

**DERMAL AND TRANSDERMAL DELIVERY OF OXICAMS USING
DEFORMABLE LIPOSOMES**

by

ZHANG JULIA ZHANG

A dissertation submitted to the

School of Graduate Studies

Rutgers, The State University of New Jersey

in partial fulfillment of the requirements

for the degree of

Doctor of Philosophy

Graduate Program in Pharmaceutical Science

Written under the direction of

Bozena Michniak-Kohn

and approved by

New Brunswick, New Jersey

January, 2021

ABSTRACT OF THE DISSERTATION

DERMAL AND TRANSDERMAL DELIVERY OF OXICAMS USING DEFORMABLE LIPOSOMES

By ZHANG JULIA ZHANG

Dissertation Director:

Bozena Michniak-Kohn, Ph.D.

Oxicams are a class of non-steroidal anti-inflammatory drugs (NSAID) structurally related to the enolic acid class of 4-hydroxy-1,2-benzothiazine carboxamides. Most oxicams are unselective inhibitors of the cyclooxygenase (COX) enzymes. They are used clinically to treat inflammation, relieve both acute and chronic pain associated with arthritis. However, adverse effects, such as gastro-intestinal toxicity/bleeding, headaches, rash, increased risk of cardiovascular events, etc., are frequently reported when Oxicams are administrated at high doses and on long-term treatment.

Topical drug delivery across the stratum corneum can provide local (dermal), or systemic (transdermal) effects, which can greatly reduce side-effects. However, the barrier function of the skin impairs the penetration and absorption of drugs. In the past three decades, nanotechnology and nanocarriers, such as microemulsion, solid lipid nanoparticles, polymeric nanoparticles, dendrimers, liposome, etc., have been extensively assessed to improve drug transport into the skin. The unique

physicochemical properties of nanoparticles allow them to overcome the biological barriers and hence, improve the bioavailability of their payload.

Among these innovative drug delivery systems, liposomes have drawn a great attention during the last few decades as a drug delivery system due to the biodegradable and biocompatible composition of liposomes and their distinctive capacity to accommodate both water-soluble and lipid-soluble agents. They showed a number of advantages over other nanocarrier systems, such as enhanced delivery of drug, protection of active drug from environmental factors, improved performance features of the product, preventing early degradation of the encapsulated drug, cost-effective formulations of expensive drugs and efficient treatment with reduced systemic toxicity. However, the conventional liposomes have been shown to be incapable of deeply penetrating the skin due to their rigid structure and size. In 1990s, transfersome, the first generation of deformable liposomes, has been introduced to greatly enhance the skin permeability of the encapsulated drugs.

The goal of this research was to explore and optimize the dermal and transdermal delivery of meloxicam (MX), a model oxicam drug, using deformable liposome delivery system. MX loaded deformable liposomal formulations have been developed and characterized for particle size, drug entrapment efficiency, zeta potential, morphology, stability and skin permeability.

In order to appropriately characterize the deformable liposomes, an HPLC method was developed for the determination of drug entrapment efficiency, drug

loading and drug content in permeation study samples. The method had been subsequently validated and proven to be specific, linear, sensitive, accurate, reproducible and stable at room temperature for the simultaneous quantitation of MX, quercetin (QCT) and dihydroquercetin (DHQ).

To conduct predictive bioavailability of topical formulations, *ex vivo* skin permeation tests using Franz Diffusion Cells have been performed to assess the skin kinetics of topical formulations. In this study, human cadaver skin model was used to generate a concentration profile following topical application of liposomal suspension or hydrogel formulations by conducting skin deposition study on both epidermal and dermal layers, flux determination on permeated samples, and visualization using Confocal Laser Microscopy (CLSM).

The composition and preparation process of conventional liposomes and transfersomes were investigated. It was found that the type, grade and the content of phospholipids played a key role in the characteristics of liposomes, such as vesicle size, PDI, zeta potential and entrapment efficiency. Based on the obtained data, vesicles were prepared using 0.8% USPC which showed the highest loading of MX, and particle size less than 200 nm with uniform size distribution (PDI less than 0.3). This finding helped guide the optimal liposomal formulations using 0.8% USPC in further experiments.

The prepared vesicles along with two different types of microemulsions were evaluated as potential dermal delivery carriers for MX. When comparing the

water-in-oil (w/o) and oil-in-water (o/w) microemulsion performance with the use of an *ex vivo* model involving human cadaver skin, the highest flux and permeation values were obtained for transfersomes, indicating these drug carriers as the most promising in terms of topical drug delivery.

Thus, the transfersome composition served as the base formulation. In order to impart stability and enhanced permeability to transfersomes, flavonoids were selected leading to the discovery of flavosomes, as novel deformable liposomes for the topical delivery of anti-inflammatory compounds. These carriers were prepared by incorporating flavonoids, specifically quercetin (QCT) and dihydroquercetin (DHQ), into transfersomes. Characterization of the flavosomes was conducted in terms of their vesicle size, zeta potential, entrapment efficiency and deformability index. These vesicles exhibited homogeneous particle size of less than 150 nm with a higher degree of deformability as compared to transfersome. *Ex-vivo* skin permeation and confocal laser scanning microscopy studies demonstrated that the flavosome formulations improved the skin permeation of MX compared to that for transfersomes.

Notably, significant skin distribution of the two flavonoids, QCT and DHQ was observed in *ex-vivo* skin permeation studies. Since flavonoids are natural anti-inflammatory compounds, flavosomes might be used as potential nanocarriers for co-delivery of other anti-inflammatory compounds such as MX.

To increase the encapsulated content of MX and improve the stability of deformable liposomal formulations (transfersomes and flavosomes), the formulation

and preparation processes were further optimized. These deformable liposomal vesicles exhibited homogeneous particle size of less than 120 nm with a significantly higher entrapment rate and deformability as compared to conventional liposomes. The liposomal gel formulation was prepared by incorporating these liposomal vesicles into 20% (w/w) poloxamer P407 hydrogel. The gel formulations were evaluated for content uniformity, rheology, particle size, morphology, stability and skin permeability.

The deformable liposomal gel formulations showed improved permeability compared to a conventional liposomal gel and a liposome-free gel. The enhancement effect was also visible by confocal laser microscopy. These deformable liposomal hydrogel formulations have the potential of being a promising alternative to conventional oral delivery of non-steroidal anti-inflammatory drugs (NSAIDs) with enhanced local and systemic onset of action and reduced gastrointestinal side effects. Notably, flavosome loaded gel formulations displayed the highest permeability through the deeper layers of the skin and shortened lag time, indicating a potential faster on-site pain relief and anti-inflammatory effect.

Acknowledgement

I would like to express my sincere and heartfelt gratitude to all the people and organizations that have helped and supported me in this endeavor with their valuable guidance, cooperation and encouragement.

My foremost gratitude goes to my advisor, Dr. Bozena Michniak-Kohn who warmly welcomed me to her Laboratory of Drug Delivery in Spring 2016 and introduced me to Dermal research, challenged me intellectually to think as a Research Scholar. She guided me to choose my own research path and has been supportive along the entire journey.

I am ineffably grateful to Dr. Aqeel Fatmi for motivating and encouraging me to pursue the Ph.D. program, which has significantly broadened my vision, knowledge and experience. During this exciting but challenging journey, he has always been there to encourage, motivate and guide me.

I would like to thank Department of Pharmaceutics at Ernest Mario School of Pharmacy for giving me the opportunity to pursue my Ph.D. in Pharmaceutical Sciences; my thesis committee members, Dr. Tamara Minko, and Dr. Leonid Kagan for taking the time out of their busy schedules to review my NIH proposal/dissertation and provide valuable critiques, comments, and guidance; all professors who taught me and showed me the advancement in the area of pharmaceutical science. I am very grateful to the administrative staff of the department of Pharmaceutics, Division of Life Sciences and Center for

Biomaterials. My special thanks go to Ms. Hui Pung and to the Center for Dermal Research CDR under the directorship of Dr. Michniak-Kohn for providing the funding for my dissertation researches.

I've enjoyed working with all past and current lab colleagues, visiting scholars and undergraduate students. I am thankful for their assistance and inputs in my research; especially thankful to Dr. Anna Froelich, Dr. Tomasz Osmalek and Dr. Paulina Skupin-Mrugalska from ORBIS program and Ms. Adelle Abady for their collaboration, support and generously sharing their knowledge and expertise. I will always cherish their friendship, and wonderful memories that we made together.

I also want to extend my appreciation to Dr. Joachim Kohn, Dr. Patrick Sinko, Dr. Nicola Francis, Dr. Rajesh Patel and their lab members who trained and assisted me to use their facilities and equipment for the analysis of my samples; Lipoid LLC and BASF for generously providing samples of soybean phosphatidylcholine and polymers as gifts.

Finally, no words can express my love and gratitude to my dearest family: my amazing husband, Qian, wonderful sons, Victor and Bowen who stood by me for this entire journey, surrounded me with love and joy, and accompanied me to overcome all obstacles and challenges; my parents, brother and his family, though, thousands of miles away, but were

always there for me. I am truly blessed to have their unconditional love, support, and encouragement. I know that I can always count on them.

Dedications

I dedicate this dissertation to my family: my husband, Qian Zhang, sons, Victor Zhang and Bowen Zhang for their unconditional love, encouragement and support. Together, we went through this challenging, but joyous and rewarding journey. I owe them an eternal debt of love and gratitude.

Table of Contents

Abstract of the Dissertation	ii
Acknowledgement	vii
Dedications.....	x
Chapter 1. Introduction	1
1.1. Oxicams: Mechanism of Action	1
1.2. Topical Delivery	5
1.3. Nanocarrier Drug Delivery Systems	9
1.4. Liposomes	16
1.5. Deformable Liposomes.....	24
1.6. Model Drug Selection	28
1.7. Specific Aims.....	32
Chapter 2. Analytical Methodology for the Quantitation and Characterization of Liposomal Formulations	33
2.1 Introduction	33
2.2 Materials and Equipment	36
2.2.1 Materials.....	36
2.2.2 Equipment	36
2.3 Development and Evaluation of Analytical Methodology for the Simultaneous Quantitation of Oxicam Model Drugs, Meloxicam (MEL) and Tenoxicam (TEN).....	37
2.3.1 Methodology.....	37
2.3.2 Results and Discussion	37
2.4 Development of Analytical Methodology for the Simultaneous Quantitation of Meloxicam (MX), Quercetin (QCT) and Dihydroquercetin (DHQ)	39
2.4.1. Methodology	39
2.4.2. Results and Discussion	39
2.5 Optimization and Validation of Analytical Methodology for the Simultaneous Quantitation of Meloxicam (MX), Quercetin (QCT) and Dihydroquercetin (DHQ)	42
2.5.1 Methodology.....	42
2.5.2 Results and Discussion.....	43
2.5.3 Conclusion	46
2.6 <i>Ex Vivo</i> Skin Permeation Study	46
2.6.1. Materials.....	46
2.6.2 Equipment-Franz Diffusion Cells	46

2.6.3. Methodology	47
2.7 Publication Information.....	48
Chapter 3. Development of Meloxicam Loaded Liposomes and Comparative Study of Liposomal vs Microemulsion Formulations.....	
3.1 Introduction	50
3.2 Materials.....	53
3.3 Methodology.....	53
3.3.1. Preparation of Liposomes	53
3.3.2. HPLC Method of the Quantification of MX	54
3.3.3. Measurement of Vesicle Size, Size Distribution, Zeta Potential and Morphology for Liposomes	55
3.3.4. Determination of MX Entrapment Efficiency	56
3.3.5. Preparation of Drug-Loaded Microemulsions.....	56
3.3.6. Pseudoternary Phase Diagrams	57
3.3.7. Electrical Conductivity Studies	58
3.3.8. Viscosity Studies	59
3.3.9. Measurement of Particle Size and Size Distribution <i>for Microemulsions</i> ...	59
3.3.10. <i>Ex Vivo</i> Skin Permeation Study.....	60
3.3.10.1 Materials	60
3.3.10.2 Equipment-Franz Diffusion Cells.....	60
3.3.10.2 Methodology	60
3.3.11. Statistical Analysis	62
3.4 Results and Discussion	63
3.4.1. Liposomes.....	63
3.4.1.1. Selection of Phosphatidylcholine	63
3.4.1.2. Development of Liposome Preparation Procedure.....	68
3.4.2. Microemulsions.....	72
3.4.2.1 Pseudoternary Phase Diagrams.....	72
3.4.2.2 Conductivity Studies.....	74
3.4.2.3 Viscosity Studies.....	77
3.4.2.4 Dynamic Light Scattering (DLS) Studies	79
3.4.3. Comparative Drug Permeation Studies.....	81
3.5 Conclusions	87
3.6 Publication Information.....	87
Chapter 4. Formulation and Process Development of Meloxicam Loaded Deformable Liposomes	
4.1. Introduction	89

4.2. Materials.....	92
4.3. Methodology.....	93
4.3.1.Preparation of Liposomal Formulations	93
4.3.2.HPLC Method of the Quantification of MX	93
4.3.3.Measurement of Vesicle Size, Size Distribution and Zeta Potential	94
4.3.4.Determination of MX Entrapment Efficiency	95
4.3.5. <i>Ex Vivo</i> Skin Permeation Study	95
4.3.5.1 Materials.....	95
4.3.5.2 Equipment-Franz Diffusion Cells	96
4.3.5.3 Methodology.....	96
4.3.6.Degree of Deformability	98
4.3.7.Fluorescence Microscopy	98
4.3.8.Study Statistical Analysis.....	99
4.4. Results and Discussion	99
4.4.1 Screening of Flavonoids Concentration	99
4.4.2 Optimization of the flavosome formulation	104
4.4.3 Deformability of Flavosome.....	110
4.5. Conclusions	112
4.6. Publication Information.....	113
Chapter 5. Development and Characterization of Meloxicam-loaded Deformable Liposomal Topical Gel Formulation	114
5.1. Introduction	114
5.2. Materials.....	118
5.3. Methodology.....	119
5.3.1 Preparation of Liposomes.....	119
5.3.2.HPLC Method of the Quantification of MX	120
5.3.3.Measurement of Vesicle Size, Size Distribution and Zeta Potential	121
5.3.4.Determination of MX Entrapment Efficiency and Drug Loading.....	122
5.3.5.Degree of Deformability	122
5.3.6.Preparation of Liposomal Gel	123
5.3.7.Morphology of Liposomal Vesicles and Gel Formulations.....	123
5.3.8.Oscillatory Rheology Studies.....	124
5.3.9 <i>Ex Vivo</i> Skin Permeation Study	125
5.3.10. Fluorescence Microscopy	127
5.3.11. Effect of Storage	128
5.3.12. Statistical Analysis	128
5.4. Results	129

5.4.1. Characterization of MX-loaded Liposomes	129
5.4.2. Characterization of MX-Loaded Hydrogels	135
5.4.3. Ex Vivo Skin Permeation Study	140
5.4.4. Skin Penetration of DiI-Labeled Liposomal Gel Formulations	145
5.4.5. Effect of Storage Study for Liposomal Formulation and Gel Formulation....	146
5.5. Conclusions	148
5.6. Publication Information.....	148
Chapter 6. Thesis Study Conclusions and Future Plans	150
References.....	156

List of Tables

Table 1. Evaluation of Meloxicam and Tenoxicam as Candidates for Topical/Transdermal Delivery	5
Table 2. Liposomal formulation present in clinical trials.....	17
Table 3. List of Deformable Liposomes.....	27
Table 4. HPLC gradients for Option 1	40
Table 5. HPLC gradients for Option 2	41
Table 6. Optimized HPLC gradients as used in the study.....	43
Table 7. Summary Table for Standard linearity, Limit of Detection (LOD) and Limit of Quantitation (LOQ).....	44
Table 8. Summary Table for Accuracy and Method Precision	45
Table 9. Summary Table for System Suitability and Solution Stability.....	46
Table 10. The composition of microemulsions used for Meloxicam (MX) incorporation	57
Table 11. Composition of the samples investigated in phase studies.....	58
Table 12. The composition and type of the vesicles investigated in the study	64
Table 13. Physicochemical properties of the obtained vesicles	66
Table 14. Physicochemical properties of the samples F1, F2 and F3 subjected to the sonication procedure ($n = 3$).....	70
Table 15 Steady state flux (J_{ss}) and permeation coefficients (K_p) obtained for the investigated formulations. ME-1 and ME-2 are w/o and o/w microemulsions, respectively. Data are presented as means \pm SD ($n = 3$ for each formulation).....	83
Table 16. Physicochemical Properties of Meloxicam (MX), Quercetin (QCT) and Dihydroquercetin (DHQ)	91
Table 17. Optimized HPLC gradients as used in the study.....	94
Table 18. Physical properties of the obtained vesicles. Data are presented as means \pm S.D. ($n=3$)	100
Table 19. Entrapment Efficiency (%EE) of the obtained vesicles. Data are presented as means \pm S.D. ($n=3$)	100
Table 20. Physical properties of the obtained vesicles. Data are presented as means \pm S.D. ($n=3$)	105
Table 21. %Entrapment Efficiency of the obtained vesicles. Data are presented as means \pm S.D. ($n=3$)	105
Table 22. Steady state flux (J_{ss}) and permeation coefficients (K_p) obtained for the investigated formulations. Data are presented as means \pm S.D. ($n=3$ for each formulation).....	108
Table 23. Deformability index of flavosomes and transfersomes. Data are presented as means \pm S.D. ($n=3$ for each formulation).....	110
Table 24. The composition and type of the vesicles investigated in the study	120

Table 25. Physiochemical properties of the obtained vesicles. Data are presented as means \pm S.D. (n=3).....	130
Table 26. Deformability index of liposomal vesicles. Data are presented as means \pm S.D. (n=3 for each formulation).....	133
Table 27. Physiochemical properties of the obtained vesicles. Data are presented as means \pm S.D. (n=3).....	140
Table 28. Permeation parameter obtained for the investigated gel formulations. Data are presented as means \pm S.D. (n=3 for each formulation).....	142
Table 29. Kinetic models for the investigated gel formulations.....	144

List of Figures

Figure 1. Representative Structure of Oxicams	1
Figure 2 Prostaglandin Synthesis Pathway	2
Figure 3. Prostaglandin Synthesis Pathway	3
Figure 4. Skin Structure and Skin Layers	6
Figure 5. Schematic representation of the transport processes involved from the release of the drug from the formulation to its eventual uptake by the dermal capillaries.	8
Figure 6. The proposed structures of nanoparticles.	10
Figure 7. Diagram of three types of solid lipid nanoparticles.	11
Figure 8. Diagram of Nanosphere and Nanocapsule	12
Figure 9. Diagram of Dendrimers.	14
Figure 10. Advantages of lipid nanoparticles applied in topical delivery systems	20
Figure 11. Possible topical delivery mechanisms liposomes.	21
Figure 12. Diagram of intact vesicles into and through the skins.	23
Figure 13. Schematic representation of the different types of lipid-based vesicular delivery systems.	26
Figure 14. Deformable Liposome	28
Figure 15. Molecular structure of meloxicam.	29
Figure 16. UV spectra and typical chromatogram of tenoxicam (Ten) and meloxicam (Mel).....	38
Figure 17. Linearity Curve for Tenoxicam and Meloxicam.	38
Figure 18. Typical HPLC Chromatogram for DHQ, QCT and MX (Option 1)	40
Figure 19. Typical HPLC Chromatogram for DHQ, QCT and MX (Option 2)	41
Figure 20. Linearity Curve for MX, QCT and DHQ for Method Option 2.	42
Figure 21. UV spectra of (a) Dihydroquercetin (DHQ) (b) Quercetin (QCT) (c) Meloxicam (MX) (d) Typical HPLC Chromatogram for DHQ, QCT and MX	44
Figure 22. Schematic of Franz diffusion cell	47
Figure 23. Dilution lines followed in conductivity studies. Lines L1, L2, L3 and L4 correspond to O:S_{mix} ratios 1:9, 2:8, 3:7 and 4:6 (w/w), respectively.....	59
Figure 25. Effect of different grade of phospholipids (PL) on entrapment efficiency of meloxicam (MX). SL: soybean lecithin, USPC: unsaturated soybean phosphatidylcholine, SSPC: saturated soybean phosphatidylcholine. Bars are means ± standard deviation (SD), n = 3.	65
Figure 26. Effect of different grade of phospholipids (PL) on drug loading of meloxicam (MX). SL: soybean lecithin, USPC: unsaturated soybean phosphatidylcholine, SSPC: saturated soybean phosphatidylcholine.	65

Bars are means \pm SD, $n = 3$.	65
Figure 27. Transmission Electron Microscopy images of (a) F2, conventional liposome, (b) F3, transfersome.	71
Figure 28. Pseudoternary phase diagrams obtained for the systems with triacetin (1A–1C) and oleic acid (2A–2C).	73
Figure 29. Conductivity plotted as a function of water content along the dilution lines L1–L4 for system 1B (Triacetin/Tween® 85/Isopropanol). The transition points are marked with green dashed lines. The transition point estimation procedure is depicted in L1. Error bars have been omitted for clarity, and standard deviation values did not exceed 5%.	76
Figure 30. Pseudoternary phase diagram with w/o (red) and o/w (blue) microemulsion areas estimated based on the conductivity studies. Microemulsions selected for the further analyses are depicted as red and blue points (ME-1 and ME-2, respectively).	77
Figure 31. Dynamic viscosity plotted as a function of water content along the dilution lines L1–L4. The transition points estimated in conductivity studies are marked with green dashed lines. Error bars have been omitted for clarity, and standard deviation values did not exceed 5%.	79
Figure 32. Particle size (A) and polydispersity index (B) obtained for placebo (red bars) and meloxicam-loaded (gray bars) w/o and o/w microemulsions.	80
Figure 33. Hypothetical mechanism of drug incorporation in w/o and o/w microemulsions.	80
Figure 34. Ex vivo drug permeation profiles of MX across human cadaver skin obtained for different carriers. ME-1 and ME-2 are w/o and o/w microemulsions, respectively. Data are plotted as means \pm SD ($n = 3$ for each formulation).	82
Figure 35. Amounts of meloxicam deposited in the skin layers after 24 h of experiment. Data are plotted as means \pm SD ($n = 3$ for each formulation).	86
Figure 37. a) The amount of meloxicam (MX) ($\mu\text{g}/\text{cm}^2$) found in the receptor compartment of the Franz diffusion cell at 24 hours; b) the amount of MX ($\mu\text{g}/\text{cm}^2$) deposited in different skin layers after permeation study ($n=3$ for each formulation)	104
Figure 38. (a) Ex vivo drug permeation profiles of Meloxicam (MX) over 24 hours; (b) MX deposited in the different layers of skin after 24-hour skin permeation study, (c) Quercetin (QCT) deposited in the different layers of skin after 24-hour skin permeation study, (d) Dihydroquercetin (DHQ) deposited in the different layers of skin after 24-hour skin permeation study. Data are presented as means \pm S.D. ($n=3$ for each formulation).	108

Figure 39. Confocal Laser Scanning Microcopy Images taken at different depths of the full thickness human cadaver skin after 24 hours permeation of Dil-labeled vesicles a) transfersome, b) Q5, c) D5 (magnification 10X)	112
Figure 40. Flow diagram of liposomal hydrogel formulation preparation.	118
Figure 41. Transmission Electron Microscopy images of (A) conventional liposomes; (B) transfersomes; (C) flavosomes-Q; (D) flavosomes-D. ..	134
Figure 42. Amplitude sweeping plots obtained for the gels (a) and calculated cross-over values (b) (n=3 for each formulation, data are presented as means \pm S.D.)	137
Figure 43. Temperature sweeping of the gels. (n=3 for each formulation, data are presented as means \pm S.D.).	138
Figure 44. Transmission Electron Microscopy images of (A) MX-Gel (B) CLP-Gel (C) TFS-Gel (D) FLSQ-Gel (E) FLSD-Gel.	139
Figure 45. (a) <i>Ex Vivo</i> drug permeation profiles of Meloxicam (MX) loaded liposomal gel formulations over 24 hours; (b) MX deposited in the different layers of skin after 24-hour skin permeation study from formulations tested (n =3 for each formulation, data are presented as means \pm S.D.).	141
Figure 46. Confocal Laser Scanning Microcopy Images taken at different depths of the full thickness human cadaver skin after 24 hours permeation of Dil-labeled gel formulations containing a) Untreated skin, b) CLP-gel, c) TFS-gel, d) FLSQ-gel and d) FLSD-gel (magnification 10X).	145
Figure 47. Stability study results of a) meloxicam loaded liposomal suspensions at 5 ± 3 °C for 30, 60 and 90 days, b) meloxicam loaded liposomal gel formulations at 25 ± 5 °C for 30, 60 and 90 days (n=3 for each formulation).	147

Chapter 1. Introduction

1.1. Oxicams: Mechanism of Action

Oxicams are non-steroidal anti-inflammatory drugs (NSAIDs) belonging to the enolic acid class of 4-hydroxy-1,2-benzothiazine 3-carboxamide derivatives¹, which was first developed by the Pfizer group as a new, potent, non-carboxylic acid-containing inflammatory agents^{2,3}. The first member of this class, Feldene (piroxicam), was introduced in the United States in 1982 and gained immediate acceptance in the market, becoming one of the top 50 prescribed drugs for several years¹. After piroxicam, other oxicams, such as isoxicam, meloxicam, tenoxicam, and lornoxicam, were introduced. The representative structure is displayed in Figure 1.

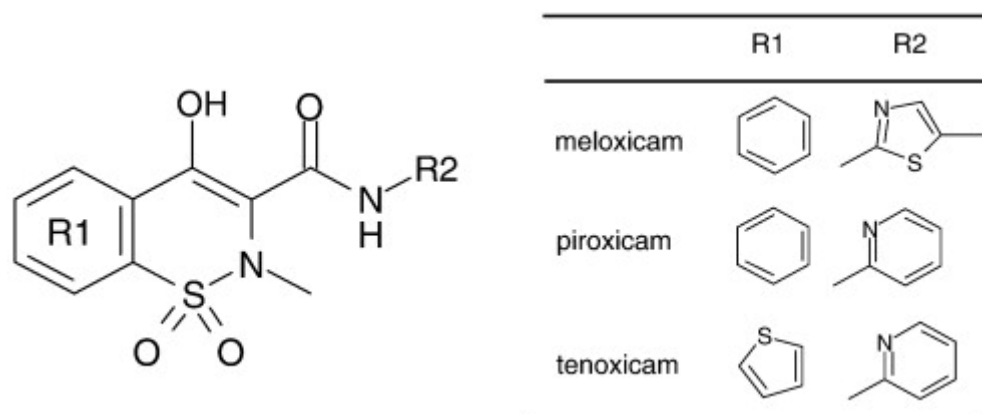


Figure 1. Representative Structure of Oxicams⁴

Most oxicams are unselective inhibitors of the cyclooxygenase (COX) enzymes. They are used clinically to treat both acute, chronic pain and inflammation associated with arthritis. Products of the prostaglandin (PG) biosynthetic pathway (Figure 2) are chief physiological mediators of both acute and chronic inflammation, involving in the recruitment of inflammatory cells, lowering the pain threshold and in the genesis

of the stimulus pyrogenic⁵. Two cyclooxygenase (COX) isoforms, COX-1 and COX-2, are the rate-limiting enzymes in this pathway. COX-1 is responsible for the baseline levels of prostaglandins, while COX-2 produces prostaglandins through stimulation, such as inflammation and growth.

As demonstrated in Figure 2, when activated by cell to cell signaling or injury/stress, cytoplasmic phospholipase A₂ (PLA₂) liberates arachidonic acid (AA) from the cell membrane. COX-1 and COX-2 metabolize AA to form specific prostaglandins (PGs) as needed. PGs act as local homeostatic regulators as well as secreted mediators of pain, fever, inflammation and vascular tone, etc. Corticosteroids can block PG production by inhibiting PLA₂, while NSAIDs inhibit PG production by inactivating COX 1&2.

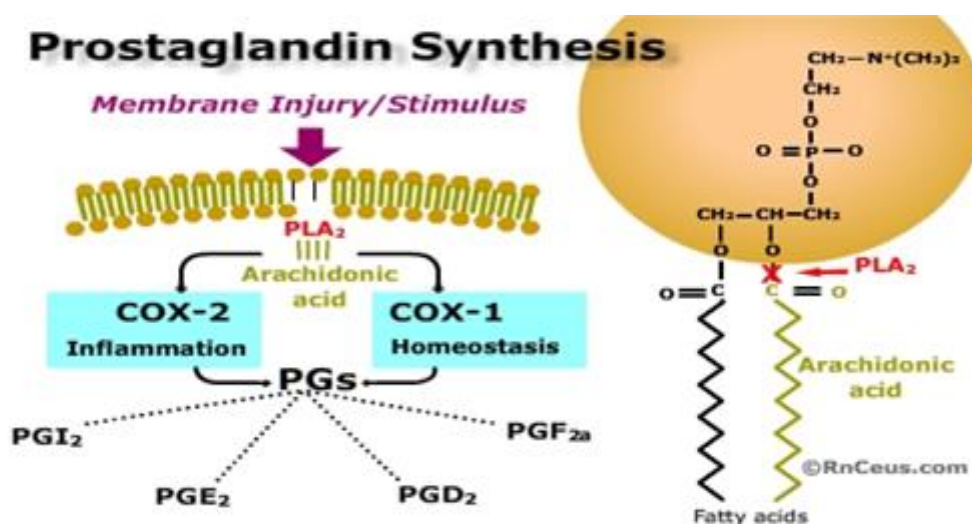


Figure 2 Prostaglandin Synthesis Pathway⁵

Recently, interest in this class of NSAIDs has increased due to the discovery that oxicams are not only inhibitors of COX1/2, but also potent inhibitors of mPGES-1

(microsomal prostaglandin E synthase-1) as displayed in Figure 3. These findings suggested the potential use of these compounds for the treatment of various cancers. Many studies have been conducted to use oxicams as a viable adjuvant therapeutic agent to treat different cancers, such as lung, colorectal, prostate and urinary bladder cancers⁶⁻¹⁰.

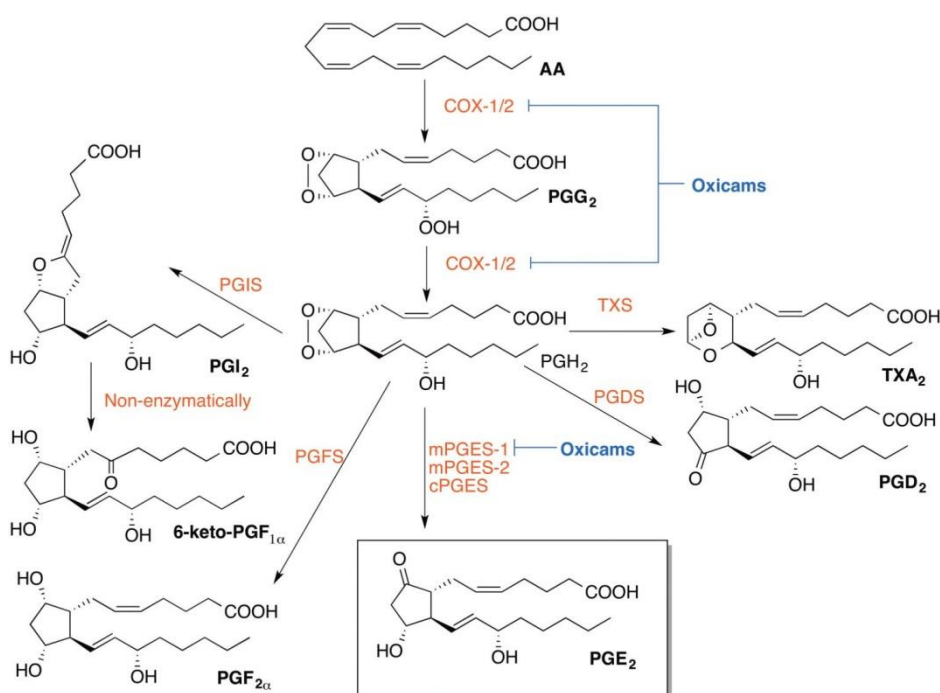


Figure 3. Prostaglandin Synthesis Pathway¹

However, adverse effects, such as gastro-intestinal toxicity/bleeding, headaches, rash, increased risk of cardiovascular events, etc., are frequently reported when administered oxicams at high doses and on the long-term treatment.¹¹

Topical administration provides a number of advantages over oral NSAIDs: the ability to deliver the drug substance more selectively to a specific site for both local and systemic effects, to avoid first pass effect, to reduce gastro-intestinal side effects

and to improve patient compliance. As per European League Against Rheumatism (EULAR) and National Institute for Health and Care Excellence (NICE) guidelines¹², topical administrations of NSAIDs are recommended for the management of mild to moderate osteoarthritis pain before the oral route.

However, topical administration cannot be used for a large number of drug because the barrier function of stratum corneum would only allow small quantities of any drug to penetrate over a period of time¹³. The selection of drug candidates for permeation through the skin depends on their physicochemical properties (solubility, crystallinity, molecular weight, polarity, melting point and partition coefficient LogP), drug interactions with the membrane, and pharmacokinetic considerations. The ideal physicochemical properties of a drug selected for cutaneous administration are low molecular weight because the diffusion coefficient will be high; solubility in water and oils to achieve a high concentration gradient and increase the diffusion force across the skin; balanced partition coefficient because very high partition coefficients may inhibit drug clearance from the skin and increase drug retention; and a low melting point which is related to an appropriate solubility affected by the skin temperature.¹⁴⁻¹⁹ The pharmacokinetic information is another critical factor because topical administration is suitable only for relatively potent drugs whose daily dose is in few milligrams¹³. Hence, there are only a few formulations of oxicams for skin use available in the global market, none in the US market due to their physiochemical

properties²⁰. Table 1 demonstrates the ideal candidate for skin delivery and the evaluation of meloxicam and tenoxicam as model drugs in this regard.

Table 1. Evaluation of Meloxicam and Tenoxicam as Candidates for Topical/Transdermal Delivery

Items	Ideal Candidate	Meloxicam		Tenoxicam	
		Value	Fit or Not	Value	Fit or Not
Aqueous solubility	> 1mg/mL	0.007 mg/mL	Not	0.014 mg/mL	Not
Lipophilicity	$1 < \log P < 3$	3.4	Not	1.9	Yes
Molecular weight	< 500 Da	351.4	Yes	337.4	Yes
Melting point	< 200°C	254	Not	211	Not
Dose deliverable	< 10 mg/day	7.5	Yes	20	Not

Therefore, the inherent properties of these oxacam compounds make them not suitable for topical delivery.

1.2. Topical Delivery

Skin of an average adult body covers a surface of approximately 2 m² and receives about one-third of the blood circulating through the body. It is the largest organ of the human body and posts great potential for application of drugs. It is composed of three layers, the epidermis (50–100 µm), dermis (1–2 mm) and hypodermis (1–2 mm) (Figure 4).

The outmost layer of epidermis, *stratum corneum*, is a 10–20 µm thick, composed of multilayer of flat, polyhedral-shaped, 2 to 3 µm thick, non-nucleated cells

termed *corneocytes*²¹ embedded in a continuous matrix of lipid membranous sheets. These extracellular membranes are unique in their compositions and are composed of ceramides, cholesterol and free fatty acids. The *stratum corneum* provides the barrier to percutaneous absorption which can reduce water loss, provide protection against abrasive action and microorganisms, and generally act as a permeability barrier to the environment.

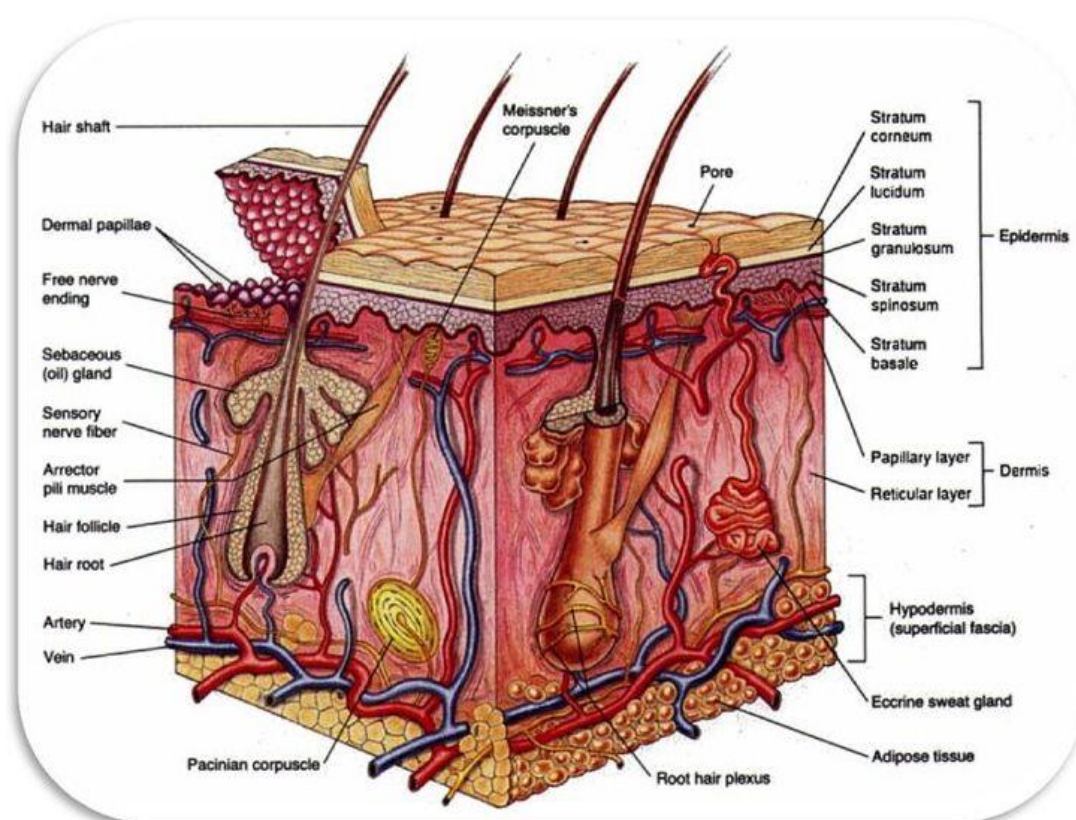


Figure 4. Skin Structure and Skin Layers²²

Delivery of drugs through the skin can be dated back in ancient Egyptian and Babylonian period in 3000 BC¹⁹. Topical remedies in the forms of ointments and potions made of animal, mineral or plant extracts were anointed, bandaged, rubbed or applied to the skin for the treatment of various skin conditions. Over the ages, it has

been recognized that products could be applied to the skin for either local or systemic effects. The progress in understanding the anatomy and physiology of the skin has facilitated to effectively and quantitatively deliver drug candidates to specific target sites in and through the skin. Advances in modern technologies are resulting in a larger number of drugs being cutaneous delivered including conventional hydrophobic small molecule drugs, hydrophilic drugs and macromolecules.

Compared to other administration routes, skin delivery provides convenient and pain-free self-administration for patients. It eliminates frequent dosing administration, maintains a constant drug concentration, and easily delivers a drug with a short half-life. All this leads to improved patient compliance, especially when long-term treatment is required, as in chronic pain management and smoking cessation therapy. Avoidance of hepatic first-pass metabolism and the GI tract for poorly bioavailable drugs is another advantage of transdermal delivery. Elimination of this first-pass effect allows the amount of drug administered to be lower, and hence safer in hepato-compromised patients as well as reduction of toxicity and adverse effects.

According to Kalia and Guy¹⁴, the release of a therapeutic agent from a formulation applied to the skin surface and its transport to the systemic circulation is a multistep process consisting of (a) dissolution within and release from the formulation, (b) partitioning into the skin's outermost layer, the SC, (c) diffusion through the SC, principally via a lipidic intercellular pathway, (i.e., the rate-limiting step for most compounds), (d) partitioning from the SC into the aqueous viable epidermis, (e)

diffusion through the viable epidermis and into the upper dermis, and (f) uptake into the local capillary network and eventually the systemic circulation (Figure 5). Therefore, an ideal drug candidate would have sufficient lipophilicity to partition into the SC, but also sufficient hydrophilicity to enable the second partitioning step into the viable epidermis and eventually the systemic circulation. For most drugs, except those possessing extreme lipophilicity ($\log P > 5$), the rate-determining step for drug transport across the skin is transit across the SC due to its barrier function impairing the penetration and absorption. Therefore, many strategies, such as physical, chemical and formulation approaches²³, have been assessed to overcome the barrier function of the stratum corneum and to improve drug transport into the skin.

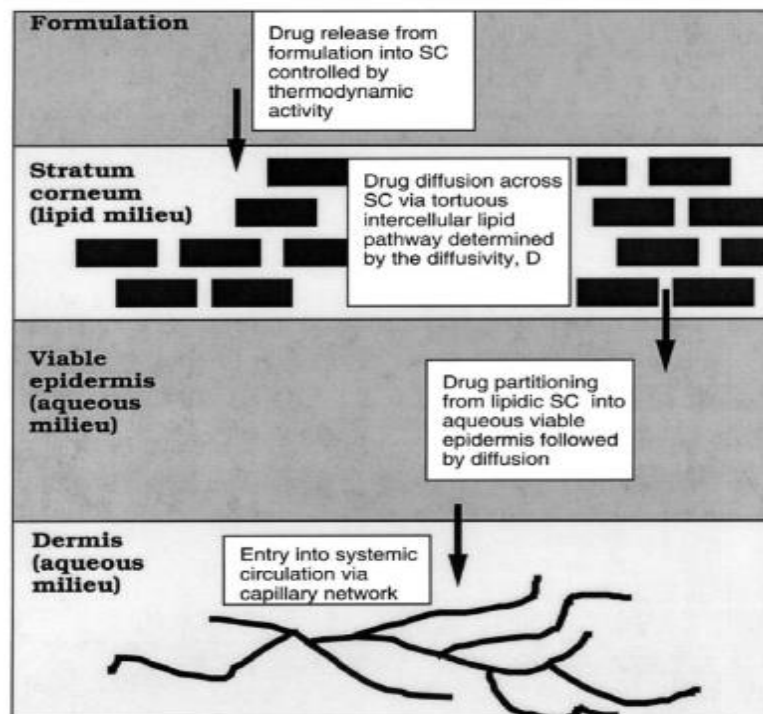


Figure 5. Schematic representation of the transport processes involved from the release of the drug from the formulation to its eventual uptake by the dermal capillaries.¹⁴

The physical approaches include iontophoresis, electroporation, microporation (microneedles), heat, needleless injection, medicated tattoos, pressure wave, sonophoresis, magnetophoresis and radiofrequency. Use of permeation enhancers and prodrugs are some of the chemical approaches used for permeation enhancement²⁴. However, the most commonly used are formulation approaches, such as creation of supersaturated systems, utilization of water as a penetration enhancer, usage of colloidal carriers, development of microemulsions etc. Among these, transporting the encapsulated active drugs via various nano-vesicles has gained significant attentions and extensive investigations have been conducted in the past few decades.

1.3. Nanocarrier Drug Delivery Systems

Nanocarriers typically have submicron particle size less than 500 μm , and can improve pharmacokinetics and biodistribution, decreased toxicities, improved solubility and stability, controlled release and site-specific delivery of therapeutic agents.²⁵ Due to their high surface area to volume ratio, these vesicles have the ability to alter basic properties and bioactivity of drugs.²⁶ Moreover, the physiochemical properties of nanocarriers can be tuned by altering their compositions (organic, inorganic or hybrid), sizes (small or large), shapes (sphere, rod or cube) and surface properties (surface charge, functional groups, PEGylation or other coating, attachment of targeting moieties), which makes them potential targeted drug delivery systems.²⁷ The overall goal of utilizing nanocarriers in drug delivery is to treat a disease effectively with minimum side effects. The commonly used nanoparticles for

dermal and transdermal delivery are solid lipid nanoparticles (SLNs), polymeric nanoparticles (PNPs), dendrimers, nanoemulsions and liposomes (Figure 6).

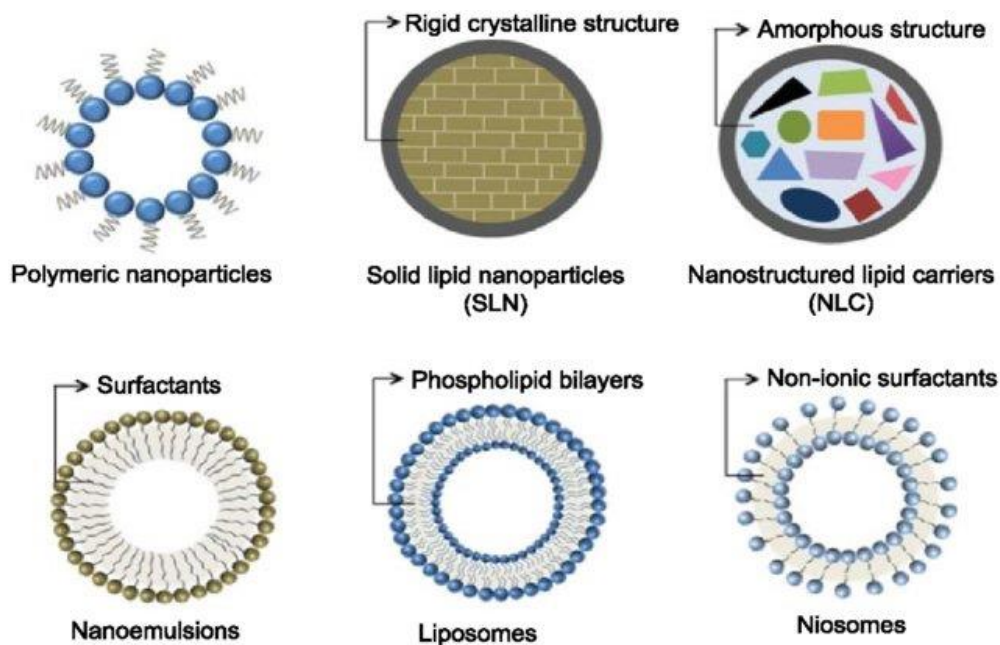


Figure 6. The proposed structures of nanoparticles.²⁸

SLN are prepared by dispersing melted solid lipids in water, with the addition of emulsifiers to stabilize the dispersion. The two most commonly used preparation procedures are high pressure homogenization and microemulsification. SLNs provide a highly lipophilic lipid matrix for drugs to be dispersed or dissolved. A wide variety of solid lipids including mono-, di- and triglycerides; free fatty acids; free fatty alcohols; waxes and steroids have been utilized for the preparation of SLNs. SLNs are quite similar to nanoemulsions except that solid lipids are used in SLNs instead of liquid lipids (oils) used in nanoemulsions.²⁵ Depending upon the composition of SLNs (lipid, drug and surfactant) and production conditions (hot or cold homogenization), drug can be dispersed homogeneously in lipid matrix (solid solution/homogeneous matrix

model), incorporated into the shell surrounding the lipid core (drug-enriched shell model) or incorporated into the core surrounded by a lipid shell (drug-enriched core model) (Figure 7).²⁹



Figure 7. Diagram of three types of solid lipid nanoparticles²⁹.

SLNs offer a number of advantages over other colloidal counterparts, including controlled drug delivery, lack of biotoxicity, high drug payload, improved bioavailability of poorly water-soluble drugs, better stability and easy as well as economical large-scale production³⁰. SLNs provide a natural platform to incorporate lipophilic drugs. However, encapsulation of hydrophilic and ionic drugs and controlling the rate and extent of drug release from SLNs are the major obstacles faced by SLNs that restrain them from becoming effective nanocarriers in dermal and transdermal drug delivery.

PNPs are solid, nanosized (10–1,000 nm) colloidal particles made up of biodegradable polymers²⁵. Based on their structural organization, PNPs can either be categorized as nanospheres (matrix type) or nanocapsules (reservoir type) (Figure 8).³¹ Nanospheres disperse or entrap the drug in the polymer matrix, while the drug is

dissolved or dispersed in liquid core of oil or water encapsulated by a solid polymeric membrane in nanocapsules. In both types of PNPs, the adsorption or chemical conjugation of drug on to the surface is also possible. The methods used to prepare PNPs can be classified into two categories, dispersion of preformed polymers and direct polymerization of monomers. The methods involving the dispersion of preformed polymers include solvent evaporation, salting out, nanoprecipitation, dialysis and supercritical fluid technology. The methods involving direct polymerization of monomers include emulsification polymerization, miniemulsion polymerization, microemulsion polymerization, interfacial polymerization and controlled/living radical polymerization³²

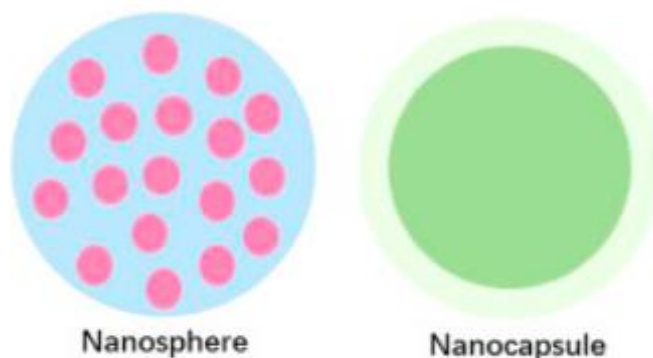


Figure 8. Diagram of Nanosphere and Nanocapsule³¹

A number of biocompatible and biodegradable, both natural and synthetic, polymers have been utilized for the preparation of PNPs, which could be degraded into individual monomers inside the body and hence removed from the body through normal metabolic pathways. Most commonly used synthetic polymers include

polylactic acid (PLA), polyglycolic acid (PGA), PLGA, PEG, polycaprolactone (PCL), *N*-(2-hydroxypropyl)methacrylamide (HPMA) copolymer, polyaspartic acid (PAA) and polyglutamic acid, whereas albumin, alginate, chitosan, collagen, dextran, gelatin and heparin are some of the commonly used natural polymers.³³ PNPs offer better stability on storage, higher drug payload, more homogeneous particle size distribution, better and controllable physicochemical properties, higher drug circulation times and more controlled drug release. However, it is difficult to scale-up the manufacturing process and there are insufficient toxicological assessments of their toxic degradation, toxic monomers aggregation, residual material associated with them, and toxic degradation process.^{34,35}

Dendrimers are nonpeptidic branched macromolecules with various arms originating from the central core with distinctive molecular weight, increased number of branching, multivalency and spherical shapes of an average diameter of 1.5–14.5 nm. (Figure 9).²⁵ Drugs can be loaded to the cavities in the dendrimers' cores through hydrogen bonds, chemical linkages or hydrophobic interactions. Each level of added branches to the core throughout the synthesis process is called as a generation. The exceedingly branched structure of dendrimers results in bulky exterior groups. Usually, they are produced by using natural or synthetic components, such as sugars, nucleotides and amino acids by either stepwise synthetic techniques or polymerization processes²⁵. The structure of these molecules results in relatively uniform shapes, sizes, and molecular weights.³⁶

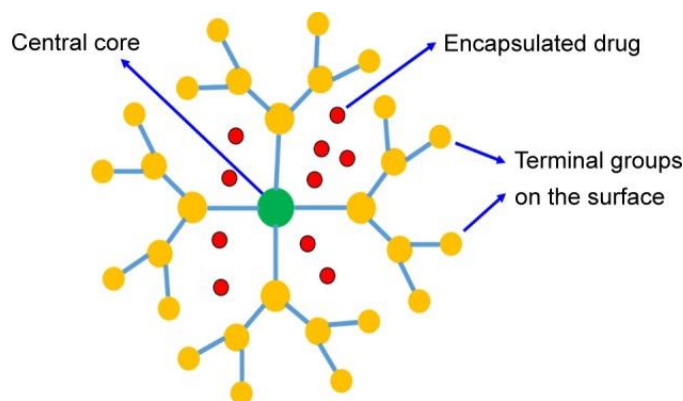


Figure 9. Diagram of Dendrimers²⁵.

Dendrimer–drug conjugate is formed when the drug is covalently bonded to a dendrimer at the core or on the terminal groups and very infrequently in the inner layers, ie, at the branching points. Being monodispersed, structurally controlled macromolecules with a definite size and molecular weight, dendrimers–drug conjugate is a carrier of choice over conventional polymeric drug delivery carriers. The permeability of dendrimers through the skin depends on physicochemical characteristics like generation size, molecular weight, surface charge, composition, and concentration. These nanocarriers have been used to transport photosensitizers for photochemical therapy and antifungal molecules. Examples of drugs delivered throughout the skin by using dendrimers are tamsulosin³⁷, indomethacin³⁸, ketoprofen, diflunisal³⁹, 5-fluorouracil⁴⁰ and peptides⁴¹.

The main advantage of dendrimers is that they have multivalency⁴² and it is possible to precisely control the functional groups on the surface⁴³ for targeted drug delivery. Due to their form and size, these molecules can carry drugs, imaging agents, etc. Dendrimers interact with lipids present in membranes, and they show better

permeation in cell cultures. Dendrimers also act like solubility enhancers, increasing the permeation of lipophilic drugs. However, they are not good carriers for hydrophilic drugs. The main problems with this kind of transdermal carrier are their poor biodegradation, inherent cellular toxicity, elimination and metabolism depending on the generation and materials, high cost for their synthesis³⁴.

Nanoemulsions are isotropic dispersed systems of two nonmiscible liquids, either an oily system dispersed in an aqueous system, or an aqueous system dispersed in an oily system but forming droplets of nanometric sizes (1-100 nm)³⁶. can be formulated in nanoemulsions. They are nontoxic and nonirritant systems and can be used for hydrophobic and hydrophilic drugs. Nanoemulsions can be prepared by three methods: high-pressure homogenization, microfluidization, and phase-inversion temperature. They are thermodynamically unstable systems because high energy is required to produce them and could break down over time and revert back to separated phase, subject to energy barrier between nanoemulsions and separated phase (Gibbs free energy, ΔG)⁴⁴. Therefore, nanoemulsions are susceptible to creaming, flocculation, and other physical instability problems. Transdermal delivery using nanoemulsions has decreased due to the inherent stability problems. Some examples of drugs using nanoemulsions for transdermal drug delivery are gamma tocopherol, caffeine, plasmid DNA, aspirin, methyl salicylate, insulin and nimesulide⁴⁵.

Liposomes are spherical vesicles consisting of one or more phospholipid bilayers and were first described by British hematologist Alec Bangham in 1960s⁴⁶⁻⁴⁹. They

were first used to study membrane processes and membrane-bound proteins due to their structure similarity to cell membrane. Due to the biodegradable and biocompatible composition of liposomes and their distinctive capacity to accommodate both water-soluble and lipid-soluble agents, liposomes have drawn a great attention during the last few decades in biomedicine, especially as a drug delivery system for antitumor drugs. They showed a number of advantages over other nanocarrier systems, such as enhanced delivery of drug, protection of active drug from environmental factors, improved performance features of the product, preventing early degradation of the encapsulated drug, cost-effective formulations of expensive drugs and efficient treatment with reduced systemic toxicity⁵⁰. Moreover, the pharmacokinetic properties of the drugs encapsulated in the liposomes have significantly changed compared to free drugs in solution⁵¹. They can be covered with polymers such as polyethylene glycol (PEG; PEGylated or stealth liposomes) to exhibit prolonged half-life in blood circulation.

1.4. Liposomes

In the past 30 years, liposomes have become one of the pharmaceutical nanocarriers of choice for various bioactive agents including drugs, vaccines, cosmetics and nutraceuticals.⁵⁰ After the approval of Doxil (doxorubicin hydrochloride liposome injection) by US FDA in 1995, many liposome-based drugs and biomedical products have been approved for clinic trials and some of them have been approved and available in global market (Table 2).

Table 2. Liposomal formulation present in clinical trials⁵²

LF	Active agent	Composition	Size (nm)	Indication	Status
ONPATTRO®	Patisiran (siRNA)	DLin-MC3-DMA, Cholesterol, DSPC, PEG ₂₀₀₀ -C-DMG	–	Hereditary transthyretin amyloidosis	Approved by FDA in August 2018
CPX-351 (Vyxeos™)	Daunorubicin + cytarabine	DSPC, DSPG, cholesterol (7:2:1) daunorubicin, cytarabine 5:1	100	Acute myeloid leukemia	Approved by FDA in 2017
Onivyde®	Irinotecan + fluorouracil + folinic acid	PEGylated liposome	80–140	Pancreatic adenocarcinoma	Approved by FDA in 2015
LEP-ETU	Paclitaxel	DOPC, cholesterol, cardiolipin (90:5:5) Lipid, PTX (33:1)	150	Ovarian cancer	Not approved by FDA
Marqibo®	Vincristine	Sphingomyelin, Cholesterol (60:40)	100	Non-Hodgkin's lymphoma and leukemia	Approved by FDA in August 2012
Exparel®	Bupivacaine	DEPC, DPPG, cholesterol, tricaprylin	3000–30,000	Pain management	Approved by FDA in 2011
Mepact®	Mifamurtide	Non-PEGylated liposome, Muramyl tripeptide PE	–	Osteosarcoma	FDA denied approval 2007. This medicine is authorized for use in the European Union
Inflexal V®	Inactivated hemagglutinin of A or B influenza virus	DOPC, DOPE (75:25)	150	Influenza	Approved by European Medicines Agency (EMA) in 2008

LF	Active agent	Composition	Size (nm)	Indication	Status
Genexol-PM	Paclitaxel	PEG-PLA polymeric micelle	20–50	Breast, lung and ovarian cancer	Approved in Korea and marketed in Europe in 2007
Epaxal®	Inactivated hepatitis A virus (strain RGSB)	DOPC, DOPE (75:25)	150	Hepatitis A	Approved in 2006 and is currently used in Switzerland and Argentina
Lipusu®	Paclitaxel	72 g PC, 10.8 cholesterol in ethanol	400	Gastric, ovarian and lung cancer	Approved by FDA in 2005
DepoDur™	Morphine sulfate	Cholesterol, triolein, DOPC, DPPG (11:1:7:1)	17,000–23,000	Pain management	Approved by FDA in 2004
Lipo-Dox®	Doxorubicin	DSPC, cholesterol, PEG 2000-DSPE (56:39:5)	20	Breast and ovarian cancer	Approved by FDA in 2012
Myocet®	Doxorubicin + cy clophosphamide	EPC, cholesterol (55:45)	190	Metastatic breast cancer	Approved by EMEA in 2000
Visudyne®	Verteporfin	EPG, DMPC (3:5)	100	Ocular histoplasmosis	Approved by FDA in 2000
Depocyt®	Cytarabine	Cholesterol, triolein, DOPC, DPPG (11:1:7:1)	20	Neoplastic meningitis	FDA status: discontinued
Abelcet®	Amphotericin B	DMPC, DMPG (7:3)	600–11,000	Invasive fungal infection	Approval FDA in 1995
Amphotec®	Amphotericin B	Cholesteryl sulfate	—		FDA status: discontinued

LF	Active agent	Composition	Size (nm)	Indication	Status
DaunoXome®	Daunorubicin	DSPC, cholesterol, daunorubicin (10:5:1)	45–80	Leukemia	FDA status: discontinued
Doxil®	Doxorubicin	HSPC, cholesterol, PEG 2000-DSPE (56:39:5)	100	Kaposi's sarcoma	Approved by FDA in 1995
AmBisome®	Amphotericin B	HSPC, DSPG, cholesterol, amphotericin B (2:0.8:1:0.4)	45–80	Invasive fungal infection	Approved by FDA in 1997
Thermodox®	Doxorubicin	DPPC, MSPC, PEG 2000-DSPE (90:10:14)	175	Hepatocellular carcinoma, solid tumors	Not approved
EndoTAG®	Paclitaxel	DOTAP, DOPC, PTX (50:47:3)	180–200	Breast cancer	Not approved
MM-302	Doxorubicin	DSPE, HER2, PEG	75–110	Breast cancer	Not approved
PTX-LDE	Paclitaxel	135 mg cholesteryl oleate, 333 mg egg PC, 132 mg miglyol 812 N, 6 mg cholesterol, 60 mg PTX	1–1000	Epithelial ovarian carcinoma	Not approved
Arikace®	Amikacin	DPPC, cholesterol (2:1)	≈ 300	Lung infections	Not approved
MRX34	miR-34a	DOTAP, cholesterol	≈ 110	Advanced solid tumors and hematological malignances	Not approved
Xemys	Myelin basic proteins	Egg PC, monomannosyl dioleoyl glycerol, α -tocopherol and lactose	–	Multiple sclerosis	Not approved

The use of liposome in topical delivery systems has many advantages, including but not limited to: increases of drug permeation through stratum corneum; lowers skin irritation caused by drugs and metabolites; extends the effective time within the skin by interaction of phospholipid bilayer with the similarly structured cell membrane;

drugs can be steadily released for extended efficacy; due to increased retention in the skin, the amount of drug which enters the epidermis/dermis and reaches systemic circulation is lowered, mitigating toxicity; for hydrophobic drugs, liposome formulation increases overall solubility without the use of skin irritating solvents (Figure 10).⁵³

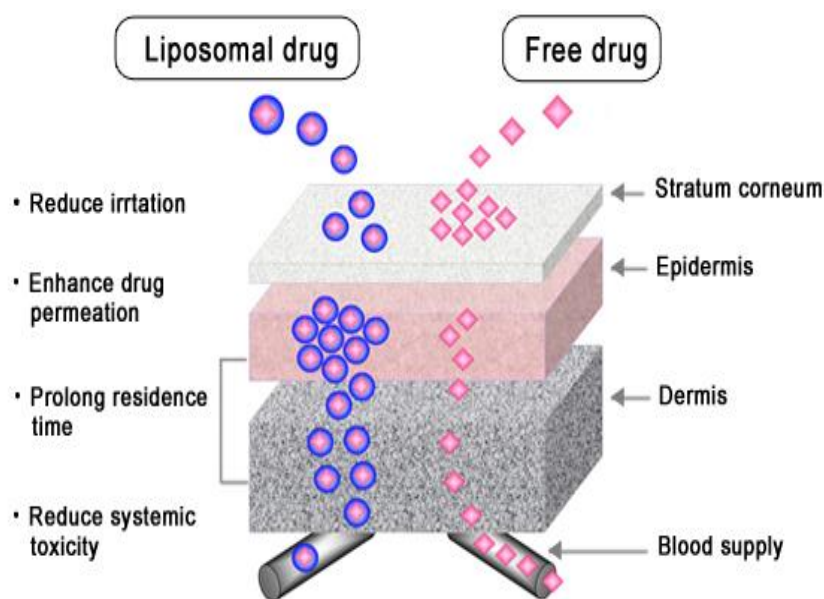


Figure 10. Advantages of lipid nanoparticles applied in topical delivery systems⁵³

As suggested by El Mahraby et al⁵⁴, possible topical delivery mechanisms of liposomes can be categorized into 5 processes (Figure 11): (A) free drug mechanisms, (B) penetration enhancing process, (C) Vesicle adsorption to and/or fusion with the SC, (D) intact vesicle penetration into and through the intact skin and (E) transappendageal penetration.

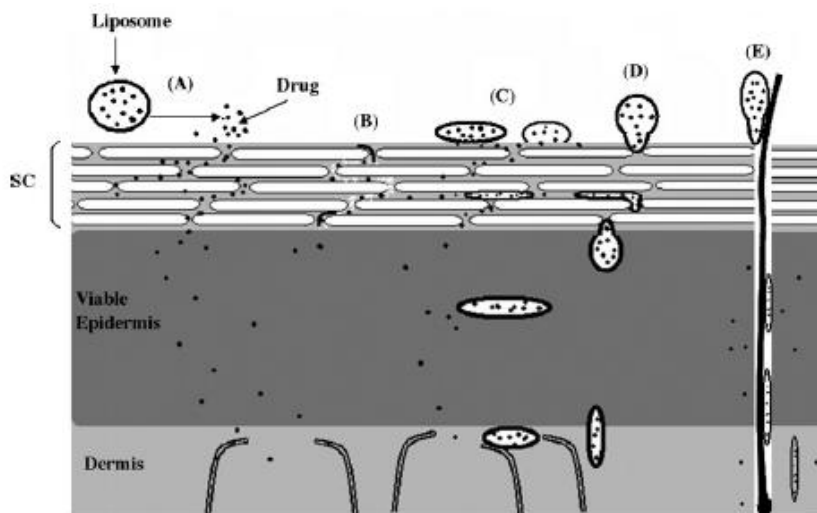


Figure 11. Possible topical delivery mechanisms liposomes⁵⁴.

According to Ganesan et al⁵⁵, the drug permeates the skin as free agent after exiting from the vesicles. However, the role of this process in transdermal delivery of estradiol was reported to be negligible by El Maghraby et al.⁵⁶ In their study, the trans-epidermal flux plot was compared with its in vitro drug release profile and the results indicated that the drug released from liposomes was negligible. This suggested that this process played minor role in liposomal topical drug delivery mechanism.

In the studies conducted by Kato et al⁵⁷, Zellmer et al⁵⁸, and Kirjavainen et al⁵⁹, the obtained results revealed that the lipids used to constructed the liposomes may penetrate deep into the SC or may fuse and mix with skin lipids to loosen their structure, suggesting a penetration-enhancing effect of the liposome components. Negative findings have also been reported by Weiner et al.⁶⁰ and Du Plessis et al⁶¹. Discrepancies observed in the penetration enhancing effects in these literature reports might be attributed to the use of different lipid components in the vesicle formulations,

with non-rigid lipids tending to produce the greatest enhancing effects. Therefore, the selection of the phospholipid types and composition of the formulations could have an impact on the liposomal permeability.

The vesicles may be adsorbed on the stratum corneum surface, then subsequently release the encapsulated drug directly from vesicles to skin, or vesicles may fuse and mix with the stratum corneum lipid matrix, increasing drug partitioning into the skin. The interaction of liposomes with human skin has been reviewed and it was concluded that they can be taken into the skin but cannot penetrate through intact healthy SC; instead, they might dissolve and form a unit membrane structure⁶². The studies conducted by Kirjavainen's group also suggested the processes of liposome lipids adhesion onto the skin surface and fusion or mixing with the lipid matrix of stratum corneum⁶³. Phospholipids was observed to increase the partitioning of estradiol, progesterone and propranolol into the stratum corneum lipid bilayers⁵⁹. The similar findings by Keith and Snipes also suggested that the major component of liposomes, phospholipids, increased the continuity of the lipid matrix of the skin and thus facilitated the movement of lipophilic molecules⁶⁴. All these studies suggested the unique delivery mechanism provided by the liposomal formulations is vesicle adsorption and/or fusion with the SC.

In respect to the intact vesicle penetration, Foldvari et al.⁶⁵ applied DPPC, CH (2:1) liposomes loaded with an electron dense marker to guinea pigs. Electron microscopic images showed the presence of intact liposomes in the dermis. The

authors proposed that liposomes carrying the drug can penetrate the epidermis. Whereas, Korting et al.⁶⁶ concluded that vesicles can penetrate diseased skin with its ruptured SC (as in eczema) but cannot invade skin with hyperkeratosis, as in psoriasis. Contrary to these findings, Du Plessis et al.⁶⁷ found that intermediate-sized and not small-sized liposomes resulted in higher skin deposition, which indicated that intact liposomes did not penetrate the skin. Furthermore, no evidence of intact carrier penetration could be found after application of DMPC or soy-lecithin liposomes by the study conducted by Zellmer et al.⁵⁸ and Korting et al.⁶⁸, separately. The route of delivery can be further classified into either intercellular or transcellular depending on the composition and the type of liposomes (Figure 12).

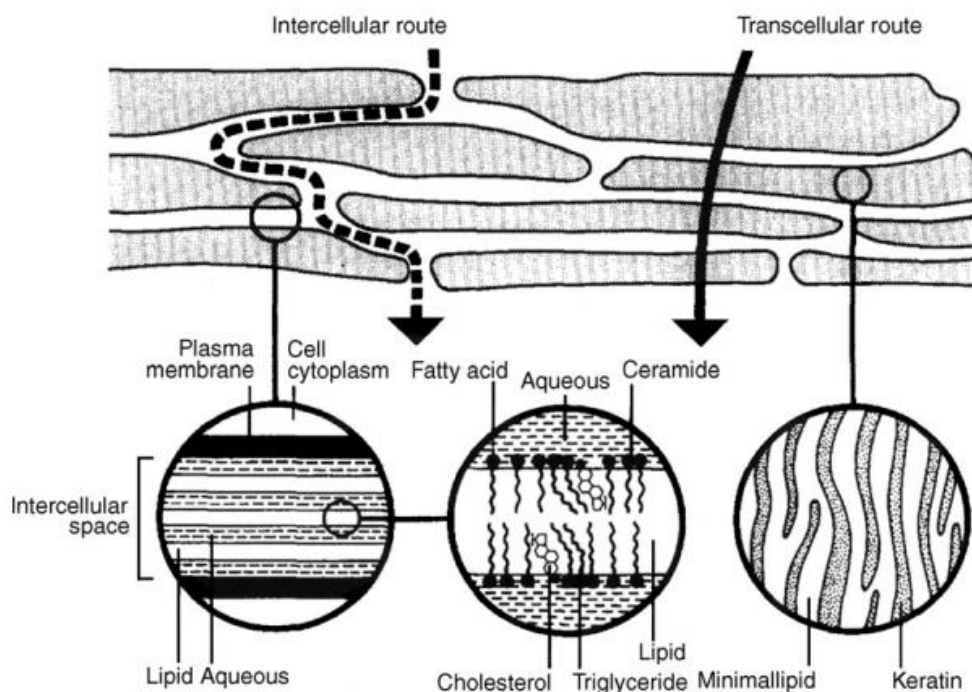


Figure 12. Diagram of intact vesicles into and through the skins⁵⁴

The last proposed liposome delivery mechanism is transappendageal penetration. From the study results reported by El Maghraby et al⁶⁹, it was concluded that the shunt routes played a minor role in estradiol transdermal delivery from liposomes. Furthermore, the transfollicular delivery from liposomes was enhanced only after combination with iontophoresis according to Han et al⁷⁰. Therefore, it appears that the shunt routes play minor role in liposomal transdermal delivery.

1.5. Deformable Liposomes

Although the liposomes provided many benefits as a biocompatible and efficient drug delivery platform, the conventional liposomes have been generally considered of little or no value as carriers for transdermal drug delivery because they are unable to penetrate through the deep layers of skin and tend to be retained in the stratum corneum (SC) layer because of its rigid structure.⁷¹ To overcome this limitation, new generation of liposomes, termed deformable liposomes, have been developed in the past twenty years.

Deformable liposomes are generally prepared by addition of a denaturant such as a surfactant (edge activator) or ethanol into the conventional liposomes⁷². Surfactants used typically include the nonionic Tween® 80, the bile salt, sodium cholate (NaC), and others.

Transfersomes® are considered the first generation of deformable vesicles developed by Cevc and Blume^{73,74}. They are a novel type of liquid-state vesicles that consist of phospholipids and an edge activator, which is often a single chain surfactant

(e.g., Sodium cholate, Span 60/65/80, and Tween 20/60/80) that destabilizes the lipid bilayers of the vesicles and increases their deformability by lowering the interfacial tension⁷⁵. This feature enables Transfersomes® to squeeze themselves through intercellular regions of the stratum corneum under the influence of the transdermal water gradient. They have been reported to penetrate intact skin *in vivo* with an efficiency similar to subcutaneous administration, provided that the elastic vesicles are topically applied in non-occlusive conditions^{73,76,77}.

Niosomes, considered the second generation of deformable liposomes, are non-ionic surfactant vesicles made up of single chain surfactant molecules in combination with cholesterol. These nanoparticles generally resemble the same characteristics as that of liposomes, but are considered more stable⁷⁷. Niosomes can reduce transepidermal water loss and increase smoothness through replenishment of lost skin lipids following fusion to corneocytes⁷⁸. Niosomes have the ability to modify the structure of the stratum corneum through their surfactant properties, in order to make the layer looser and more permeable.

Ethosomes, another novel lipid carrier developed by Touitou et al., has shown enhanced skin delivery of encapsulated compounds^{71,79}. The ethosomal system is mainly composed of phospholipids, a relatively high concentration of ethanol (20–50%) and water. Ethanol is a well-known permeation enhancer that is suggested to provide a synergistic mechanism with the vesicles and skin lipids. The inclusion of ethanol may provide the vesicles with soft flexible characteristics, which allow them to more easily

penetrate into deeper layers of the skin. Ethosome may also influence the bilayer structure of the stratum corneum to enhance drug penetration⁷⁵.

An illustration of these three deformable liposomes is presented in Fig 13.

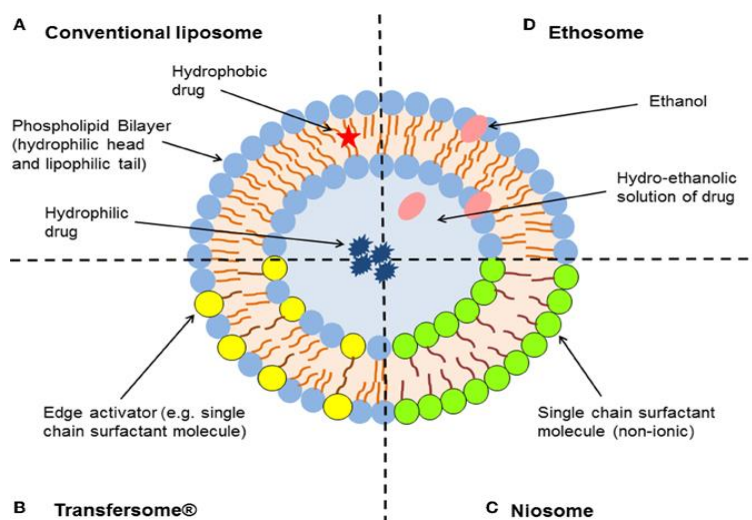


Figure 13. Schematic representation of the different types of lipid-based vesicular delivery systems⁷⁵.

Mentosomes, novel ultra-deformable vehicles, are composed of phospholipids, menthol and edge activator. Meloxicam loaded mentosomes were firstly introduced by Duangjit et al.⁸⁰, and the physicochemical characteristics and skin permeation profile were investigated. The optimal formulation composed of 0.773% phosphatidylcholine, 0.077% menthol, 0.077% MX, 0.082% cholesterol and 0.224% cetylpyridinium chloride was screened using response surface methodology, which performed best with flux of 0.31 mg/cm²/h.

Moreover, many other approaches, such as flexosome⁸¹, invasome⁸², etc., by introducing different permeation enhancers into the composition of the lipid-based

nano-delivery systems can increase both vesicle elasticity and deformability. A summary of these investigated liposomal vesicles is listed in Table 3.

Table 3. List of Deformable Liposomes

Name	Composition (Phospholipids+...)	Remarks	References
Transfersomes	Edge activator (sodium cholate)/single-chain surfactant	1 st generation, flexible, deliver large molecules	74
Niosomes	Optimal ratio of non-ionic surfactant+ cholesterol	2 nd generation, not lipid based, improve solubility of drugs, bioavailability, Chemical stability and low cost	83
Ethosomes	Ethanol	Highly lipophilic molecules, cationic drug	79
Invasomes	Ethanol + terpenes/terpenes mixtures	Increase permeation of hydrophilic drugs, control release by change the type and ratio of terpenes	84
Flexosomes	Low molecular weight heparin (LMWH)-loaded liposomes	Similar particle size with ethosomes, but higher deformability	85
Menthosomes	Menthol + edge activator (CPC)+cholesterol	Improve skin permeation by increase of drug partition and diffusion	80
Bilosomes	Bile salts + non-ionic surfactant +cholesterol	Bile salts in the lipid bilayer of niosomes make them resistant against GI bile salts and enzymes, offer protection for the entrapped drug.	86
Proniosomes	Dry product of niosomes is hydrated immediately before use	Minimize physical instability, aggregation, fusion and leaking, provide convenience in transportation, distribution, storage and dosing.	87

Compared to conventional liposomes, the denaturant embedded in the lipid bilayers can destabilize the bilayers and provide a flexible membrane, which enables these vesicles to open extracellular pathways among the cells in *stratum corneum*, and

then deform to squeeze through these passages into the deeper layers of the skin as illustrated in Figure 14.^{54,88,89}

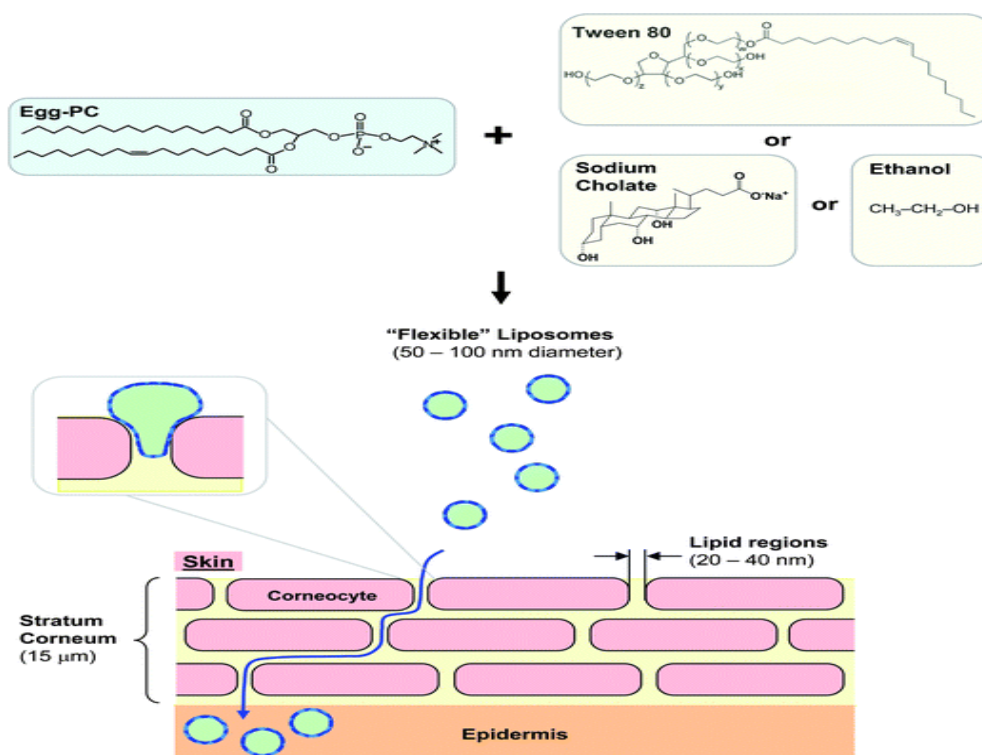


Figure 14. Deformable Liposome⁹⁰

1.6. Model Drug Selection

Meloxicam is a potent Biopharmaceutical Classification System (BCS) class II non-steroidal anti-inflammatory drug (NSAID), which is pastel yellow solid. Its IUPAC (International Union of Pure and Applied Chemistry) name is: 4-hydroxy-2-methyl-*N*-(5-methyl-1,3-thiazol-2-yl)-1,1-dioxo-1 λ^6 ,2-benzothiazine-3-carboxamide, and its molecular formula is $\text{C}_{14}\text{H}_{13}\text{N}_3\text{O}_4\text{S}_2$. The structural formula of meloxicam is demonstrated in Figure 15. Mobic® (Boehringer Ingelheim) was first approved as 7.5 mg meloxicam tablet by US FDA in 2000 and was later approved and marketed in capsule and suspension forms.

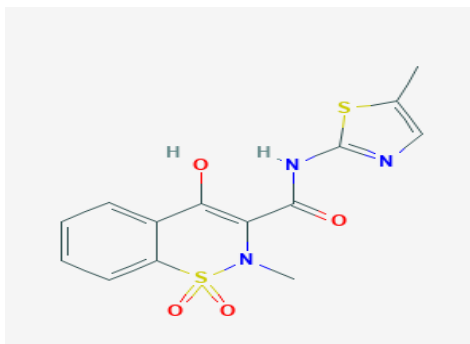


Figure 15. Molecular structure of meloxicam.

As a preferential cyclo-oxygenase-2 (COX-2) inhibitor, it has been used clinically to treat both acute and chronic pain and inflammation, relieve swelling, stiffness and pain associated with rheumatoid arthritis, osteoarthritis, ankylosing spondylitis, tendonitis, bursitis and peri-arthritis of the shoulders or hips⁹¹⁻⁹³. Additionally, it has been widely explored as a potential therapeutic agent for Alzheimer's disease and various tumors, such as lung, colorectal, prostate and urinary bladder cancers⁶⁻⁹.

As clinical pharmacology information provided in Mobic® tablets and oral suspension package insert on FDA website (https://www.accessdata.fda.gov/drugsatfda_docs/label/2012/020938s022lbl.pdf), the absolute bioavailability of meloxicam capsules was 89% following a single oral dose of 30 mg compared with 30 mg IV bolus injection. Following single intravenous doses, dose-proportional pharmacokinetics were shown in the range of 5 mg to 60 mg. After multiple oral doses the pharmacokinetics of meloxicam capsules were dose-proportional over the range of 7.5 mg to 15 mg. Mean C_{max} was achieved within four to five hours after a 7.5 mg meloxicam tablet was taken under fasted

conditions, indicating a prolonged drug absorption. With multiple dosing, steady-state concentrations were reached by Day 5. A second meloxicam concentration peak occurs around 12 to 14 hours post-dose suggesting biliary recycling.

Administration of meloxicam capsules following a high fat breakfast (75 g of fat) resulted in mean peak drug levels (i.e., C_{max}) being increased by approximately 22% while the extent of absorption (AUC) was unchanged. The time to maximum concentration (T_{max}) was achieved between 5 and 6 hours. In comparison, neither the AUC nor the C_{max} values for meloxicam suspension were affected following a similar high fat meal, while mean T_{max} values were increased to approximately 7 hours. No pharmacokinetic interaction was detected with concomitant administration of antacids. Based on these results, MOBIC can be administered without regard to timing of meals or concomitant administration of antacids.

Meloxicam is ~99.4% bound to human plasma proteins (primarily albumin) within the therapeutic dose range. The fraction of protein binding is independent of drug concentration, over the clinically relevant concentration range, but decreases to ~99% in patients with renal disease. Its penetration into human red blood cells, after oral dosing, is less than 10%. Following a radiolabeled dose, over 90% of the radioactivity detected in the plasma was present as unchanged meloxicam.

Meloxicam is extensively metabolized in the liver. Its metabolites include 5'-carboxy meloxicam (60% of dose), from P-450 mediated metabolism formed by oxidation of an intermediate metabolite 5'-hydroxymethyl meloxicam which is also

excreted to a lesser extent (9% of dose). In vitro studies indicate that CYP2C9 (cytochrome P450 metabolizing enzyme) plays an important role in this metabolic pathway with a minor contribution of the CYP3A4 isozyme. Patients' peroxidase activity is probably responsible for the other two metabolites which account for 16% and 4% of the administered dose, respectively. All the four metabolites are not known to have any in vivo pharmacological activity.

The mean elimination half-life ($T_{1/2}$) ranges from 15 hours to 20 hours. The elimination half-life is constant across dose levels indicating linear metabolism within the therapeutic dose range. Plasma clearance ranges from 7 to 9 mL/min.

Although it has been considered the first choice for treatment of chronic pain, many adverse effects, especially gastro-intestinal toxicity/bleeding, have been frequently reported when it is administrated orally ^{11,94,95}. Additionally, it has significant first pass effect as reported above. Therefore, numerous researches have been conducted to target its dermal and transdermal delivery, but until now there is no topical dosage form available in US market. As a zwitterionic drug, MX has a relatively high melting point (254 °C), low aqueous solubility (7.15 mg/L at 25 °C) and lipophilicity ($\log P = 3.43$) ⁹⁶ out of the ideal range of 1 to 3 (Table xxx), indicating that it is not an ideal candidate for topical delivery. To address the unmet need, it was selected as the model drug to develop a deformable liposomal system to overcome these challenges.

1.7. Specific Aims

The main goal of the study is to achieve dermal and transdermal delivery of the model drug, meloxicam, using deformable liposomes. The specific aims are listed below:

Aim 1: To Develop and Validate Analytical Methodology for the Characterization of Liposomal Formulations, including both Liposomes and Liposomal Hydrogel Formulations

Aim 2: To Develop and Optimize Meloxicam Loaded Deformable Liposomal Formulations and Preparation Processes

Aim 3: To Develop and Characterize MX-Loaded Deformable Liposomal Topical Gel formulations

Chapter 2. Analytical Methodology for the Quantitation and Characterization of Liposomal Formulations

2.1 Introduction

Liposomes are highly versatile structures, which can be used as potential carriers for various compounds, including the traditional small molecules, biologics and diagnostic agents. In order to assess the quality of liposomes and obtain quantitative measures that allow comparison between different batches of prepared formulations, various parameters should be monitored. The main characteristics of liposomes are entrapment efficiency, average size, size distribution (polydispersity index, PDI), surface charge and morphology.

The vesicle average size and size distribution are important parameters because vesicular size can affect the penetration of drugs through the skin to the deeper layers. Verma et al.⁹⁷ studied the influence of liposomal size on the skin penetration utilizing two fluorescently labeled substances. They found that the penetration of these fluorescent substances was inversely related to the size of the liposomes. It was concluded that vesicles with a size larger than 600 nm failed to deliver the loaded molecules into deeper layers of the skin, whereas those with a size smaller than 300 nm were able to deliver the loaded molecules into the deeper layers of the skin. Polydispersity Index (PDI) is usually measured to determine the degree of size distribution uniformity of these vesicle systems. In drug delivery applications using lipid-based carriers, such as liposomal formulations, a PDI of 0.3 and below is

considered to be acceptable and indicates a homogenous population of phospholipid vesicles.^{98,99}

Zeta potential was used to study these vesicles' surface charge, which was affected by the total net charge of the vesicle components and pH of the hydration buffer. As many studies revealed¹⁰⁰⁻¹⁰², higher positive or negative values of zeta potential of nano vesicles indicate good physical stability due to electrostatic repulsion of individual particles. On the other hand, zeta potential value close to zero can result in particle aggregation and flocculation due to the Van der Waals attractive forces.

Another key physicochemical assessment of liposomes is visualizing the morphology of the nanoparticles using microscopy. There are a number of techniques available for imaging liposomes that can be broadly categorized into light, electron, or atomic-force microscopy.¹⁰³ In our study, transmission electron microscopy (TEM) has been used to study the morphology of the vesicles and liposomal gel formulations.

Entrapment efficiency (%EE) is a key parameter to calculate the amount of drug incorporated into the liposomes by expressed as the percentage of drug encapsulated in liposomes relative to the total amount of drug. Drug loading (%DL) is the process of incorporating the drug into the vesicles. It is calculated as the percentage of drug encapsulated in liposomes relative to the total amount of phospholipids used.

As stated by Herkenne et al. in their review paper¹⁰⁴, pharmacokinetic measurements in blood, plasma or urine are usually not feasible because of the very

low concentrations achieved in these typical sampling compartments for topical products. It is also not clear whether measurable levels in the blood are relevant to local, topical drug bioavailability. Therefore, bioavailability assessment of topical formulations is challenging. One of the methods suggested by FDA is the dermatopharmacokinetic (DPK) approach, in which the drug concentration in the skin is determined continuously or intermittently for a period of time¹⁰⁵. Additionally, FDA has posted a draft guidance on acyclovir topical cream in 2016¹⁰⁶, in which a comparative IVPT (in vitro permeation test) between the test and RLD products can be conducted to demonstrate bio-equivalency instead of the in vivo option.

Human or animal skin permeation study using Franz Diffusion Cell is one of the standard in vitro tests to assess the skin kinetics of topical formulations. It is also an important model system to establish in vitro-in vivo correlation (IVIVC) used by both academia and healthcare industries¹⁰⁷. In this study, human cadaver skin model has been used to generate a concentration profile following topical application of liposomal hydrogel formulations by conducting skin deposition study on both epidermal and dermal layers, flux determination on permeated samples, and visualization using CLSM. To evaluate the feasibility and capability of the dermal and transdermal delivery using the developed vesicles or formulations, *ex vivo* skin permeation study is a key measurement.

Since the physical characterization techniques, such as particle size, size distribution, zeta potential and morphology are quite straightforward, the

corresponding methodology would be discussed in each individual chapter. As the key analytical measurement, this chapter would focus on HPLC method development for the quantitative determination of MX, Tenoxicam, QCT and DHQ. The optimized method would be validated and used for the determinations of %EE, %DL and drug content in the permeation study. The two flavonoid compounds, QCT and DHQ, have been used as permeation enhancers and will be discussed in detail in chapter 4.

2.2 Materials and Equipment

2.2.1 Materials

High-performance liquid chromatography (HPLC) grade water, phosphoric acid and acetonitrile were purchased from BDH VWR Analytical (Radnor, PA, USA). QCT was purchased from Sigma-Aldrich (St. Louis, MO). MX and Tenoxicam was supplied from Acros Organics (Morris Plains, NJ), and DHQ was purchased from Cayman Chemical Company (Ann Arbor, MI, USA).

2.2.2 Equipment

The HPLC system used in the study was an Agilent 1100 Series liquid chromatography system equipped with diode array and/or UV/Vis detector(s) and column heater (Agilent Technologies, Santa Clara, CA, USA) and Agilent Chemstation software (OpenLab CDS, ChemStation Edition, Rev. C.01.10, Agilent Technologies, Santa Clara, CA, USA). A reversed-phase C18 column (Agilent Plus C18, 5 μ m, 4.6 \times 150 mm, Agilent Technologies, Santa Clara, CA,

USA or YMC Triart C18 Ex RS Plus, 5 μ m, 4.6 \times 150 mm, 8 nm, YMC Co., Ltd., Kyoto, Japan) was used as the stationary phase.

2.3 Development and Evaluation of Analytical Methodology for the Simultaneous Quantitation of Oxicam Model Drugs, Meloxicam (MEL) and Tenoxicam (TEN)

2.3.1 Methodology

The column temperature was maintained at 30°C \pm 0.5 °C using the column heater. The mobile phase composed of 40% of 50 mM phosphate buffer (pH 6.6) and 60% of methanol at a flow rate of 1.0 mL/ min. The UV detector was set at a wavelength of 360 nm both Ten and Mel. The elution Mode was isocratic. Injection volume was set at 10 μ L and the run time was established at 3 minutes.

2.3.2 Results and Discussion

An analytical HPLC method has been developed for the analysis of oxicams model drugs, Tenoxicam (Ten) and Meloxicam (Mel). Based on the UV spectra of Ten and Mel in the region between 200 to 400 nm, shown in Figure 16, the UV detection wavelength for Ten and Mel was set at 360 nm. The retention time for Ten and Mel was approximately 1.8 and 2.2 minutes, respectively.

The method was shown to be linear (correlation coefficient, $r^2=1$ for both compounds) at a concentration ranging from 0.03 to 0.65 μ g/ml and 0.08 to 1.68 for Ten and Mel, respectively, as demonstrated in Figure 17.

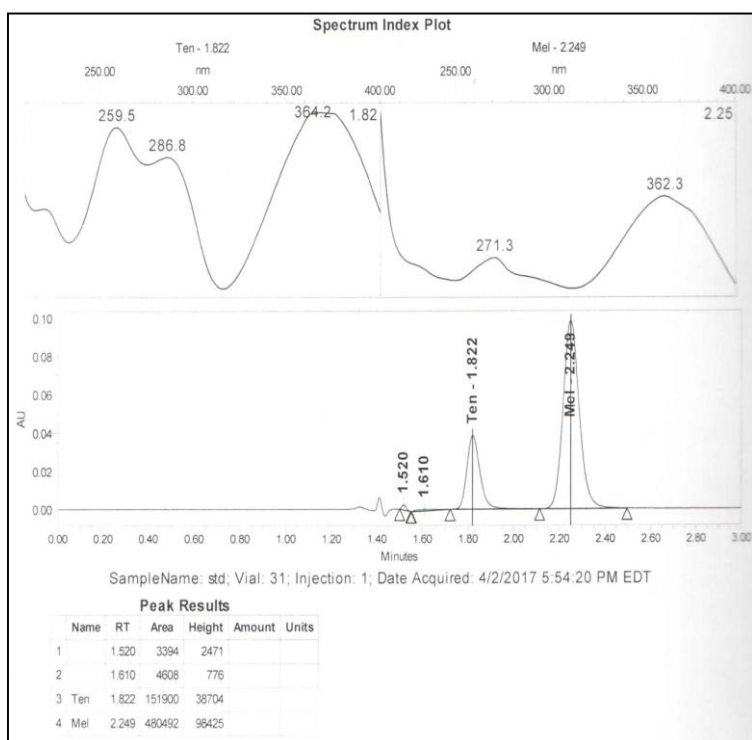


Figure 16. UV spectra and typical chromatogram of tenoxicam (Ten) and meloxicam (Mel)

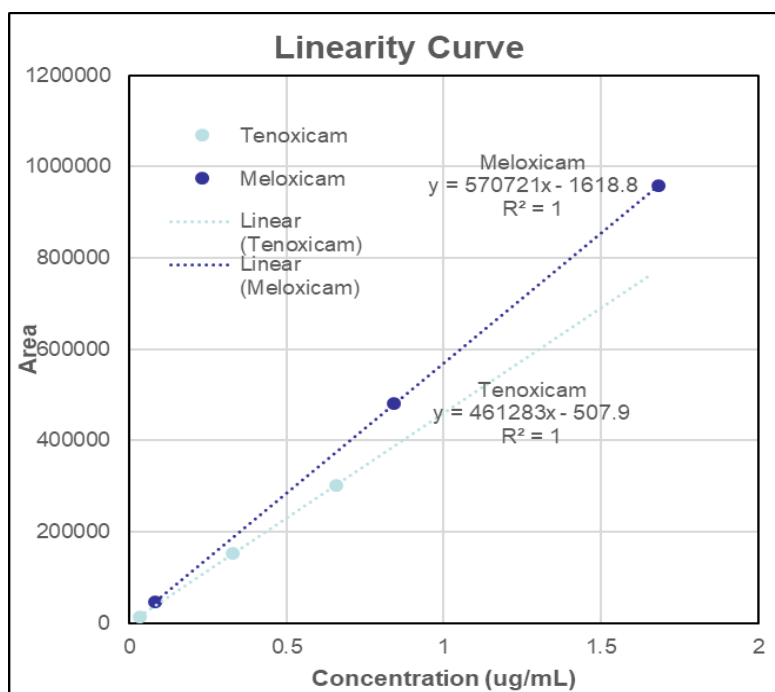


Figure 17. Linearity Curve for Tenoxicam and Meloxicam.

Therefore, this method was determined to be suitable for the quantitation of these two oxicam model drugs. However, further qualification of the method, such as recovery, specificity, stability, etc., need to be conducted.

2.4 Development of Analytical Methodology for the Simultaneous Quantitation of Meloxicam (MX), Quercetin (QCT) and Dihydroquercetin (DHQ)

2.4.1. Methodology

The column temperature was maintained at 30° C. The mobile phase composed of 1% phosphoric acid and acetonitrile at a flow rate of 1.0 mL/ min. The UV detector was set at a wavelength of 290 nm for DHQ and 360 nm for QCT and MX.

2.4.2. Results and Discussion

Two flavonoid compounds, QCT and DHQ, have been introduced in the formulation for their potential antioxidant and permeation enhancement effects. Therefore, it was beneficial to develop an HPLC method for the simultaneous qualification of MX, QCT and DHQ, which would have greatly shortened the analysis time. To achieve this goal, various HPLC running parameters were evaluated. Compared to methods described in section 2.3, the mobile phase composed of 1% phosphoric acid and acetonitrile demonstrated superior selectivity and resolution. Two options had shown satisfactory linearity and specificity and

were further evaluated. Their HPLC gradient tables and typical standard solution chromatograms are shown in Tables 4/5 and Figures 18/19, respectively.

Table 4. HPLC gradients for Option 1

Time (minutes)	Acetonitrile (%)	1% Phosphoric Acid (%)
0.0	38	62
4.5	38	62
4.8	80	20
7.8	80	20
8.0	38	62

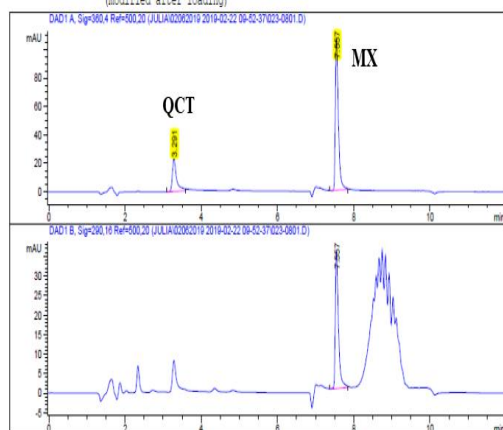
Data File C:\CHEM32\2\DATA\JULIA\02062019 2019-02-22 09-52-37\023-0001.D
Sample Name: QCT+MX

=====

Acq. Operator : JULIA Seq. Line : 8
Acq. Instrument : Instrument 2 Location : Vial 23
Injection Date : 2/22/2019 12:45:47 PM Inj : 1
Inj Volume : 5.0 µl

Acq. Method : C:\CHEM32\2\DATA\JULIA\02062019 2019-02-22 09-52-37\MELOXICAM_DQH_MX_J2.M
Last changed : 2/22/2019 11:23:36 AM by JULIA
(modified after loading)

Analysis Method : C:\CHEM32\2\METHODS\MELOXICAM_DQH_MX_J2.M
Last changed : 2/25/2019 11:22:51 AM by JULIA
(modified after loading)



Data File C:\CHEM32\2\DATA\JULIA\02062019 2019-02-22 09-52-37\022-3002.D
Sample Name: DHQ+MX

=====

Acq. Operator : JULIA Seq. Line : 30
Acq. Instrument : Instrument 2 Location : Vial 22
Injection Date : 2/22/2019 11:35:35 PM Inj : 2
Inj Volume : 5.0 µl

Acq. Method : C:\CHEM32\2\DATA\JULIA\02062019 2019-02-22 09-52-37\MELOXICAM_DQH_MX_J2.M
Last changed : 2/22/2019 11:23:36 AM by JULIA
(modified after loading)

Analysis Method : C:\CHEM32\2\METHODS\MELOXICAM_DQH_MX_J2.M
Last changed : 2/25/2019 2:04:06 PM by JULIA
(modified after loading)

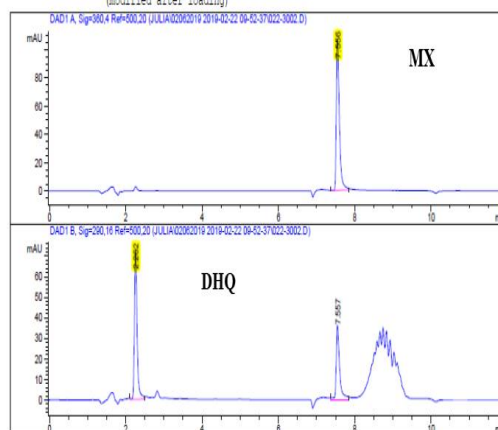


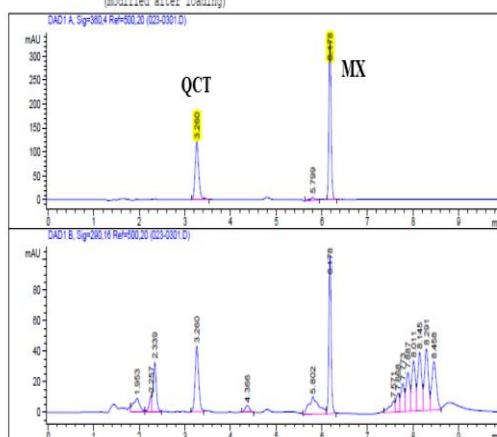
Figure 18. Typical HPLC Chromatogram for DHQ, QCT and MX (Option 1)

Table 5. HPLC gradients for Option 2

Time (minutes)	Acetonitrile (%)	1% Phosphoric Acid (%)
0.0	38	62
3.5	38	62
3.7	70	30
6.5	70	30
6.7	38	62

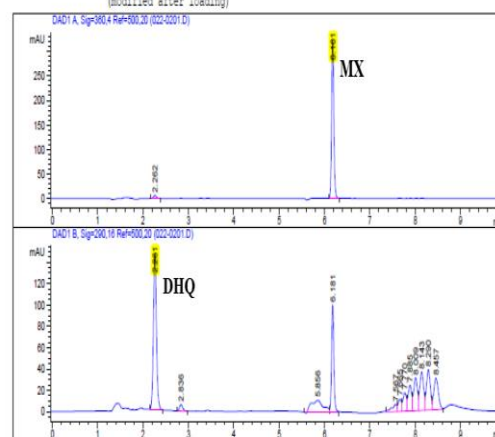
Data File C:\CHEM32\2\DATA\JULIA\02062019 2019-02-25 12-35-12\023-0301.D
Sample Name: QCT+MX-1

===== A =====
Acq. Operator : JULIA Seq. Line : 3
Acq. Instrument : Instrument 2 Location : Vial 23
Injection Date : 2/25/2019 1:12:00 PM Inj : 1
Inj Volume : 10.0 µl
Sequence File : C:\CHEM32\2\DATA\JULIA\02062019 2019-02-25 12-35-12\02062019.S
Method : C:\CHEM32\2\DATA\JULIA\02062019 2019-02-25 12-35-12\MELONICAM_DQH_JZ.M
Last changed : 2/25/2019 12:37:04 PM by JULIA
(modified after loading)



Data File C:\CHEM32\2\DATA\JULIA\02062019 2019-02-25 12-35-12\022-0201.D
Sample Name: DHQ+MX-1

===== B =====
Acq. Operator : JULIA Seq. Line : 2
Acq. Instrument : Instrument 2 Location : Vial 22
Injection Date : 2/25/2019 12:48:56 PM Inj : 1
Inj Volume : 10.0 µl
Sequence File : C:\CHEM32\2\DATA\JULIA\02062019 2019-02-25 12-35-12\02062019.S
Method : C:\CHEM32\2\DATA\JULIA\02062019 2019-02-25 12-35-12\MELONICAM_DQH_JZ.M
Last changed : 2/25/2019 12:37:04 PM by JULIA
(modified after loading)

**Figure 19. Typical HPLC Chromatogram for DHQ, QCT and MX (Option 2)**

Method option 2 displayed sharper, more symmetrical peaks and shorter run time. Therefore, it was selected for further evaluation. The method was shown to be linear (correlation coefficient, $r^2 > 0.999$) at a concentration ranging from 0.5 to 50 µg/ml for all three compounds, as demonstrated in Figure 20.

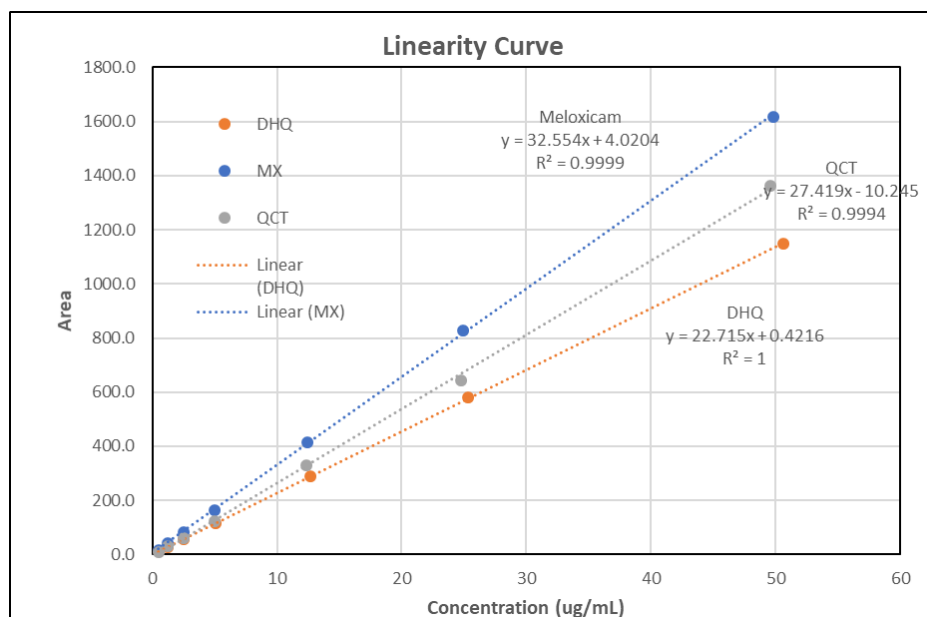


Figure 20. Linearity Curve for MX, QCT and DHQ for Method Option 2.

Therefore, this method was determined to be suitable for further optimization and validation.

2.5 Optimization and Validation of Analytical Methodology for the Simultaneous Quantitation of Meloxicam (MX), Quercetin (QCT) and Dihydroquercetin (DHQ)

2.5.1 Methodology

The column temperature was maintained at 30° C. The mobile phase composed of 1% phosphoric acid and acetonitrile at a flow rate of 1.0 mL/ min. The UV detector was set at a wavelength of 290 nm for DHQ and 360 nm for QCT and MX. The optimized HPLC gradient table is provided below in Table 6.

Table 6. Optimized HPLC gradients as used in the study

Time (minutes)	Acetonitrile (%)	1% Phosphoric Acid (%)
0.0	32	68
3.5	32	68
3.7	70	30
6.5	70	30
6.7	32	68

2.5.2 Results and Discussion

Based on the UV spectra of MX, DHQ and QCT in ethanol in the region between 200 to 400 nm, shown in Figure 21 (a), (b) and (c), the UV detection wavelength for MX and QCT was set at 360 nm and at 290 nm for DHQ, respectively. The retention time for DHQ, QCT and MX was approximately 2.7, 5.1 and 7.0 minutes, respectively (Figure 21 (d)).

The method was shown to be linear at a concentration ranging from 0.05 to 50 µg/ml for all three compounds as demonstrated in Table 7. The limit of detection (LOD) and Limit of Quantitation (LOQ) are provided in Table 7. No interference was observed from the diluent, placebo (liposome formulations without MX, DHQ and QCT) and skin samples.

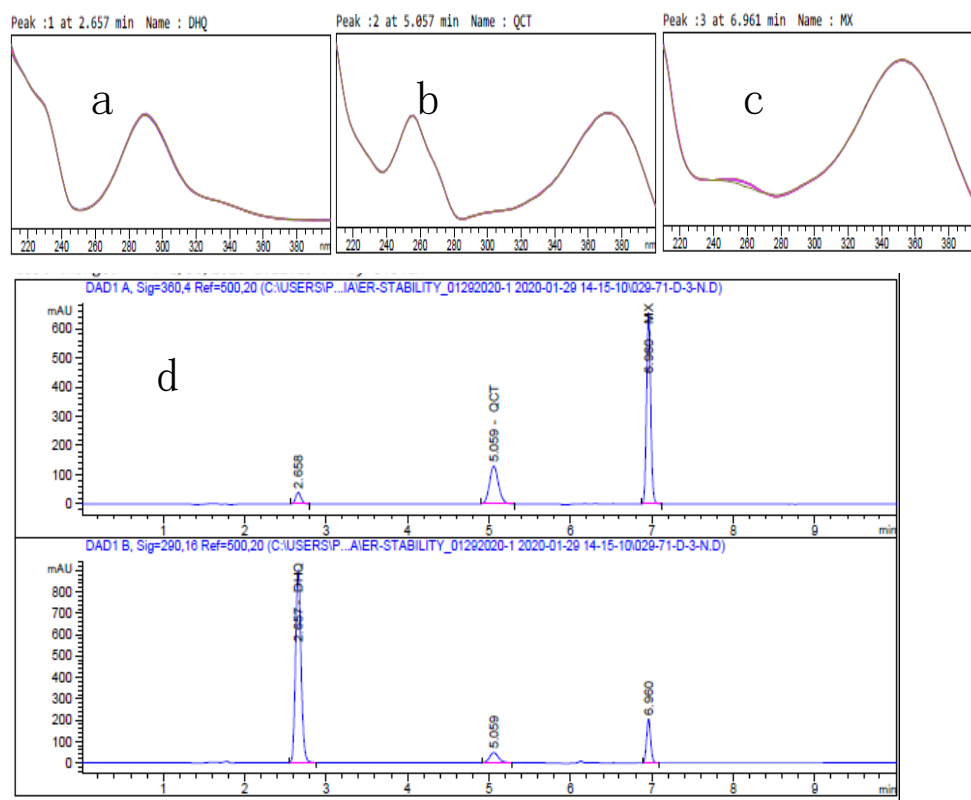


Figure 21. UV spectra of (a) Dihydroquercetin (DHQ) (b) Quercetin (QCT) (c) Meloxicam (MX) (d) Typical HPLC Chromatogram for DHQ, QCT and MX

Table 7. Summary Table for Standard linearity, Limit of Detection (LOD) and Limit of Quantitation (LOQ)

Compound Name	Slope	Intercept	R ²	LOD (µg/mL)	LOQ (µg/mL)
MX	48.055	10.295	1.000	0.01	0.05
DHQ	34.842	4.6958	0.997	0.05	0.2
QCT	131.48	23.341	1.000	0.05	0.2

The accuracy of the method was determined by a recovery test, in which placebo solutions were spiked with a known amount of MX, DHQ and QCT standard solutions at three levels (0.5, 25 and 50 µg/mL). The % average recovery for MX, DHQ and QCT at each concentration level ranged from 98.1 % to 101.5 %

with % relative standard deviation (% RSD) ranged from 0.6 % to 2.7 % (Table 8). Method precision and intermediate method precision were determined by assaying six replicate preparations of flavosomal formulations on two different days. The %RSD for these preparation on each day were found to be less than 3.0% for all three compounds (Table 8), indicating the method is precise and reproducible. These results were deemed satisfactory for the purpose of this study.

Table 8. Summary Table for Accuracy and Method Precision

Compound Name	Accuracy (% Average Recovery \pm % RSD) (n=3)			Method Precision (%RSD) (n=6)	Intermediate Method Precision (%RSD) (n=6)
	0.5 μ g/mL	25 μ g/mL	50 μ g/mL		
MX	99.1 \pm 1.6	99.5 \pm 1.1	99.9 \pm 0.6	2.8	2.9
DHQ	100.9 \pm 2.7	101.5 \pm 0.6	100.8 \pm 1.4	2.3	2.8
QCT	98.1 \pm 1.8	98.8 \pm 1.0	99.0 \pm 1.6	2.8	2.7

Additionally, system suitability was evaluated by the determination of five replicate injections of the standard solutions. The % RSDs of these injections were found to be NMT 2.0% for all three compounds, which met the requirements set by the US Pharmacopeia <621> Chromatography. Solution stability was also determined (Table 9). The standard solution was stored at room temperature (25 °C) for 30 days and the contents of MX, DHQ and QCT were determined at 7th, 14th and 30th day. The initial assay results were normalized to

100% for comparison to be made. It was found that all these compounds were stable at room temperature for 30 days.

Table 9. Summary Table for System Suitability and Solution Stability

Compound Name	System Suitability (%RSD) (n=5)	Solution Stability (n=3)			
		Initial	7 days	14 days	30 days
MX	0.4	100.0	100.6 \pm 0.7	100.3 \pm 0.5	100.5 \pm 0.9
DHQ	0.3	100.0	100.2 \pm 0.5	99.7 \pm 0.6	99.9 \pm 0.8
QCT	0.6	100.0	99.7 \pm 0.2	99.9 \pm 0.4	99.5 \pm 0.5

2.5.3 Conclusion

The above results demonstrated that the optimized HPLC method is specific, linear, sensitive, accurate, reproducible and stable at room temperature for the simultaneous quantitation of MX, DHQ and QCT.

2.6 Ex Vivo Skin Permeation Study

2.6.1. Materials

Full thickness dermatomed (approximately 500 μ m) human cadaver skin from the posterior torso was obtained from New York Firefighters Skin Bank (New York, NY). PBS Buffer (pH 7.4) was obtained from VWR International (Radnor, PA).

2.6.2 Equipment-Franz Diffusion Cells

The Franz diffusion cell was an in vitro model that is used as a standard for measuring the permeability of compounds into and across skin or other biological

membranes. The major components of a diffusion cell included a donor chamber, a receptor chamber, a sampling port, a cell clamp, and a jacket that was connected to a water source. Figure 22 shows the schematic of the Franz diffusion cell ¹⁰⁸.

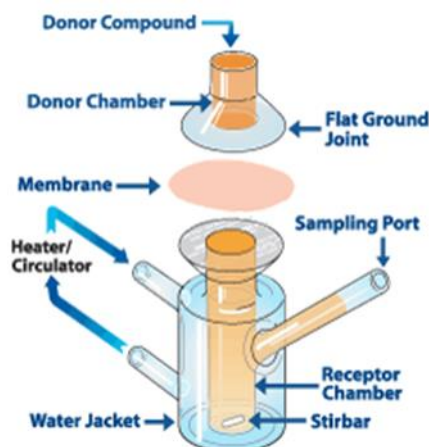


Figure 22. Schematic of Franz diffusion cell

2.6.3. Methodology

On the day of study, the frozen human cadaver skin was quickly thawed in pH 7.4 PBS at room temperature for at least 20 minutes. An appropriate size of skin was cut using a pair of scissors and carefully mounted on the receptor chamber of a vertical Franz Diffusion Cell (FDC) (Logan Instruments, Somerset, NJ, USA) filled with a known volume of pH 7.4 PBS buffer and an orifice size of 0.64 cm², the stratum corneum facing the donor chamber. The FDC was then placed into a dry block heater (Logan Instruments, Somerset, NJ) set at $37.0 \pm 0.5^{\circ}\text{C}$, and was stirred continuously with a small PTFE-coated magnetic bar at 600 rpm.

After the assembled FDC was equilibrated for at least 30 minutes, approximately 500 mg of each MX loaded liposomal gel formulations and liposome-free gel formulation was applied to the skin. At appropriate time intervals, an aliquot of the receptor medium was withdrawn, and the same volume of fresh buffer solution was replaced to the receptor chamber. The concentration of MX in the aliquot was analyzed using the HPLC method described above.

At the end of the permeation study (24 hours), removed the donor compartment, washed the skin sample with PBS buffer (pH 7.4) to remove the residual formulations and carefully dried it with cotton swab. Next, the section of skin exposed to the test formulation was cut out with scissors and the dermal and epidermal layers were separated manually with tweezers. Separated layers were cut into small pieces and collected into a bedbug prefilled tube. Then the obtained samples were homogenized with 50% ethanol and centrifuged at 10000 rpm for 5 min. The supernatant was filtered and collected into an HPLC vial using 0.45 μm syringe filters. Collected samples were analyzed using the HPLC method described above.

2.7 Publication Information

Section 2.5 was adapted from our manuscript entitled Flavosomes, novel deformable liposomes for the co-delivery of anti-inflammatory compounds to skin published in *International Journal of Pharmaceutics* (Zhang ZJ, Michniak-Kohn B.

Flavosomes, novel deformable liposomes for the co-delivery of anti-inflammatory compounds to skin. *Int J Pharm.* 2020; 585:119500) and has been reproduced here.

Chapter 3. Development of Meloxicam Loaded Liposomes and Comparative Study of Liposomal vs Microemulsion Formulations

3.1 Introduction

Meloxicam is a non-steroidal anti-inflammatory drug (NSAID) structurally related to the enolic acid class of 4-hydroxy-1,2-benzothiazine carboxamides. It was first approved as a 7.5 mg tablet (Mobic; Boehringer Ingelheim) by the United States Food and Drug Administration (US FDA) in 2000 and was later approved and marketed in capsule and suspension forms. These dosage forms are used clinically to treat acute and chronic pain and inflammation, as well as relieve swelling, stiffness and pain associated with arthritis. Additionally, meloxicam has been studied as a potential drug for Alzheimer's disease and as a viable adjuvant therapeutic agent to treat different cancers, such as lung, colorectal, prostate and urinary bladder cancers^{6-9,109}. However, adverse effects, such as gastro-intestinal toxicity/bleeding, headaches, rash, increased risk of cardiovascular events, etc., are frequently reported when this drug is administered at high doses and with long-term treatment¹¹.

Topical administration provides a number of advantages over oral NSAIDs: the ability to deliver the drug substance more selectively to a specific site for both local and systemic effects, to avoid first pass effect, to reduce gastro-intestinal side effects and to improve patient compliance. As per European League Against Rheumatism (EULAR) and National Institute for Health and Care Excellence (NICE) guidelines¹²,

topical administrations of NSAIDs is recommended for the management of mild to moderate osteoarthritis pain before the oral route.

However, the barrier function of the skin impairs the penetration and absorption of drugs. Therefore, many formulation strategies, such as liposomes, nanoparticles, microemulsions, etc., have been assessed to overcome the barrier function of the *stratum corneum* (SC) and to improve drug transport into the skin.

Liposomes are spherical vesicles consisting of one or more phospholipid bilayers. Over the past 20 years, many studies have been conducted on liposomal delivery systems due to their biocompatibility, biodegradability, low toxicity and capability to encapsulate both hydrophilic and lipophilic drugs. However, the conventional liposome does not deeply penetrate skin but rather remains in the upper layer of the *stratum corneum*⁷⁹ due to its rigid structure and size⁷¹.

Transfersomes[®] belong to a class of highly elastic or deformable vesicles, which were first introduced by Cevc and Blume⁷³. These are liquid-state vesicles that consist of phospholipids and an edge activator, which is often a single chain surfactant, e.g., sodium cholate, sorbitan esters (Span[®] 60/65/80) and polysorbates (Tween[®] 20/60/80), that destabilizes the lipid bilayers of the vesicles and increases their deformability by lowering the interfacial tension⁷⁵. This feature enables the Transfersomes[®] to squeeze themselves through intercellular regions of the *stratum corneum* under the influence of the transdermal water gradient. They have been reported to penetrate intact skin *in vivo* with an efficiency similar to that of

subcutaneous administration, provided that the elastic vesicles are topically applied in non-occlusive conditions^{76,77}.

Microemulsions are thermodynamically stable liquid dispersions composed of polar and non-polar phases stabilized by one or more surfactants. One of the most important microemulsion features is an extremely low interfacial tension between the phases of different polarity. This is usually achieved with the use of a co-surfactant, an additional component revealing low molecular weight and good miscibility with both phases¹¹⁰. Another important property of microemulsions is small diameter of dispersed phase particles. It is noteworthy that numerous studies regarding topical and transdermal delivery of drugs incorporated in microemulsions indicate their significant potential as carriers that enhance absorption of the active ingredient¹¹¹⁻¹¹⁶. Despite the fact that these systems have been known and investigated for more than 70 years¹¹⁷, the exact mechanism explaining this phenomenon has not been elucidated. It has been hypothesized that several different factors might contribute to the increased topical absorption of the drug. One of them is the presence of surfactants and co-surfactants also acting as permeation enhancers and temporarily disrupting the organization of lipids in the *stratum corneum*. Another important feature of microemulsions is the small droplet diameter which may contribute to better penetration of the dispersed phase into the deeper skin layers. Moreover, in the case of oil in water (o/w) microemulsions, the oil phase might act as a drug reservoir, maintaining a high concentration gradient between the formulation and the skin¹¹⁸.

In this study, we present both liposomal and microemulsion formulations investigated as potential carriers for the dermal delivery of meloxicam. In order to analyze the impact of structural features on the potential therapeutic efficacy, two different types of vesicles and two different microemulsion types were prepared and tested. Both liposomes and microemulsions were subjected to structural studies and applied to *ex vivo* skin in Franz diffusion cell studies.

3.2 Materials

Soybean lecithin (SL) was purchased from Acros Organics (Morris Plains, NJ). Unsaturated Soybean Phosphatidylcholine (USPC) and Saturated Soybean Phosphatidylcholine (SSPC) were generously donated by LIPOID LLC (Newark, NJ, USA). Cholesterol (Chol) was purchased from Alfa Aesar (Haverhill, MA, USA). Cetylpyridinium chloride (CPC) was purchased from Sigma-Aldrich (St. Louis, MO, USA). Meloxicam (MX) was supplied from Acros Organics (Morris Plains, NJ, USA). Tween[®] 85, triacetin, oleic acid, ethanol and isopropanol were purchased from Sigma-Aldrich. Transcutol[®] P was kindly donated by Gattefosse (Paramus, NJ, USA). All other chemicals used were of reagent grade and purchased from VWR International (Radnor, PA, USA).

3.3 Methodology

3.3.1. Preparation of Liposomes

Meloxicam (MX)-loaded liposomes were prepared by the thin film hydration method followed by sonication¹¹⁹. Briefly, lipid mixtures of phosphatidylcholine (PC), cholesterol (Chol), MX and/or cetylpyridinium chloride (CPC), were

dissolved in chloroform. The solvent was then evaporated under a nitrogen gas stream. The lipid film was placed in a desiccator for at least 12 h to remove any remaining solvent. The dried lipid film was hydrated with sodium acetate buffer solution (pH 5.5). Vesicles were subsequently sonicated in a sonicator bath (Tru-sweep Crest Bath Ultrasonicator, Cortland, NY, USA) for one hour followed by two cycles of 12 min probe sonication (SFX Branson Ultrasonic Processor, Emerson Industrial Automation, St. Louis, MO, USA) at continuous mode with 2-min intervals between the cycles in an ice-water bath. Liposome suspension was then centrifuged at 3000 g for 30 min. The prepared vesicle formulations (supernatant) were stored in airtight containers at 4 °C prior to use.

3.3.2. HPLC Method of the Quantification of MX

MX was quantified using high-pressure liquid chromatography (HPLC) with UV detection. The HPLC system included an Agilent 1100 Series liquid chromatograph (Agilent Technologies, Santa Clara, CA, USA) and the Agilent Chemstation software (OpenLab CDS, ChemStation Edition, Rev. C.01.10, Agilent Technologies). A reversed-phase C18 column (YMC Triart C18 ExRS plus, 5 μ m, 4.6 \times 150 mm, YMC America Inc., Allentown, PA, USA) was used as the stationary phase. The column temperature was maintained at 30.0 \pm 0.2 °C. The mobile phase composed of 1% phosphoric acid (A) and acetonitrile (B) at a flow rate of 1.0 mL/min. The gradient program is: 0 min, 35% B; 5.5 min, 75% B; 7.2 min, 35% B. The UV detector was set at a wavelength of 360 nm for MX. The retention time for MX was about 8.5 min. The method was linear at a concentration

range of 0.05–50 µg/mL with R^2 of 0.9995 for meloxicam. The limit of detection (LOD) was found to be 0.05 µg/mL and the limit of quantification (LOQ) was 0.22 µg/mL. The relative standard deviation for both intra-day and inter-day precision was less than 2%.

3.3.3. Measurement of Vesicle Size, Size Distribution, Zeta Potential and Morphology for Liposomes

Average vesicle size and size distribution (Polydispersity Index, PDI) of the liposome formulations were measured by Dynamic Light Scattering (DLS) (Zetasizer Nano-S, Malvern Panalytical, Westborough, MA, USA). Zeta potential was measured by Electrophoretic Light Scattering (ELS) (Zetasizer Nano series, Malvern Panalytical, Westborough, MA, USA). All formulation samples without further treatment were analyzed at room temperature.

The morphology of liposomes was characterized by transmission electron microscopy (TEM) (CM 12 TEM, Philips, Amsterdam, Netherlands). One drop of liposomal vesicle preparation was placed onto a copper grid, and the excess suspension was immediately adsorbed using filter paper. The sample was then stained by adding a drop of 2% phosphotungstic acid. The excess solution was immediately removed by filter paper, and then the sample was dried at room temperature. Afterward, the grid was observed using a TEM with AMT Image Capture Engine V602 (Advance, Microscopy Techniques Corp, Woburn, MA, USA).

3.3.4. Determination of MX Entrapment Efficiency

The concentration of MX in the vesicle formulation was determined by HPLC analysis after disruption of the vesicles with 50% v/v ethanol in water. The extracted solution was sonicated for 10 min in a sonicator bath (Tru-sweep Crest Bath Ultrasonicator, Cortland, NY, USA). The resulting solution was then filtered with a 0.45 µm nylon syringe filter (Midland Scientific, Omaha, NE, USA). The entrapment efficiency and drug loading of MX loaded in the liposomes were calculated according to Equations (1) and (2)¹²⁰, respectively.

$$\% \text{ entrapment efficiency} = (C_M/C_i) \times 100 \quad (1)$$

$$\% \text{ drug loading} = (C_M/C_L) \times 100 \quad (2)$$

where C_M is the concentration of MX loaded in the liposome, as described in the above methods, C_i is the initial concentration of MX added into the vesicle formulation and C_L is the concentration of phosphate lipid added into the vesicle formulation.

3.3.5. Preparation of Drug-Loaded Microemulsions

The composition of the microemulsions (ME) used in skin permeation experiments is presented in Table 10. In the first step, triacetin was mixed with surfactant and co-surfactant and subsequently MX (0.08% w/w) was dissolved in the resulting mixture. Next, water was added, and the sample was gently mixed and inspected visually for clarity.

Table 10. The composition of microemulsions used for Meloxicam (MX) incorporation

Component (%, w/w)	Sample	
	ME*-1	ME-2
Triacetin	19.0	11.0
Tween 85	38.0	22.0
Isopropyl alcohol	38.0	22.0
Water	5.0	45.0

*: Microemulsion

3.3.6. Pseudoternary Phase Diagrams

Pseudoternary phase diagrams were obtained with a water titration procedure¹²¹. The composition of the investigated systems is presented in Table 11. In the first step, the mixture of surfactant and co-surfactant (Smix) at a 1:1 ratio (w/w) was prepared. Next, the systems containing oil and Smix at 1:9, 2:8, 3:7, 4:6, 5:5, 6:4, 7:3, 8:2 and 9:1 ratio (w/w) were obtained. The water phase was added to each sample dropwise, with gentle stirring during the titration process, until transparency loss was observed. Moreover, the viscosity of the system was visually inspected during the experiment. The transparent systems revealing low viscosity were classified as microemulsions. All experiments were performed at 25.0 ± 0.5 °C.

Table 11. Composition of the samples investigated in phase studies.

No	Oil Phase	S _{mix}		Water Phase
		Surfactant	Co-Surfactant	
1A			Ethanol	
1B	Triacetin		Isopropanol	
1C		Tween [®] 85	Transcutol [®] P	Water
2A			Ethanol	
2B	Oleic acid		Isopropanol	
2C			Transcutol [®] P	

3.3.7. Electrical Conductivity Studies

Electrical conductivity tests were performed with Thermo Orion model 105A+ (Thermo Fisher Scientific, Waltham, MA, USA) for the formulation 1B (Table 11). The device was calibrated with 12896, 1413 and 100 $\mu\text{S cm}^{-1}$ standard solutions. The conductivity studies were performed along the dilution lines L1, L2, L3 and L4 (Figure 23) corresponding to the initial mixture containing oil and S_{mix} at 1:9, 2:8, 3:7 and 4:6 ratios (w/w), respectively. Each sample was gradually diluted with 0.05% solution of sodium chloride and after the addition of each aliquot, the sample was gently mixed. All measurements were performed in triplicate at ambient temperature.

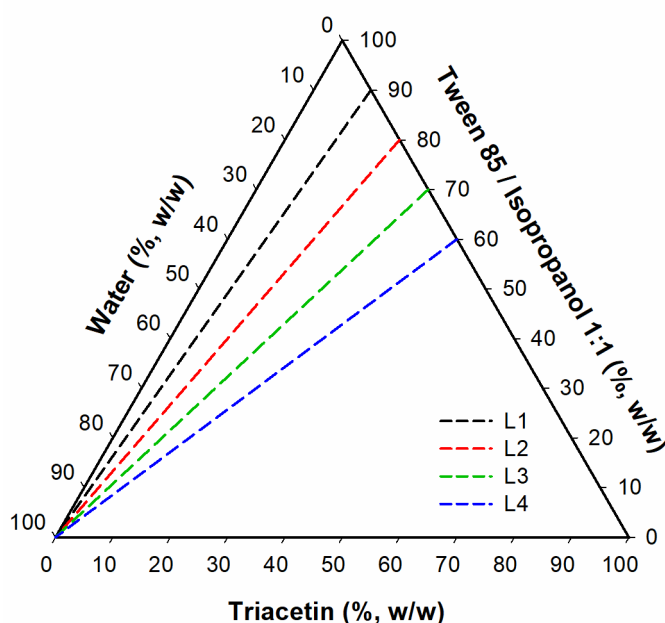


Figure 23. Dilution lines followed in conductivity studies. Lines L1, L2, L3 and L4 correspond to O:S_{mix} ratios 1:9, 2:8, 3:7 and 4:6 (w/w), respectively.

3.3.8. Viscosity Studies

The viscosity of microemulsion was monitored along the dilution lines depicted in Figure 23. The measurements were performed with Kinexus Ultra+ rotational rheometer (Malvern, UK) equipped with coaxial cylinders geometry (diameter: 25 mm, measurement gap: 4.2 mm). Each sample was analyzed in triplicate at 25.0 ± 0.2 °C. The shear rate was increasing linearly from 0 to 100 s^{-1} over 120 s.

3.3.9. Measurement of Particle Size and Size Distribution for Microemulsions

The particle size analysis was performed for selected microemulsions with Zetasizer Nano S equipped with a 632.8 nm He-Ne laser light source (4 mW).

The measurements were done at 25.0 °C using non-invasive backscatter mode (NIBS) at an angle of 173°. Each sample was equilibrated prior the experiment for 180 s.

3.3.10. *Ex Vivo* Skin Permeation Study

3.3.10.1 Materials

Full thickness dermatomed (approximately 500 µm) human cadaver skin from the posterior torso was obtained from New York Firefighters Skin Bank (New York, NY). PBS Buffer (pH 7.4) was obtained from VWR International (Radnor, PA).

3.3.10.2 Equipment-Franz Diffusion Cells

The Franz diffusion cell was an in vitro model that is used as a standard for measuring the permeability of compounds into and across skin or other biological membranes. The major components of a diffusion cell included a donor chamber, a receptor chamber, a sampling port, a cell clamp, and a jacket that was connected to a water source.

3.3.10.2 Methodology

On the day of study, the frozen human cadaver skin was quickly thawed in pH 7.4 PBS at room temperature for 20 minutes. An appropriate size of skin was cut using a pair of scissors and carefully mounted on the receptor chamber of a vertical Franz Diffusion Cell (FDC) (Logan Instruments, Somerset, NJ, USA) filled with a known volume of pH 7.4 PBS buffer and

an orifice size of 0.64 cm², the stratum corneum facing the donor chamber. The FDC was then placed into a dry block heater (Logan Instruments, Somerset, NJ) set at $37.0 \pm 0.5^{\circ}\text{C}$, and was stirred continuously with a small PTFE-coated magnetic bar at 600 rpm.

After the assembled FDC was equilibrated for at least 30 minutes, approximately 500 mg of each MX loaded liposomal gel formulations and liposome-free gel formulation was applied to the skin. At appropriate time intervals, an aliquot of the receptor medium was withdrawn, and the same volume of fresh buffer solution was replaced to the receptor chamber. The concentration of MX in the aliquot was analyzed using the HPLC method described above.

At the end of the permeation study (24 hours), removed the donor compartment, washed the skin sample with PBS buffer (pH 7.4) to remove the residual formulations and carefully dried it with cotton swab. Next, the section of skin exposed to the test formulation was cut out with scissors and the dermal and epidermal layers were separated manually with tweezers. Separated layers were cut into small pieces and collected into a bedbug prefilled tube. Then the obtained samples were homogenized with 50% ethanol and centrifuged at 10000 rpm for 5 min. The supernatant was filtered and collected into an HPLC vial using 0.45 μm syringe filters. Collected samples were analyzed using the HPLC method described above.

The cumulative amount of MX permeated per unit area was calculated according to Equation 3 ¹²²:

$$Q_n = \frac{C_n V_r + \sum_{i=0}^{n-1} C_i V_s}{A} \quad (3)$$

where Q_n is the cumulative amount of the drug permeated per unit area ($\mu\text{g}/\text{cm}^2$) at different sampling times, C_n is the drug concentration in the receiving medium at different sampling times ($\mu\text{g}/\text{mL}$), C_i is the drug concentration in the receiving medium at the i th ($n-1$) sampling time ($\mu\text{g}/\text{mL}$), V_r is the volume of the receptor solution (mL), V_s is the volume of the sample withdrawn (mL), and A is the effective permeation area of the diffusion cell (cm^2). The Q_n values were plotted against time, and then the steady-state flux (J_{ss}) was calculated from the slope of the linear portion of the plot.

The permeability coefficient (K_p) was calculated with Equation 4 ¹²²:

$$K_p = \frac{J_{ss}}{C_d} \quad (4)$$

where:

J_{ss} —steady state flux ($\mu\text{g cm}^{-2} \text{h}^{-1}$), and

C_d —concentration of MX in the donor compartment ($\mu\text{g mL}^{-1}$).

3.3.11. Statistical Analysis

The data were reported as means \pm S.D. ($n = 3$). The obtained results were analyzed with one-way analysis of variance (ANOVA) followed with post-hoc

Tukey test. Statistical significance in the differences of the means was determined by Student's t-test. The statistical significance level in all tests was set at 5%. All calculations were performed with JMP[®] Pro 14.2.0 (SAS Institute Inc., Cary, NC, USA).

3.4 Results and Discussion

3.4.1. Liposomes

3.4.1.1. Selection of Phosphatidylcholine

As demonstrated in many published studies, liposome properties are considerably affected by the lipid type/composition, surface charge, size and the method of preparation. Furthermore, the choice of bilayer components determines the ‘rigidity’ or ‘fluidity’ and the charge of the vesicles. For instance, unsaturated phosphatidylcholine from natural sources (egg or soybean) yields much more permeable and less stable bilayers, while the saturated phospholipid with long acyl chains (for example, dipalmitoylphosphatidylcholine) forms rigid, rather impermeable vesicles^{119,123-125}.

The initial formulations were based on the MX-loaded mentosomes developed by Duangjit et al.¹²⁰. The compositions of each formulation are listed in Table 12. The preparation procedure was as described in Section 3.3.1, but with only one cycle of 6 minutes probe sonication at continuous mode.

Table 12. The composition and type of the vesicles investigated in the study.

Formulation ID	Description	Wt (mg)/100 mL			
		PC ¹	MX ² (0.08%)	Chol ³ (0.04%)	CPC ⁴ (0.10%)
F1	Conventional Liposome	400/800/1200	80	-	-
F2	Conventional Liposome	400/800/1200	80	40	-
F3	Transfersome	400/800/1200	80	40	100

¹Phosphatidylcholine, ²Meloxicam, ³Cholesterol, ⁴Cetylpyridinium chloride

In this study, the type and grade of PC were evaluated. Specifically, soybean lecithin (SL), unsaturated phosphatidylcholine (USPC) and saturated soybean phosphatidylcholine (SSPC) were used for the preparation of liposome formulations at the concentration levels of 0.4, 0.8 and 1.2%.

As Figure 25 demonstrates, compared to soybean lecithin, the entrapment efficiency improved dramatically with USPC and SSPC, in which USPC yielded the best results. The entrapment efficiency of transfersomes was significantly higher than that of the conventional liposomes. These results might be attributed to the intrinsic properties of the cationic surfactant as a solubilizer and the interactions among the surfactant, MX and lipid bilayer. The encapsulation rates increased with increased concentration of lipids, however, the drug loading decreased from 0.8% to 1.2%, as demonstrated in Figure 26. The physical characteristics of the investigated formulations are described in Table 13.

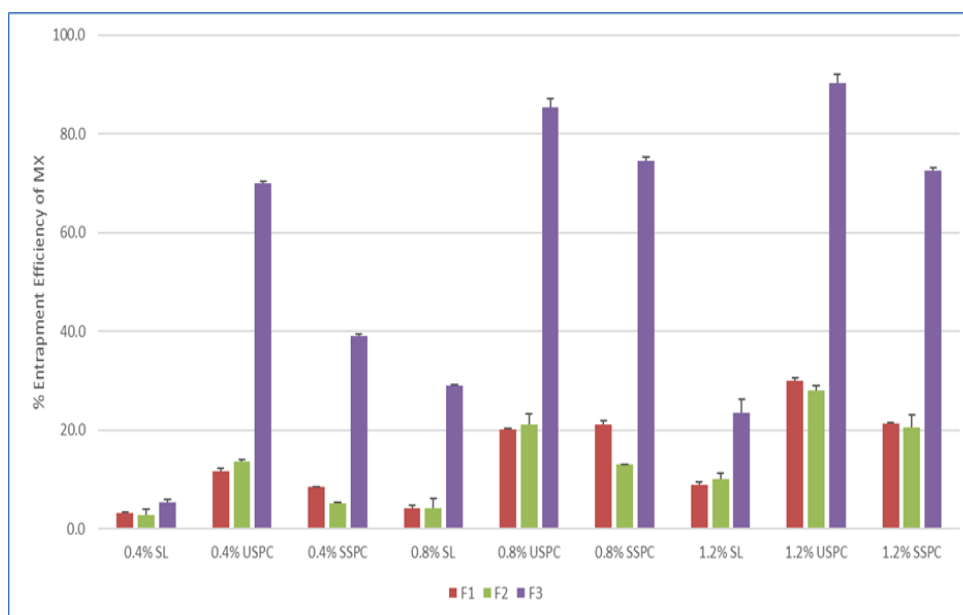


Figure 24. Effect of different grade of phospholipids (PL) on entrapment efficiency of meloxicam (MX). SL: soybean lecithin, USPC: unsaturated soybean phosphatidylcholine, SSPC: saturated soybean phosphatidylcholine. Bars are means \pm standard deviation (SD), $n = 3$.

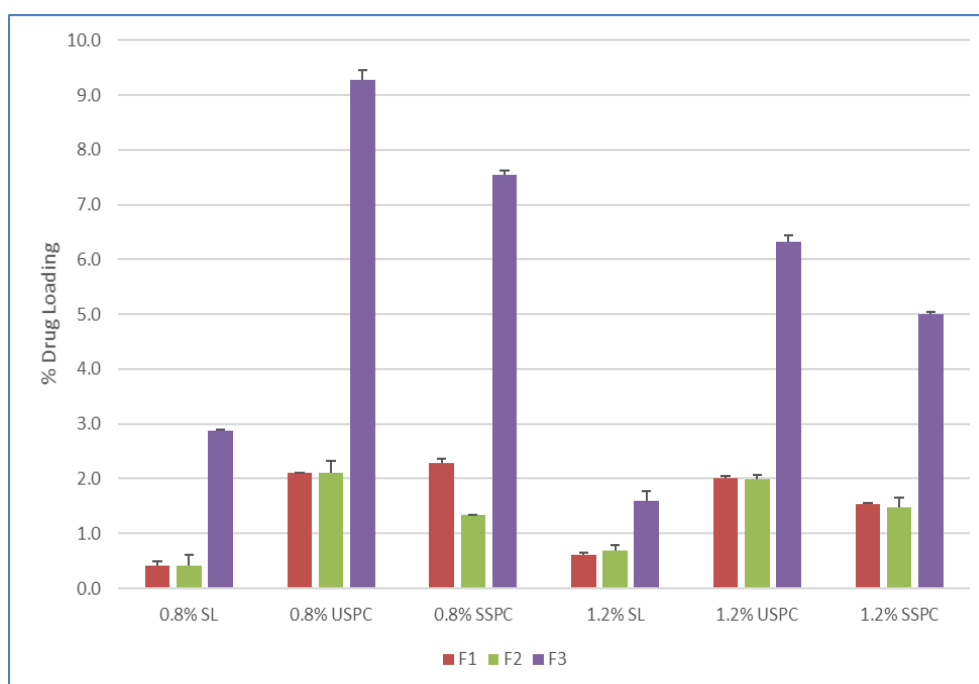


Figure 25. Effect of different grade of phospholipids (PL) on drug loading of meloxicam (MX). SL: soybean lecithin, USPC: unsaturated soybean phosphatidylcholine, SSPC: saturated soybean phosphatidylcholine. Bars are means \pm SD, $n = 3$.

Table 13. Physicochemical properties of the obtained vesicles ($n = 3$)

SL ^a		0.4%			0.8%			1.2%	
ID	Ave Diameter (nm)	PDI	Zeta Potential (mV)	Ave Diameter (nm)	PDI	Zeta Potential (mV)	Ave Diameter (nm)	PDI	Zeta Potential (mV)
F1	113.4 ± 2.0	0.173 ± 0.010	-11.6 ± 0.3	119.6 ± 2.6	0.185 ± 0.011	-25.7 ± 0.5	133.7 ± 0.2	0.191 ± 0.013	-23.4 ± 1.3
F2	130.5 ± 1.8	0.212 ± 0.010	-26.5 ± 0.8	125.7 ± 2.5	0.178 ± 0.019	-23.0 ± 0.5	133.9 ± 2.0	0.192 ± 0.019	-23.7 ± 0.5
F3	128.0 ± 2.8	0.219 ± 0.014	6.7 ± 0.5	155.4 ± 11.2	0.215 ± 0.027	-10.7 ± 0.6	172.1 ± 1.8	0.150 ± 0.014	-9.6 ± 0.4
USPC ^b		0.4%			0.8%			1.2%	
ID	Ave Diameter (nm)	PDI	Zeta Potential (mV)	Ave Diameter (nm)	PDI	Zeta Potential (mV)	Ave Diameter (nm)	PDI	Zeta Potential (mV)
F1	125.0 ± 3.0	0.226 ± 0.020	0.2 ± 0.5	126.2 ± 0.9	0.259 ± 0.024	0.0 ± 1.5	120.5 ± 0.4	0.186 ± 0.006	-1.3 ± 1.7
F2	114.2 ± 3.9	0.256 ± 0.008	-0.1 ± 0.8	125.7 ± 4.9	0.274 ± 0.052	-0.2 ± 0.6	121.7 ± 0.9	0.205 ± 0.017	-0.3 ± 0.3
F3	103.0 ± 0.3	0.254 ± 0.009	27.1 ± 0.8	136.7 ± 5.7	0.185 ± 0.019	20.0 ± 0.6	174.0 ± 3.1	0.408 ± 0.021	16.9 ± 0.1
SSPC ^c		0.4%			0.8%			1.2%	
ID	Ave Diameter (nm)	PDI	Zeta Potential (mV)	Ave Diameter (nm)	PDI	Zeta Potential (mV)	Ave Diameter (nm)	PDI	Zeta Potential (mV)
F1	2347 ± 325.9	0.859 ± 0.126	1.1 ± 0.3	445.5 ± 3.6	1.000 ± 0.000	0.7 ± 0.3	270.4 ± 20.7	0.947 ± 0.091	1.0 ± 0.3
F2	168.5 ± 4.4	0.308 ± 0.021	2.7 ± 0.8	190.1 ± 1.4	0.430 ± 0.026	3.4 ± 1.2	160.6 ± 5.2	0.510 ± 0.023	1.1 ± 0.3
F3	445.1 ± 11.7	0.318 ± 0.041	40.7 ± 1.9	199.0 ± 0.6	0.351 ± 0.062	34.3 ± 1.5	178.8 ± 3.6	0.405 ± 0.017	27.8 ± 0.5

a: soybean lecithin, b: unsaturated soybean phosphatidylcholine, c: saturated soybean phosphatidylcholine, d: Polydispersity Index (PDI).

As suggested in Table 13, the incorporation of different components in the liposome systems affected the size, zeta potential and size distribution of the vesicle formulation. Generally, liposomes prepared using USPC had smaller particle sizes than those prepared using SSPC but similar size with those prepared with SL. For example, at 0.8% concentration level, the particle sizes of F2 (conventional liposome with cholesterol) were found to be 125.7 ± 2.5 nm using SL, 125.7 ± 4.9 nm using USPC and 190.1 ± 1.4 nm using SSPC, respectively. A similar finding was observed for F3 (transfersome) at the same concentration level, the particle sizes for the vesicles prepared using SL, USPC and SSPC were 155.4 ± 11.2 , 136.7 ± 5.7 and 199.0 ± 0.6 nm, respectively. The impact of the liposomes' composition on the size was assessed because vesicular size has the ability to influence the penetration of drugs through the skin to the deeper layers. The size of the investigated vesicular systems using SL and USPC at all three concentration levels were less than 200 nm, which means that these investigated systems have the potential to deliver MX through the skin, as suggested by the study conducted by Verma et al ⁹⁷.

Polydispersity Index (PDI) had been measured to determine the degree of size distribution uniformity of these vesicle systems. In drug delivery applications using lipid-based carriers, such as liposomal formulations, a PDI of 0.3 and below is considered to be acceptable and indicates a homogenous population of phospholipid vesicles^{98,99}. As elucidated in Table 13, the PDI of liposomal formulations prepared using SL and USPC was less than 0.3, with the only exception of F3 prepared using 1.2% USPC. However, the PDI of the vesicles prepared using SSPC were generally greater than 0.3, indicating that these nanoparticles are heterogeneously sized.

Zeta potential was used to study these vesicles' surface charge, which was affected by the total net charge of the vesicle components and pH of the hydration buffer. The isoelectric point (pI) of MX is 2.6¹²⁰, which is lower than the pH of hydration buffer (pH 5.5). Therefore, MX is in the negatively charged form. Cholesterol is a neutral material, while CPC, a cationic surfactant, is positively charged. Since PC is the major component in the formulation, it plays the key role in determining the vesicles' surface charge. As displayed in Table 13, SL is negatively charged, so zeta potentials of F1 and F2 were found to be negative, while F3 had positive zeta potential with lower level of PC but became negatively charged when the concentration of PL increased. USPC and SSPC are neutral materials, so the zeta potentials of F1 and F2 prepared using these two PC were found to be in the range of -0.1 to 3 mV. F3 prepared using these two PCs carried a positive charge due to the positively charged CPC.

Based on the obtained data, vesicles prepared using 0.8% USPC has the highest loading of MX, with particle size less than 200 nm and uniform size distribution (PDI less than 0.3). Therefore, liposomal formulations would be prepared using 0.8% USPC in the further experiments.

3.4.1.2. Development of Liposome Preparation Procedure

In this study, liposomes were prepared by the thin film hydration method followed by sonication. Sonication is perhaps the most widely used passive loading technique for the preparation of liposomes¹¹⁹. There are two sonicating techniques: probe and bath sonication. The effect of sonication techniques and time were studied with respect to entrapment efficiency and physical properties of the liposomal formulations. It was found that the highest entrapment efficiency was obtained by using both techniques. Initially, the liposome

dispersion in a scintillation vial was placed into a bath sonicator for 1 hour (Cycle 0, Table 14). Vesicles were subsequently sonicated for two cycles of 12 minutes using a sonication probe at continuous mode with 2 minutes intervals between the cycles (Cycle 1 and 2, Table 14). It was observed that prolonged sonication resulted in excessive heat in the liposomal formulations, which led to precipitation of the lipids due to the phospholipids oxidation. Therefore, the samples were kept in an ice-water bath to avoid possible oxidation. The physicochemical characteristics of F1, F2 and F3 are shown in Table 14.

The entrapment rates of MX in the vesicles were in the range of approximately 20%–80% (160–640 $\mu\text{g/mL}$). The solubility of MX in acetate buffer solution (pH 5.5) was determined to be 7 $\mu\text{g/mL}$, indicating that liposomal formulations provided substantial enhancement of MX solubility. Furthermore, the results indicated that the entrapment efficiency for transfersome incorporating CPC (84%) were much higher than that of conventional liposomes (around 20%). The intrinsic properties of the edge activator, CPC, increased the solubility of MX in vesicle bilayers. As demonstrated in Table 14, entrapment efficiency increased with increase of sonication time and plateaued at the second sonication cycle. Similar results were obtained by He et al.¹²⁶ when investigating the influence of probe-sonication on drug entrapment efficiency of ibuprofen-loaded liposomes.

Table 14. Physicochemical properties of the samples F1, F2 and F3 subjected to the sonication procedure ($n = 3$).

Formulation ID	Cycle No	%Entrapment Efficiency	Average Diameter (nm)	PDI *	Zeta Potential (mV)
F1	0	17.60 ± 0.64	126.4 ± 2.0	0.221 ± 0.013	0.78 ± 0.27
	1	20.96 ± 0.47	121.3 ± 0.9	0.243 ± 0.005	0.82 ± 0.23
	2	21.91 ± 0.52	96.1 ± 1.3	0.283 ± 0.008	0.73 ± 0.34
F2	0	19.83 ± 0.26	129.7 ± 5.3	0.235 ± 0.003	1.17 ± 0.26
	1	20.17 ± 0.40	111.4 ± 0.2	0.257 ± 0.008	1.01 ± 0.36
	2	22.13 ± 0.35	100.6 ± 1.1	0.237 ± 0.010	0.89 ± 0.54
F3	0	74.26 ± 2.83	96.72 ± 1.5	0.258 ± 0.008	20.8 ± 0.5
	1	83.57 ± 1.89	85.36 ± 0.8	0.266 ± 0.004	19.9 ± 1.2
	2	83.59 ± 0.73	73.46 ± 1.3	0.253 ± 0.007	21.4 ± 0.6

* PDI: Polydispersity Index.

As illustrated in Table 14, the vesicle sizes of different liposomal formulations were in the nano-size range of 80–130 nm with the size distribution (polydispersity index; PDI) less than 0.3, suggesting that the sonication method can prepare nano-size homogeneous vesicles. The addition of cholesterol has no impact on particle size and PDI in this study. Transfersome had smaller vesicle sizes compared to conventional liposomes, due to the incorporation of edge activator, CPC, which can achieve higher curvature, thus resulting in decrease in vesicle size compared to conventional liposomes. It is also observed that particle size decreased with increasing sonication time and cycles. This observation agreed with the sonication study conducted by Silva et al.¹²⁷, and Nam et al.¹²⁸, in which a decrease of the particle size with the increase of the sonication time until a plateau size was obtained.

The zeta potentials of these vesicles were in a positive charge range of approximately 0.7–20 mV. Transfersome had much higher positive zeta potential compared to the conventional liposomes, which might resist aggregation and therefore provide better stability. Unlike the other two

physical properties, zeta potential was not affected by the sonication time and cycles. As also indicated in the results from Section 3.4.1.1, addition of cholesterol has not much effect on the physiochemical properties of these liposomal vesicles. However, to keep the closest resemblance to the transfersome, F2 were used as conventional liposomes for ex vivo skin permeation study.

To further characterize these two vesicle systems, a TEM study was conducted and Figure 27 shows a spherical shape for both formulations.

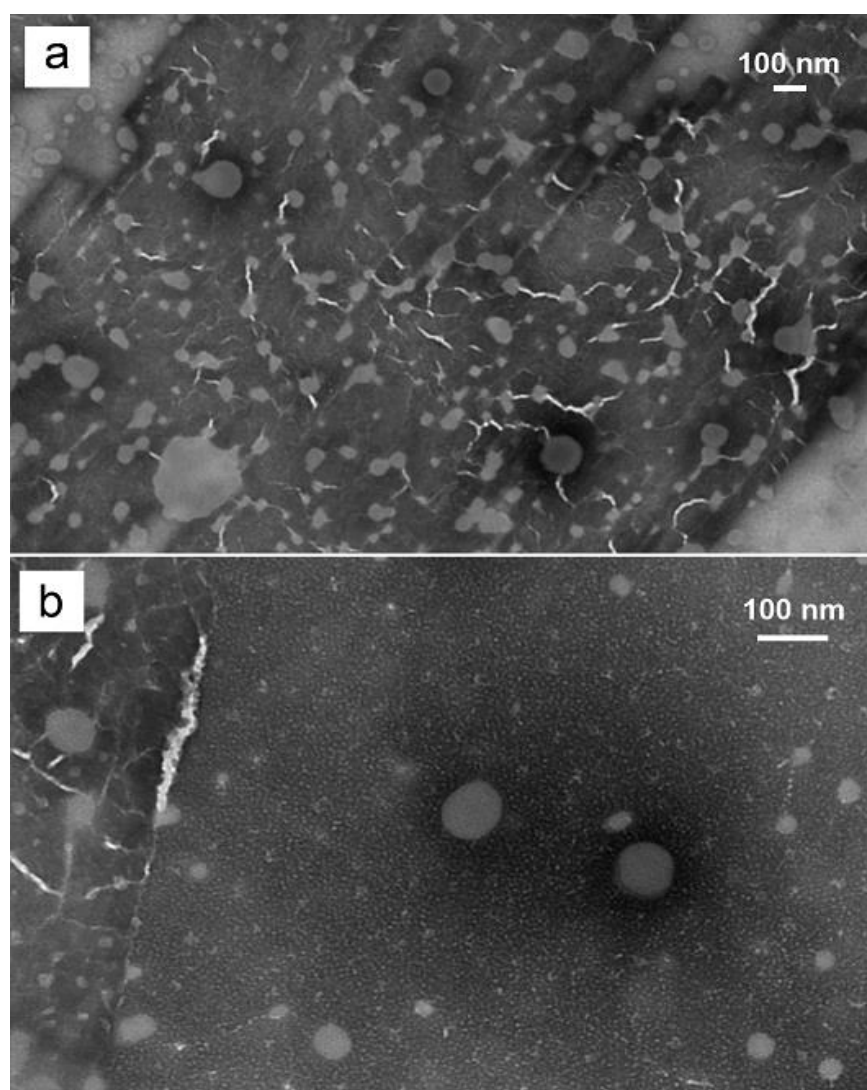


Figure 26. Transmission Electron Microscopy images of (a) F2, conventional liposome, (b) F3, transfersome.

3.4.2. Microemulsions

3.4.2.1 Pseudoternary Phase Diagrams

The surfactant applied in the preliminary phase studies was selected based on the active ingredient solubility. According to Yuan et al.¹²⁹, among different sorbitan esters, Tween[®] 85 reveals the best properties in terms of solubilizing MX. For the oil phase, relatively polar components were tested, in order to provide the best water solubilization capacity¹³⁰.

Pseudoternary phase diagrams obtained with different oil phases and co-surfactants are presented in Figure 28. Gray areas correspond to transparent, monophasic liquids of low viscosities identified as microemulsions, while white ones correspond to non-transparent coarse emulsions. The monophasic areas observed for the systems with triacetin (Figure 28, 1A–1C) were larger than the corresponding ones obtained for the systems with oleic acid (Figure 28, 2A–2C). The observed differences might be explained with different polarity of the applied oil phases. The values of log P reported for triacetin and oleic acid are -0.075^{131} and 3.50^{132} , respectively. Lower value in the case of triacetin indicates relatively higher polarity, which results in higher water solubilization capacity. Similar results were observed by Yang et al.¹³³. On the other hand, it has been hypothesized that low molecular weight oils can partially behave as co-surfactants¹³⁴,

which might also contribute to the differences observed between the systems with triacetin and oleic acid investigated in this study.

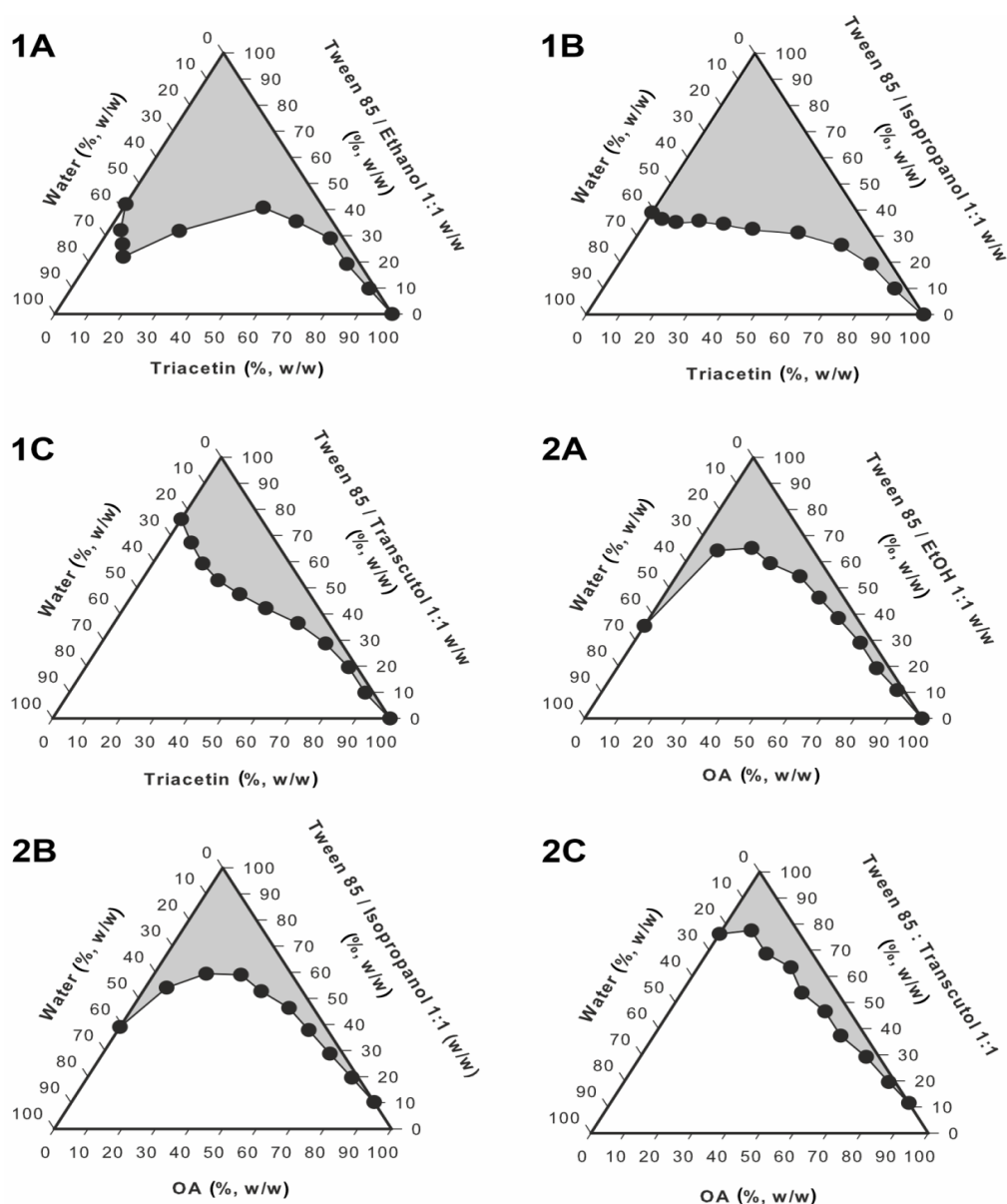


Figure 27. Pseudoternary phase diagrams obtained for the systems with triacetin (1A–1C) and oleic acid (2A–2C).

In the next step, the differences observed between the systems containing different co-surfactants were taken into consideration. In both investigated sets, a significantly smaller monophasic area was observed for the systems containing Transcutol[®] P. In the case of the systems with ethanol and

isopropanol, the results are similar. However, in the case of isopropanol, monophasic areas are slightly bigger. Therefore, for the further analyses, a system with triacetin as an oil phase and isopropyl alcohol as a co-surfactant was selected.

3.4.2.2 Conductivity Studies

Conductivity experiments were performed to assess the regions of the occurrence of particular microemulsion types. According to numerous studies¹³⁵⁻¹³⁸, the conductivity changes observed as a result of microemulsion dilution with polar phase reflect the microstructural changes related to the transitions from one microemulsion type to another. In the initial step of the study, the observed conductivity values are close to zero, which is related to the structure and properties of water in oil (w/o) microemulsion containing isolated water droplets. The external phase in such case reveals low polarity, which is reflected by low electrical conductivity. As a result of water addition, isolated droplets start to coalesce forming polar channels which results in the transition into bicontinuous type and is reflected by the significant increase of conductivity versus water content plot slope. With further water addition, the number of channels increases which contributes to the increase of conductivity values. Finally, the bicontinuous system transforms into oil in water (o/w) microemulsion with polar external phase and electrical conductivity reaches plateau. In some cases, only a single

transition point is observed and the system transforms from w/o into o/w without any discernible region corresponding to the bicontinuous system^{139,140}.

The results obtained in this study for the dilution lines L1, L2, L3 and L4 (Figure 29) indicate the presence of only one transition point corresponding to the transformation from w/o to water-continuous systems. Similar effects have been reported for other microemulsions¹⁴¹⁻¹⁴³.

The points corresponding to the transition from w/o to water-continuous microemulsions were obtained as intersections of the extrapolated approximately linear parts of the conductivity curve, as presented in Figure 29. The transition points and the areas reflecting the occurrence of particular microemulsion types are depicted in Figure 30. Based on these findings, two microemulsion compositions from both areas were selected and applied in further experiments (Figure 30).

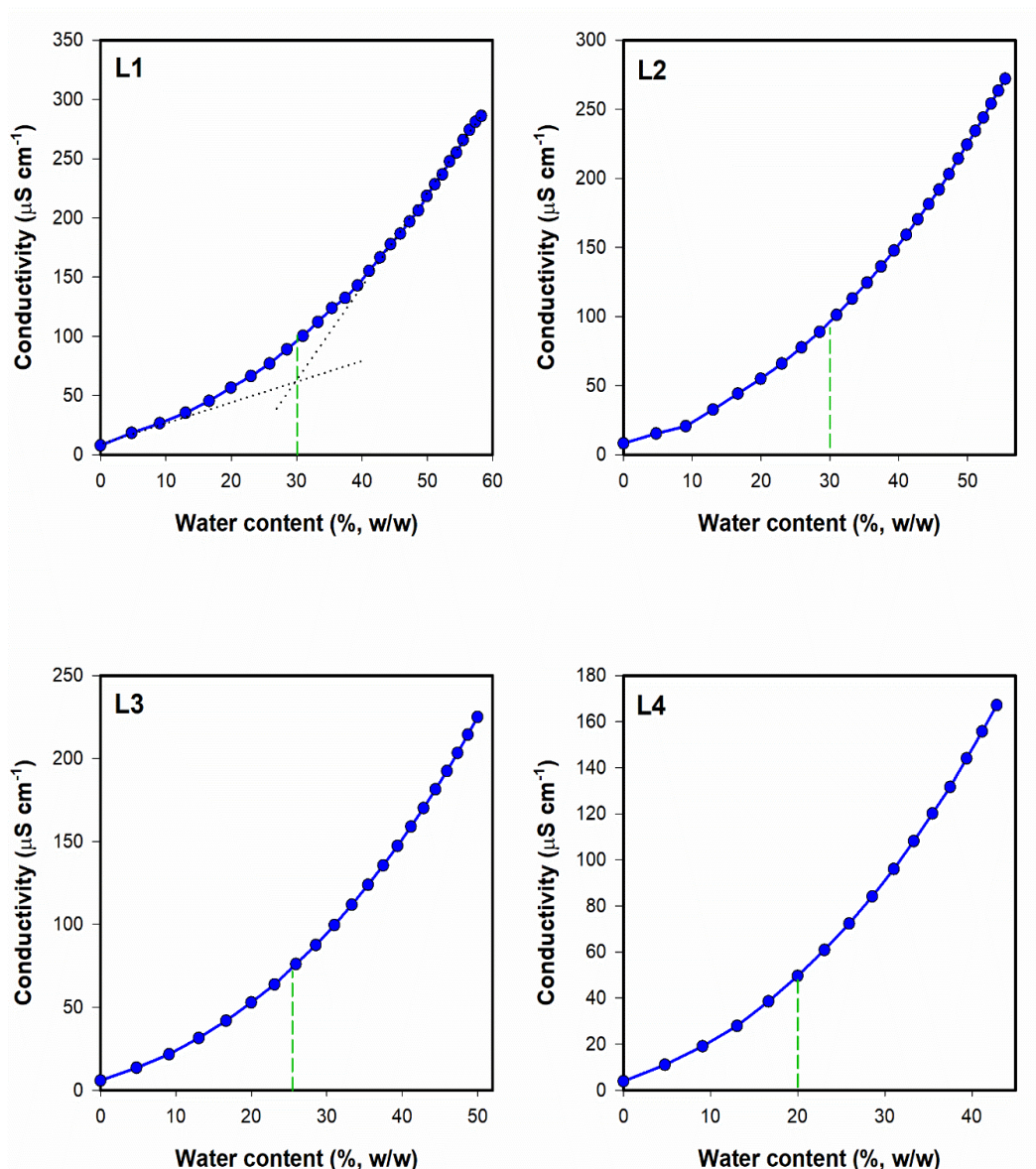


Figure 28. Conductivity plotted as a function of water content along the dilution lines L1–L4 for system 1B (Triacetin/Tween[®] 85/Isopropanol). The transition points are marked with green dashed lines. The transition point estimation procedure is depicted in L1. Error bars have been omitted for clarity, and standard deviation values did not exceed 5%.

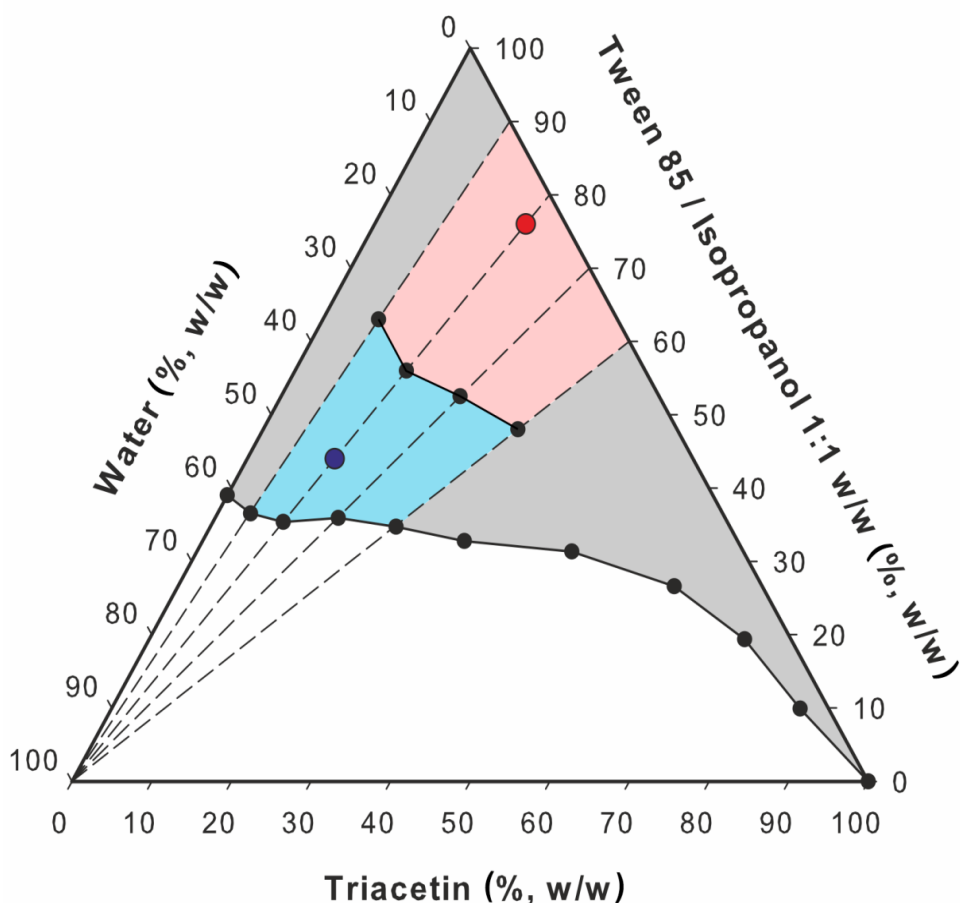


Figure 29. Pseudoternary phase diagram with w/o (red) and o/w (blue) microemulsion areas estimated based on the conductivity studies. Microemulsions selected for the further analyses are depicted as red and blue points (ME-1 and ME-2, respectively).

3.4.2.3 Viscosity Studies

In general, all investigated systems revealed Newtonian behavior, which is considered as typical for microemulsions¹⁴⁴, except for bicontinuous systems containing intertwining polar and non-polar domains forming an internal structure that might contribute to slightly shear-thinning behavior¹⁴⁵. On the other hand, high initial viscosity of the system and highly pseudoplastic properties indicate the presence of lamellar systems which are

not classified as microemulsions. It is important to notice that all analyzed systems remained liquid during the dilution and no gelation was observed. The viscosity values ranged from 10 to 28 mPa s. The plots depicting the relationship between the water content and the viscosity of microemulsions monitored along the dilution lines L1–L4 are presented in Figure 31.

Viscosity changes observed during the dilution of microemulsion can be applied for monitoring structural transitions from one microemulsion type to another¹⁴⁴. In the initial phase of the experiment, w/o microemulsion is formed. The increase of viscosity in this case is related to the increased amount of the dispersed phase droplets which interact with each other. At about 25%–30% of water, the viscosity increases slower (L1 and L2, Figure 31) or reaches plateau (L3 and L4). The observed effect might be related to the structural transition leading to the formation of continuous water phase. It is noteworthy that the approximate transition points observed in viscosity curves correspond to those recorded with electrical conductivity measurements.

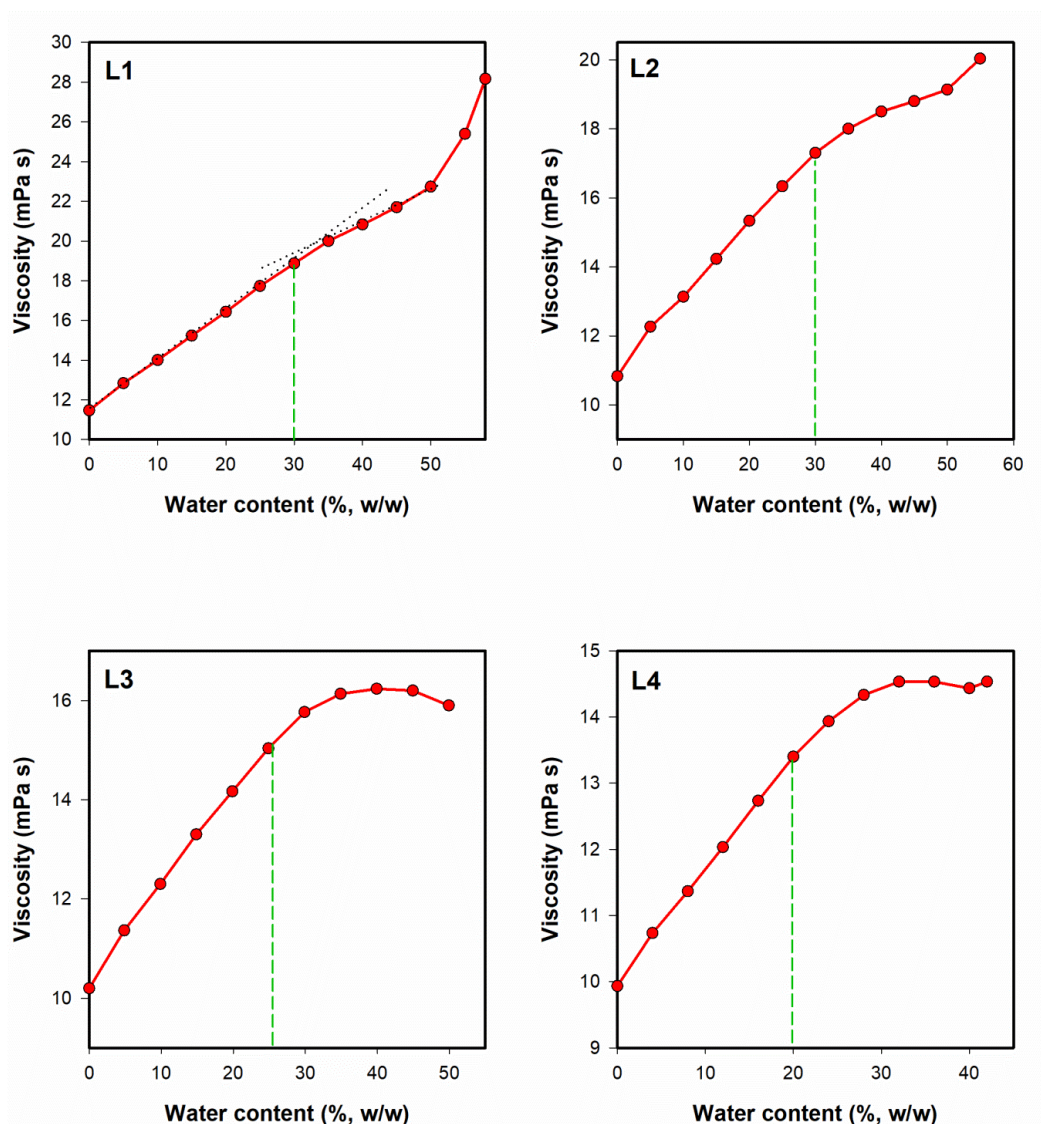


Figure 30. Dynamic viscosity plotted as a function of water content along the dilution lines L1–L4. The transition points estimated in conductivity studies are marked with green dashed lines. Error bars have been omitted for clarity, and standard deviation values did not exceed 5%.

3.4.2.4 Dynamic Light Scattering (DLS) Studies

The particle size diameter and polydispersity index (PDI) values obtained for placebo and drug-loaded microemulsions are presented in Figure 32. It is noteworthy that the droplet diameter in case of water-continuous microemulsion increased with the addition of meloxicam. The obtained result might theoretically indicate the decrease of stability of the system. However,

all microemulsions remained transparent during three months of storage. On the other hand, the increase of particle diameter might be related to the incorporation of an active ingredient in microemulsion droplets. In the case of an oil-continuous system, the drug remains in the external phase and its presence does not affect the particle size (Figure 33).

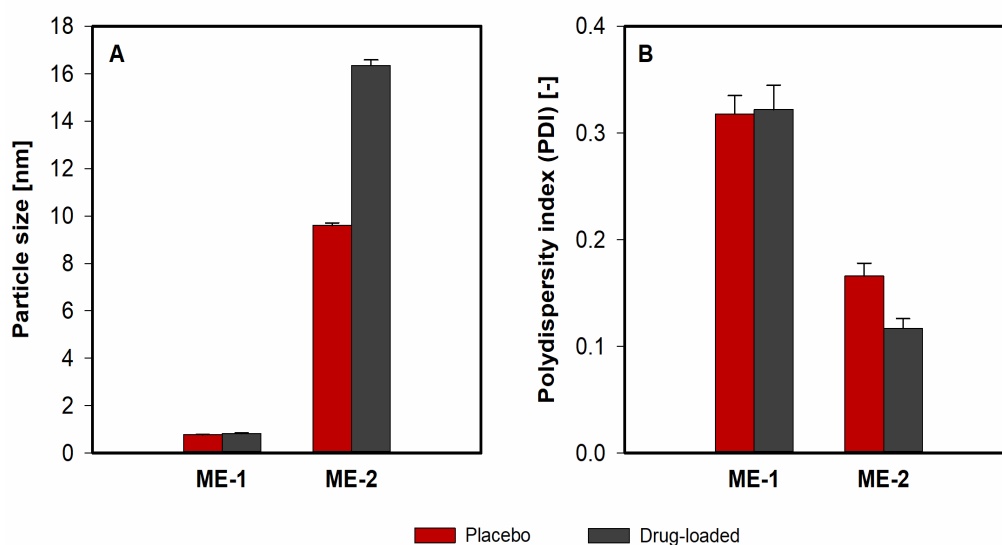


Figure 31. Particle size (A) and polydispersity index (B) obtained for placebo (red bars) and meloxicam-loaded (gray bars) w/o and o/w microemulsions.

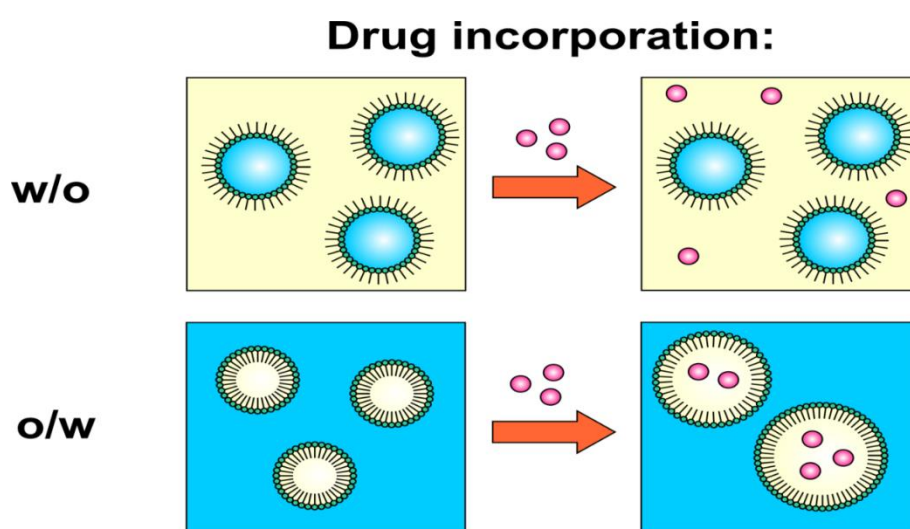


Figure 32. Hypothetical mechanism of drug incorporation in w/o and o/w microemulsions.

3.4.3. Comparative Drug Permeation Studies

Ex vivo skin permeation studies were conducted with both liposome and microemulsion formulations applied to human cadaver skin using Franz diffusion cells. The results of skin permeation experiments yielded plots of cumulative drug amount versus time and are presented in Figure 34, while the values of steady state flux (J_{ss}) and permeability coefficients (K_p) are presented in Table 15. Steady state flux values were calculated as a slope of the linear plots presented in Figure 34, while permeability coefficients were calculated with the use of Equation (4). Both parameters calculated for liposomal formulations clearly indicate that transfersomes reveal a greater ability to penetrate the skin compared to the classical non-deformable liposomes, suggesting that the deformable liposomes greatly enhanced the permeation of MX compared to the rigid vesicles. The mechanisms underlying the differences observed in this study have been described in the literature related to deformable vesicles¹⁴⁶⁻¹⁴⁸. The most important structural feature of transfersomes is the presence of surfactants acting as edge activators and destabilizing lipid bilayers. As a result, the modified vesicles are more flexible and susceptible to deformation than the conventional ones, which allows for more efficient penetration through the pores present in the skin. Another important factor in the permeation enhancement is osmotic gradient, which acts as a driving force pushing transfersomes from the relatively dehydrated skin surface into the deeper layers of skin. It is worth mentioning that the osmotic effect was reported as crucial in non-occlusive conditions¹⁴⁹ while in this study, all samples placed in Franz diffusion cells were protected from water evaporation. Therefore, it may be hypothesized that the differences observed between conventional and deformable vesicles could be even higher in a non-occlusive environment.

$$K_p = \frac{J_{ss}}{C_d} \quad (4)$$

where:

J_{ss} —steady state flux ($\mu\text{g cm}^{-2} \text{ h}^{-1}$), and

C_d —concentration of MX in the donor compartment ($\mu\text{g mL}^{-1}$).

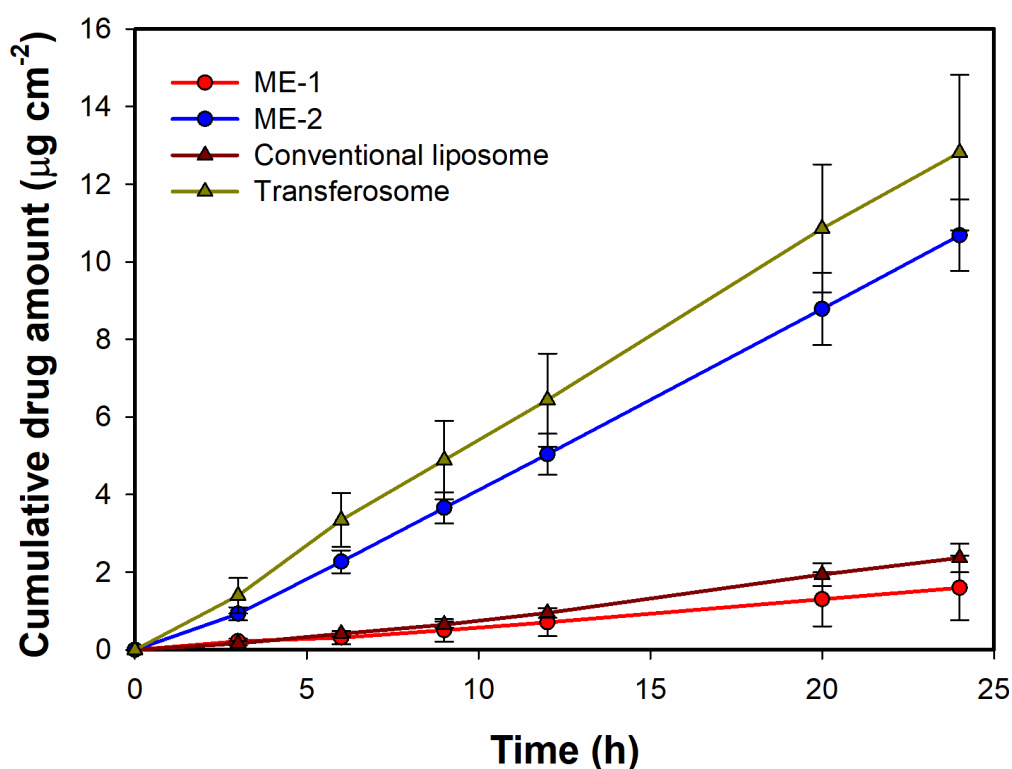


Figure 33. Ex vivo drug permeation profiles of MX across human cadaver skin obtained for different carriers. ME-1 and ME-2 are w/o and o/w microemulsions, respectively. Data are plotted as means \pm SD ($n = 3$ for each formulation).

The drug permeation results obtained for two different microemulsions investigated in this study indicate that the effectiveness of the carrier depends on the type of microemulsion or water content in the system. In the case of o/w microemulsion, the steady state flux value is significantly higher than that in the w/o system. Similar effects have been reported by Zhang and Michniak-Kohn¹⁵⁰. It

was shown that the increase of water content in the system resulted in the increased drug permeation, which was more pronounced for lipophilic drugs when compared to a hydrophilic one. However, in the case of active ingredients revealing low solubility in water, the described effect might be related to the increased thermodynamic activity of the drugs in water-rich systems.

Table 15 Steady state flux (J_{ss}) and permeation coefficients (K_p) obtained for the investigated formulations. ME-1 and ME-2 are w/o and o/w microemulsions, respectively. Data are presented as means \pm SD ($n = 3$ for each formulation).

Formulation	J_{ss} ($\mu\text{g cm}^{-2} \text{ h}^{-1}$)	Concentration ($\mu\text{g mL}^{-1}$)	K_p (cm h^{-1})
Conventional liposome	0.11 ± 0.02	177.04	$(60.75 \pm 11.94) \times 10^{-5}$
Transfersomes	0.54 ± 0.08	668.75	$(80.82 \pm 12.28) \times 10^{-5}$
ME-1	0.07 ± 0.04	735.50	$(9.59 \pm 4.84) \times 10^{-5}$
ME-2	0.46 ± 0.04	768.71	$(60.50 \pm 5.12) \times 10^{-5}$

Similar tendencies were described in the study focusing on hydrophilic caffeine¹⁵¹. The highest flux values were observed for o/w microemulsions, while the lowest ones were recorded for oil-continuous systems. However, the authors indicated lower permeation differences observed between the particular microemulsion types than in the case of less polar actives reported in the literature. The statistically significant differences obtained in this study for two structurally different microemulsion systems can also be related to the hydrophobic character of the applied drug.

The comparison of the drug flux values calculated for different microemulsions and liposomal formulations revealed statistically significant results between the investigated formulations. According to Figure 34,

conventional liposomes displayed similar properties as w/o microemulsion, while for transfersomes and o/w microemulsion, higher flux values were obtained. Comparing the potential therapeutic utility of the investigated formulations, it may be expected that the latter two will perform better. A similar tendency was also observed for the amounts of the drug deposited in the skin (Figure 35). The highest concentration of meloxicam in both skin layers was recorded for transfersomes, which indicated the highest ability to overcome *stratum corneum* and also explained the highest concentration in the receptor medium. The amounts observed for o/w microemulsion were lower, even though the drug flux was very similar. This may indicate a higher tendency to penetrate deeper with apparently lower affinity to the dermis and epidermis. The observed effect can be explained with the composition of both systems. Transfersomes contain naturally derived phospholipids which display high biocompatibility and high affinity to skin structures. Therefore, it might be expected that higher amounts of the drug incorporated in the vesicles will be retained in the skin. On the other hand, conventional liposomes containing the same phospholipids reveal lower elasticity and ability to deform, which decreases their ability to overcome the skin barriers and stay in the skin structures. These results suggested that the transfersomes containing cationic surfactant may affect the lipids of SC and therefore produce an enhancing effect in terms of dermal drug delivery.

In the case of microemulsions, it might be hypothesized that the presence of surfactants and co-surfactants contributed to the increased ability to penetrate through the *stratum corneum* into the deeper layers of the skin without binding to them, as was observed in transfersomes. However, the tendency was not the same for different types of microemulsions, which indicated the possible impact of the

structural features and thermodynamic activity of the incorporated drug. It is noteworthy that the literature reports showing the comparison between microemulsions and liposomal formulations are quite scarce. According to El-Badry et al.¹⁵², microemulsions with two different co-surfactants revealed higher drug flux than liposomal formulations containing croconazole, a poorly water-soluble antimycotic drug. Nevertheless, the experiment was conducted with the use of an animal skin model, which might provide different results when compared to human cadaver skin. Moreover, the efficacy of microemulsion is dependent on its composition. The study presented by Yuan et al.¹²⁹ investigating meloxicam-loaded microemulsions showed significantly higher drug flux values. However, isopropyl myristate applied as an oil phase is less polar than triacetin applied in our study, which might potentially contribute to the observed differences.

Taking into consideration the permeation coefficients calculated for all investigated formulations, it may be assumed that the observed differences are partially related to different drug content occurring mostly as a result of different encapsulation efficiency in liposomes. The highest value was obtained for transfersomes, while conventional liposomes and water-continuous microemulsion revealed similar properties. The lowest value of permeation coefficient was observed for oil-continuous microemulsion. The comparison made between two different types of vesicles confirmed the results described in the literature¹⁵³⁻¹⁵⁵ [62–64]. The available studies show that transfersomes reveal better properties in terms of dermal drug delivery, which is related to higher deformability allowing for better penetration into deeper skin layers. Moreover, because of the presence of cationic surfactant, transfersomes may disrupt the organization of lipids in the

stratum corneum. Similar results, indicating that transfersomes also had higher tendency to be retained in skin when compared to conventional liposomes, were presented by Alvi et al.¹⁵⁴.

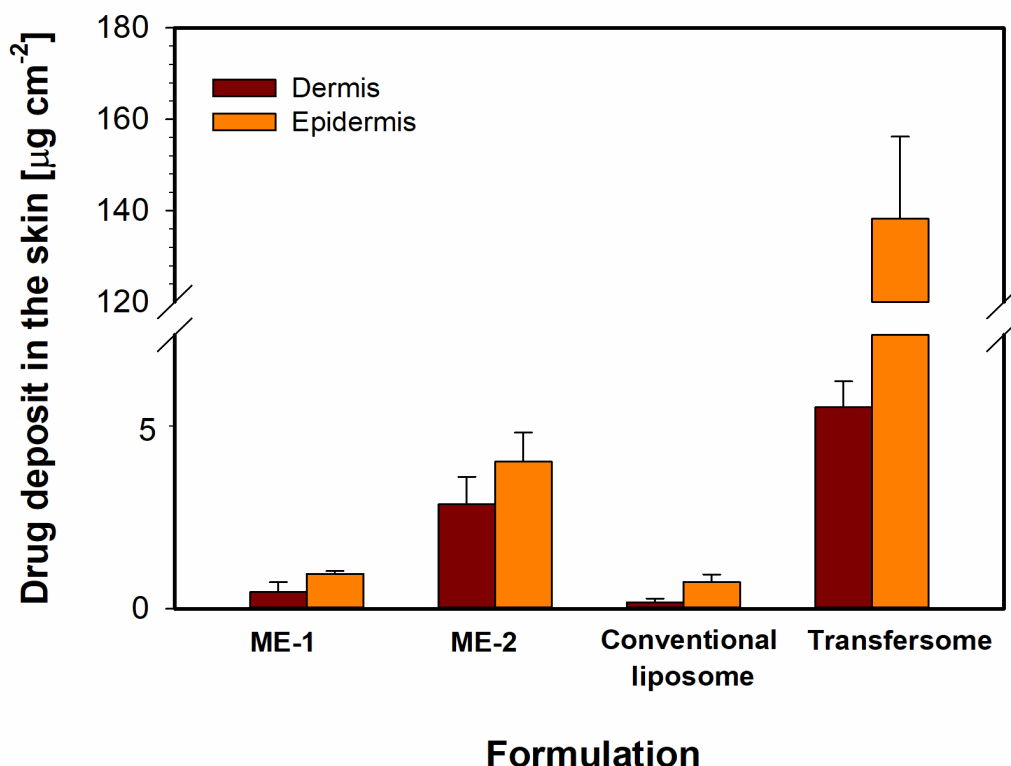


Figure 34. Amounts of meloxicam deposited in the skin layers after 24 h of experiment. Data are plotted as means \pm SD ($n = 3$ for each formulation).

Considering advantages and disadvantages of the investigated dermal delivery systems, it can be assumed that transfersomes reveal better properties as potential drug carriers, efficiently enhancing the absorption of the active ingredient. Another important feature of phospholipid-based vesicles is their high compatibility with the skin and low irritancy, which is particularly important in longer therapies requiring multiple applications. According to Mahrhauser et al.¹⁵⁶, liposomes and multiple emulsions had no negative effects on the skin, while microemulsion-based formulation temporarily increased transepidermal water

loss, which resulted in dehydration. The observed side effects related to microemulsion administration might be related to high surfactants and co-surfactants content. On the other hand, microemulsions are thermodynamically stable dispersions, which means that the formation process is spontaneous and does not require high amounts of energy and complicated multi-step technological processes. Therefore, several technological difficulties, such as non-uniformity, instability or high variability of the final product, can be avoided.

3.5 Conclusions

In the study, conventional liposomes and deformable transfersomes were obtained and compared to two different types of microemulsions as potential dermal delivery carriers for meloxicam, a non-steroidal anti-inflammatory drug. The performed studies allowed for optimization of the preparation method and composition of the investigated systems. When comparing the w/o and o/w microemulsion performance with the use of an *ex vivo* model involving human cadaver skin, the highest flux and permeation values were obtained for transfersomes, indicating these drug carriers as the most promising in terms of topical drug delivery. The developed liposomal formulations and preparation process would be used for further studies.

3.6 Publication Information

This chapter is a slightly modified version of Topical Delivery of Meloxicam using Liposome and Microemulsion Formulation Approaches published in *Pharmaceutics* (Zhang, J., Froelich, A., and Michniak-Kohn, B. Topical Delivery of Meloxicam using Liposome and Microemulsion Formulation Approaches.

Pharmaceutics. 2020, 12, 282. doi:10.3390/pharmaceutics12030282) and has been reproduced here.

The microemulsion development, preparation and analysis were performed by Dr. Anna Froelich from Chair and Department of Pharmaceutical Technology, Poznań University of Medical Sciences, Poland.

Chapter 4. Formulation and Process Development of Meloxicam Loaded Deformable Liposomes

4.1. Introduction

Compared to the rigid structure of conventional liposomes, the surfactants embedded in the lipid bilayers of transfersome can destabilize the bilayers and provide a flexible membrane, which makes transfersome highly deformable. The flexibility enables transfersomes to open extracellular pathways among the cells in stratum corneum, and then deform to squeeze through these passages into the deeper layers of the skin⁵⁴. In the case of ethosomes, incorporating ethanol into the liposomal formulation can solubilize the drug and create deformable lipid structures which could easily pass between skin corneocytes and subsequently enhance the skin retention and permeation^{88,89}. According to the study conducted by Niu et al¹⁵⁷, ethosomes could change the fluidity of the stratum corneum by disturbing its lipid domain, which enable the encapsulated drug to penetrate through deeper layers of the skin. These studies suggested that the added denaturants (edge activators or ethanol) can not only change the fluidity of the lipid bilayer of liposomes but the lipid domain of stratum cornea as well, which enhance the skin permeability of encapsulated drug.

Flavonoids are a class of polyphenolic compounds which could be further categorized into 6 groups: isoflavonoids, flavanones, flavanols, flavonols, flavones and anthocyanidins¹⁵⁸. They are present in a wide variety of fruits and vegetables and

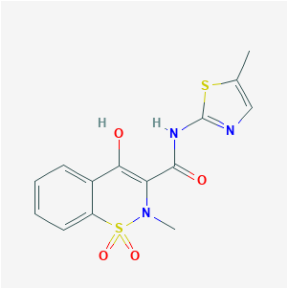
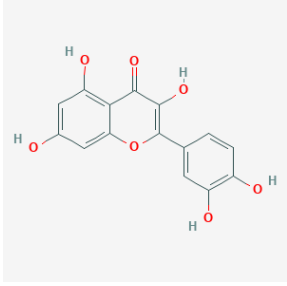
have been generally used as antioxidant and anti-inflammatory supplements. Recent studies also disclosed other therapeutic benefits related to flavonoids such as: immunomodulatory¹⁵⁹, anticancer¹⁶⁰ and anti-diabetic¹⁶¹ activities. Quercetin, a widely studied flavonol, has a wide range of biological actions including anti-carcinogenic, antiviral activities, attenuating lipid peroxidation, platelet aggregation and capillary permeability^{162,163}. It is a versatile antioxidant known to possess protective abilities against tissue injury induced by various drug toxicities¹⁶⁴.

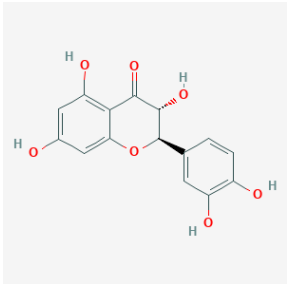
To study the mechanisms of flavonoids' antimicrobial activities, Ulrih et al¹⁶⁵ used four flavonoid-loaded liposomal vesicles as biological membrane models. The membrane fluidity characteristics of these multilamellar liposomes were determined using Electron Paramagnetic Resonance (EPR) spectroscopy. The obtained EPR spectra disclosed incorporation of these flavonoids could alter the fluidity of the liposomal membrane. Two similar studies were conducted by Saija et al¹⁶⁶ and Arora's group¹⁶⁷ to explore the mechanism of the antioxidant activity of flavonoids using liposomes as a bio-membrane model as well. The results obtained by both studies revealed that flavonoids could interact with and penetrate the lipid bilayers. Moreover, according to the study conducted by Huang et al¹⁶⁸, Raman and IR spectroscopy images revealed that flavonoids could modify the dynamic and packing order of lipid bilayer, hence to stabilize the flavonoid-loaded liposome. Based on these literature reports, we speculated that flavonoid-loaded liposomes could be a potential drug delivery system to affect the permeability of the co-encapsulated drug

in these liposomes by modulating the deformability of the liposomal vesicles and fluidity of stratum cornea membrane.

In this study, novel deformable liposomes, flavosomes, consisting of phospholipids, cholesterol, edge activator (cetylpyridinium chloride), flavonoids and meloxicam (model drug) have been developed to enhance the solubility and permeation of meloxicam for topical drug delivery. To be specific, among the various flavonoids, quercetin (QCT) and dihydroquercetin (DHQ) have been selected and evaluated due to their closely related structure but different solubility. Their physiochemical properties are presented in Table 16 together with those of MX.

Table 16. Physiochemical Properties of Meloxicam (MX), Quercetin (QCT) and Dihydroquercetin (DHQ)

Compound Name	Chemical Structure	Molecular Weight (g/mol)	Log P	Predicted Caco-2 Permeable	Melting Point (°C)	Aqueous Solubility (mg/mL)	pKa
Meloxicam		351.4	1.9	0.8484	254	0.007	4.08
Quercetin		302.2	1.8	0.8957	317	0.06	6.44

Compound Name	Chemical Structure	Molecular Weight (g/mol)	Log P	Predicted Caco-2 Permeable	Melting Point (°C)	Aqueous Solubility (mg/mL)	pKa
Dihydroquercetin (Taxifolin)		304.3	0.95	0.8957	237	1.16	7.8

Note: Data was collected from DrugBank (Wishart DS 2006).

4.2. Materials

Phosphatidylcholine (PC) from soybean source was a gift from LIPOID LLC (Newark, NJ, USA). Cholesterol (Chol) was purchased from Alfa Aesar (Haverhill, MA). Cetylpyridinium chloride (CPC), quercetin (QCT), ethanol and isopropanol were purchased from Sigma-Aldrich (St. Louis, MO). Meloxicam (MX) was supplied from Acros Organics (Morris Plains, NJ). Dihydroquercetin (DHQ) was purchased from Cayman Chemical Company (Ann Arbor, MI, USA). High-performance liquid chromatography (HPLC) grade water and acetonitrile were purchased from Sigma-Aldrich (St. Louis, MO) and Midland Scientific (Omaha, NE), respectively. 1,1-Dioctadecyl-3,3,3,3-tetramethylindocarbocyanine perchlorate (Dil) was procured from AAT Bioquest (Sunnyvale, CA, USA). Dermatomed human cadaver skin was obtained from New York Firefighter Skin Bank (NY, USA). All other chemicals used were of reagent grade and purchased from VWR International (Radnor, PA).

4.3. Methodology

4.3.1. Preparation of Liposomal Formulations

Meloxicam loaded liposomes were prepared by the thin film hydration method followed by sonication. Different levels of QCT and DHQ were added to the liposomal formulation based on the studies conducted in Chapter 3. In these formulations, the concentration of MX, PC, Cholesterol and CPC remained the same as 0.08%, 0.8%, 0.04% and 0.1%, respectively. Briefly, lipid mixtures of PC, Chol, CPC, MX and flavonoids (QCT or DHQ) were dissolved in chloroform. The solvent was then evaporated under a nitrogen gas stream and the lipid film was placed in a desiccator for at least 12 hours to remove any remaining solvent. Following this, the dried lipid film was hydrated with sodium acetate buffer solution (pH 5.5). Vesicles were subsequently sonicated at a sonicator bath (Tru-sweep Crest Bath Ultrasonicator, Cortland, NY) for one hour followed by 6 minutes probe sonication (SFX Branson Ultrasonic Processor, Emerson Industrial Automation, U.S.A.) at continuous mode in an ice-water bath. Liposome suspension was then centrifuged at 3000g for 30 minutes. The prepared vesicle formulations (supernatant) were stored in airtight containers at 4 °C prior to use.

4.3.2. HPLC Method of the Quantification of MX

The HPLC system used in the study was an Agilent 1100 Series liquid chromatography system (Agilent Technologies, Santa Clara, CA, USA) and Agilent Chemstation software (OpenLab CDS, ChemStation Edition, Rev.

C.01.10, Agilent Technologies, Santa Clara, CA, USA). A reversed-phase C18 column (Agilent Plus C18, 5 μm , 4.6 \times 150 mm, Agilent Technologies, Santa Clara, CA, USA) was used as the stationary phase. The column temperature was maintained at 30.0 ± 0.2 °C. The mobile phase composed of 1% phosphoric acid and acetonitrile at a flow rate of 1.0 mL/ min. The UV detector was set at a wavelength of 290 nm for DHQ and 360 nm for QCT and MX. The optimized HPLC gradient table is provided below in Table 17.

Table 17. Optimized HPLC gradients as used in the study

Time (minutes)	Acetonitrile (%)	1% Phosphoric Acid (%)
0.0	32	68
3.5	32	68
3.7	70	30
6.5	70	30
6.7	32	68

4.3.3. Measurement of Vesicle Size, Size Distribution and Zeta Potential

Average vesicle size and size distribution (Polydispersity Index, PDI) of the liposome formulations were measured by Dynamic Light Scattering (DLS) (Zetasizer Nano-S, Malvern Panalytical, Westborough, MA, USA). Zeta potential was measured by Electrophoretic Light Scattering (ELS) (Zetasizer Nano series, Malvern Panalytical, Westborough, MA, USA). All formulation samples without further treatment were analyzed at room temperature.

4.3.4. Determination of MX Entrapment Efficiency

The concentration of MX in the vesicle formulation was determined by HPLC analysis after disruption of the vesicles with 50% v/v ethanol in water. The extracted solution was sonicated for 10 min in a sonicator bath (Tru-sweep Crest Bath Ultrasonicator, Cortland, NY, USA). The resulting solution was then filtered with a 0.45 μm nylon syringe filter (Midland Scientific, Omaha, NE, USA). The entrapment efficiency and drug loading of MX loaded in the liposomes were calculated according to Equations (1) and (2) ¹²⁰, respectively.

$$\% \text{ entrapment efficiency} = (C_M/C_i) \times 100 \quad (3)$$

$$\% \text{ drug loading} = (C_M/C_L) \times 100 \quad (4)$$

where C_M is the concentration of MX loaded in the liposome, as described in the above methods, C_i is the initial concentration of MX added into the vesicle formulation and C_L is the concentration of phosphate lipid added into the vesicle formulation.

4.3.5. *Ex Vivo* Skin Permeation Study

4.3.5.1 Materials

Full thickness dermatomed (approximately 500 μm) human cadaver skin from the posterior torso was obtained from New York Firefighters Skin Bank (New York, NY). PBS Buffer (pH 7.4) was obtained from VWR International (Radnor, PA).

4.3.5.2 Equipment-Franz Diffusion Cells

The Franz diffusion cell was an in vitro model that is used as a standard for measuring the permeability of compounds into and across skin or other biological membranes. The major components of a diffusion cell included a donor chamber, a receptor chamber, a sampling port, a cell clamp, and a jacket that was connected to a water source.

4.3.5.3 Methodology

On the day of study, the frozen human cadaver skin was quickly thawed in pH 7.4 PBS at room temperature for 20 minutes. An appropriate size of skin was cut using a pair of scissors and carefully mounted on the receptor chamber of a vertical Franz Diffusion Cell (FDC) (Logan Instruments, Somerset, NJ, USA) filled with a known volume of pH 7.4 PBS buffer and an orifice size of 0.64 cm², the stratum corneum facing the donor chamber. The FDC was then placed into a dry block heater (Logan Instruments, Somerset, NJ) set at $37.0 \pm 0.5^{\circ}\text{C}$, and was stirred continuously with a small PTFE-coated magnetic bar at 600 rpm.

After the assembled FDC was equilibrated for at least 30 minutes, approximately 500 mg of each MX loaded liposomal gel formulations and liposome-free gel formulation was applied to the skin. At appropriate time intervals, an aliquot of the receptor medium was withdrawn, and the same volume of fresh buffer solution was replaced to the receptor chamber. The

concentration of MX in the aliquot was analyzed using the HPLC method described above.

At the end of the permeation study (24 hours), removed the donor compartment, washed the skin sample with PBS buffer (pH 7.4) to remove the residual formulations and carefully dried it with cotton swab. Next, the section of skin exposed to the test formulation was cut out with scissors and the dermal and epidermal layers were separated manually with tweezers. Separated layers were cut into small pieces and collected into a bedbug prefilled tube. Then the obtained samples were homogenized with 50% ethanol and centrifuged at 10000 rpm for 5 min. The supernatant was filtered and collected into an HPLC vial using 0.45 µm syringe filters. Collected samples were analyzed using the HPLC method described above.

The cumulative amount of MX permeated per unit area was calculated according to Equation 3 ¹²²:

$$Q_n = \frac{C_n V_r + \sum_{i=0}^{n-1} C_i V_s}{A} \quad (3)$$

where Q_n is the cumulative amount of the drug permeated per unit area ($\mu\text{g}/\text{cm}^2$) at different sampling times, C_n is the drug concentration in the receiving medium at different sampling times ($\mu\text{g}/\text{mL}$), C_i is the drug concentration in the receiving medium at the i th ($n-1$) sampling time ($\mu\text{g}/\text{mL}$), V_r is the volume of the receptor solution (mL), V_s is the volume of

the sample withdrawn (mL), and A is the effective permeation area of the diffusion cell (cm²). The Qn values were plotted against time, and then the steady-state flux (J_{ss}) was calculated from the slope of the linear portion of the plot.

The permeability coefficient (K_p) was calculated with Equation 4¹²²:

$$K_p = \frac{J_{ss}}{C_d} \quad (4)$$

where:

J_{ss} —steady state flux (μg cm⁻² h⁻¹), and

C_d —concentration of MX in the donor compartment (μg mL⁻¹).

4.3.6. Degree of Deformability

The vesicles were passed through 50 nm polycarbonate membrane (GE Healthcare, Chicago, IL, USA) fitted on an extruder (Avanti Polar Lipids, Alabaster, Alabama, USA). Vesicles before and after extrusion were analyzed for vesicle size and deformability index. Vesicle size was analyzed following the procedure described in section 4.3.3. Deformability index was calculated by dividing vesicle size before and after extrusion¹⁶⁹.

4.3.7. Fluorescence Microscopy

The depth of the skin penetration of liposomal formulations was evaluated by fluorescence microscopy (LSM 780 Confocal Laser Scanning Microscope; Zeiss Research Microscopy Solutions, Pleasanton, USA). Dil dye as a fluorescence marker¹⁷⁰ was added in the lipid-chloroform solution (1 to 50 w/w) before the

drying process. Dil-loaded liposomal formulations were prepared as the procedure described in section 4.3.1. Permeation studies were performed under the same conditions as in Section 4.3.5. After application for 24 hours, the residual amount of the liposome formulations was removed from the donor compartment. The skin exposed to the formulation was washed with deionized water and then dried with cotton swab. Subsequently, the skin sample was mounted on a microscope slide. The specimen was optically scanned at 10 μ m increments without any additional staining or treatment through a 10 \times objective using a fluorescence microscope equipped with a filter for Dil dye. The images were then analyzed using ImageJ 1.52p software (NIH, USA)

4.3.8. Study Statistical Analysis

The data were reported as means \pm S.D. ($n = 3$). The obtained results were analyzed with one-way analysis of variance (ANOVA) followed with post-hoc Tukey test. Statistical significance in the differences of the means was determined by Student's t-test. The statistical significance level in all tests was set at 5%. All calculations were performed with JMP[®] Pro 14.2.0 (SAS Institute Inc., Cary, NC, USA).

4.4. Results and Discussion

4.4.1 Screening of Flavonoids Concentration

Three concentration levels of QCT and DHQ have been added to the initial liposomal formulation as described in section 4.3.1. In these formulations, the concentration of MX, PC, Cholesterol and CPC remained the same. As many

published studies demonstrated, the incorporation of different components in the liposome systems affected the size, size distribution, zeta potential, drug content, and entrapment efficiency of the vesicle formulation, which will ultimately determine the efficacy of these liposomes¹⁷¹⁻¹⁷⁴. Therefore, the prepared MX-loaded liposomes were characterized with respect to their particle size, polydispersity index (PDI), zeta potential (Table 18) and %EE (Tables 19).

Table 18. Physical properties of the obtained vesicles. Data are presented as means \pm S.D. (n=3)

Sample ID	Flavonol Content (% w/v)	Ave Diameter (nm)	PDI ^a	Zeta Potential (mV)
Q-1	0.04	84.5 \pm 1.9	0.293 \pm 0.022	20.3 \pm 1.7
Q-2	0.06	89.7 \pm 1.1	0.275 \pm 0.026	22.0 \pm 0.7
Q-3	0.08	99.1 \pm 1.2	0.341 \pm 0.016	22.8 \pm 1.1
D-1	0.08	82.1 \pm 0.7	0.292 \pm 0.020	15.8 \pm 0.9
D-2	0.16	99.3 \pm 0.5	0.288 \pm 0.028	16.4 \pm 1.2
D-3	0.20	108.0 \pm 1.7	0.209 \pm 0.014	17.0 \pm 1.0

a: Polydispersity Index

Table 19. Entrapment Efficiency (%EE) of the obtained vesicles. Data are presented as means \pm S.D. (n=3)

SPL ID	Flavonol Content (% w/v)	MX ^a		QCT ^b		DHQ ^c	
		%EE ^d	Content (mg/mL)	%EE	Content (mg/mL)	%EE	Content (mg/mL)
Q-1	0.04	70.69 \pm 0.78	0.56 \pm 0.01	82.91 \pm 1.79	0.25 \pm 0.01	-	-
Q-2	0.06	66.67 \pm 0.50	0.53 \pm 0.01	95.70 \pm 2.26	0.57 \pm 0.01	-	-
Q-3	0.08	63.73 \pm 1.60	0.51 \pm 0.01	80.42 \pm 0.44	0.72 \pm 0.01	-	-
D-1	0.08	71.42 \pm 0.95	0.57 \pm 0.01	-	-	93.47 \pm 1.40	0.70 \pm 0.01
D-2	0.16	74.75 \pm 0.79	0.59 \pm 0.01	-	-	88.70 \pm 0.59	1.33 \pm 0.01
D-3	0.20	76.40 \pm 0.50	0.61 \pm 0.01	-	-	84.65 \pm 0.64	1.59 \pm 0.01

a: Meloxicam; b: Quercetin; c: Dihydroquercetin; d: % Entrapment Efficiency

The vesicle sizes of all these liposomal formulations were in the nano-size range of 80 – 110 nm with the size distribution (polydispersity index; PDI) of 0.2 – 0.4. The particle size increased with increasing concentrations of QCT/DHQ probably because more components had been encapsulated in these liposomes. As the studies conducted by Verma's group⁹⁷ revealed, the penetration of the fluorescent substances was inversely related to the size of the liposomes. Specifically, vesicles with size less than 300 nm were able to deliver their loaded molecules into the deeper layers of the skin while those with size greater than 600 nm were not effective. As shown in Table 14, the sizes of these investigated vesicular systems were all less than 150 nm, suggesting that these systems have potential to deliver both MX and the flavonoids through the skin. Zeta potential was used to study the surface charge of these vesicles. The zeta potentials of these vesicles were in positive range of 15–22 mV (Table 18). QCT loaded liposomes had a higher positive zeta potential (20-22 mV) compared to DHQ loaded liposomes (15-17 mV).

It was observed (Table 19) that with the increase of QCT concentration, the %EE for MX decreased, while the opposite effect was observed for DHQ loaded liposomes. The % EE for MX were 70.69%, 66.67% and 63.73% for Q1, Q2 and Q3, respectively; while the %EE for MX were 71.42%, 74.75% and 76.40% for D1, D2 and D3, respectively. The described effects may be related to the difference in solubility of these compounds. Based on the data summarized in

Table 16, QCT has similar water solubility and log P value as MX, while DHQ has higher aqueous solubility with lower log P value. Therefore, DHQ is likely to be retained in the inner core with less competition to MX, while QCT is likely to embed within the lipid layer and compete with MX. Additionally, the %EE for both QCT and DHQ were also determined, and the highest %EE for QCT was found with Q2 and %EE for DHQ was found to decrease as the level of DHQ increased.

To study the permeability of these formulations, the *ex vivo* skin permeation study through human cadaver skin was conducted using Franz diffusion cells. PBS is the most frequently selected medium in skin studies which is related also by to its pH close to the physiological values and also possesses the best compatibility with human cadaver skin which is an important factor for in 24-hour experiments.

The aqueous solubility of MX is pH dependent. As study conducted by Luger et al.¹⁷⁵ revealed, increasing pH resulted in significant increase in solubility. In their study, the solubility of MX in pH 7.0 and 8.0 buffer was found to be 0.27 mg/mL and 1.55 mg/mL, respectively. The solubility of MX at pH 7.4 PBS buffer was evaluated in our laboratory and was determined to be 0.44 mg/mL. Assuming the total amount of MX applied could permeate through the skin and be collected in receptor cells, the theoretical concentration of MX in the receptor cells was calculated to be around 0.09 mg/mL, which is about 1/5 of the solubility of MX

in pH 7.4 PBS buffer. Moreover, the observed concentration of MX in the study was found to be well below this level. Therefore, the solubility of MX in pH 7.4 PBS buffer was determined not to be a restricting factor in the ex vivo skin permeation study and pH 7.4 PBS buffer was selected as a physiologically similar medium.

Figure 37 shows (a) MX found in the receptor compartment after 24 hours (b) MX deposited in the different layers of skin after skin permeation study. As demonstrated in these two figures, the highest amount of MX was obtained in the receptor cell and deposited in the skin following topical application of Q2 and D3, indicating that these two vesicle formulations demonstrated the highest skin permeability within their own group. For the DHQ group, the formulation permeability increased with increasing DHQ concentrations, which also may be due to the increase of MX entrapment efficiency. However, in the QCT group, the permeability did not directly relate to MX entrapment efficiency, but rather exhibited a “V” shape curve. This may suggest that the concentration ratio of MX to QCT (4 to 3) in Q2 could be at the optimal level to demonstrate a synergic effect on its skin permeability. Further studies will have to be conducted to confirm these findings.

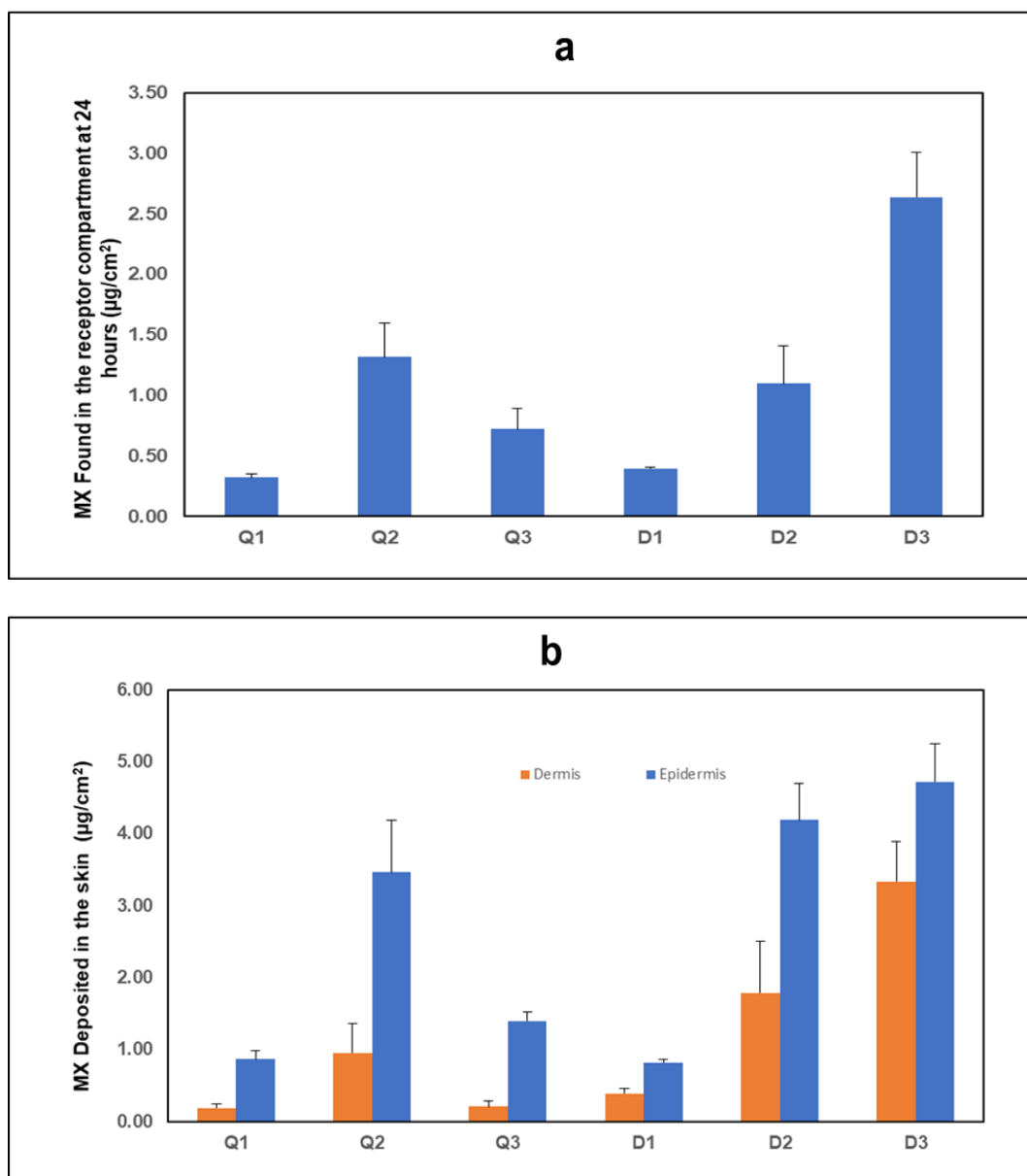


Figure 35. a) The amount of meloxicam (MX) ($\mu\text{g}/\text{cm}^2$) found in the receptor compartment of the Franz diffusion cell at 24 hours; b) the amount of MX ($\mu\text{g}/\text{cm}^2$) deposited in different skin layers after permeation study (n=3 for each formulation)

4.4.2 Optimization of the flavosome formulation

Based on the screening study data summarized in section 4.4.1, further concentrations of QCT and DHQ were explored as illustrated in Table 20. In these formulations, the concentration of MX, PC, Cholesterol and CPC remained the same as described in section 4.3.1. Additionally, transfersomes (containing

MX, PC, Cholesterol and CPC) were also prepared as control. The physicochemical characteristics of these investigated vesicle systems are shown in Tables 21 and 22.

Table 20. Physical properties of the obtained vesicles. Data are presented as means \pm S.D. (n=3)

Sample ID	%Flavonol (wt/v)	Ave Diameter (nm)	PDI ^a	Zeta Potential (mV)
Control	-	67.25 \pm 1.85	0.249 \pm 0.012	20.8 \pm 0.6
Q-4	0.03	80.97 \pm 2.19	0.242 \pm 0.006	19.6 \pm 1.1
Q-5	0.06	99.33 \pm 1.46	0.261 \pm 0.003	21.4 \pm 0.7
Q-6	0.09	114.8 \pm 0.52	0.282 \pm 0.031	22.9 \pm 0.8
D-4	0.15	95.47 \pm 2.66	0.245 \pm 0.005	15.4 \pm 1.5
D-5	0.20	99.36 \pm 1.94	0.242 \pm 0.008	16.6 \pm 1.0
D-6	0.25	115.80 \pm 2.47	0.200 \pm 0.009	17.0 \pm 0.9

a: Polydispersity Index

Table 21. %Entrapment Efficiency of the obtained vesicles. Data are presented as means \pm S.D. (n=3)

SPL ID	%Flavonol (wt/v)	MX ^a		QCT ^b		DHQ ^c	
		%EE ^d	Content (mg/mL)	%EE	Content (mg/mL)	%EE	Content (mg/mL)
Con ^e	-	76.52 \pm 2.39	0.61 \pm 0.02				
Q-4	0.03	69.31 \pm 1.11	0.55 \pm 0.01	81.71 \pm 1.01	0.24 \pm 0.01	-	-
Q-5	0.06	66.37 \pm 0.95	0.53 \pm 0.01	90.37 \pm 1.31	0.54 \pm 0.01	-	-
Q-6	0.09	62.15 \pm 1.27	0.50 \pm 0.01	77.92 \pm 1.61	0.70 \pm 0.01	-	-
D-4	0.15	69.18 \pm 2.38	0.55 \pm 0.02	-	-	90.50 \pm 1.23	1.34 \pm 0.02
D-5	0.20	71.57 \pm 0.99	0.57 \pm 0.01	-	-	87.99 \pm 2.32	1.75 \pm 0.05
D-6	0.25	59.89 \pm 2.03	0.48 \pm 0.02	-	-	91.14 \pm 2.01	2.33 \pm 0.05

a: Meloxicam; b: Quercetin; c: Dihydroquercetin; d: % Entrapment Efficiency; e: Control

As revealed in Table 20, the vesicle sizes of all these liposomal formulations were in the range of 67 – 116 nm with the size distribution (polydispersity index;

PDI) of 0.2 – 0.3. The particle size increased with the increase of QCT/DHQ concentration, probably due to the fact that more components had been encapsulated in these liposomes. Transfersome had the smallest particle size at 67 nm because it had the least components encapsulated considering the fact that preparation procedure was the same for these vesicles.

The zeta potentials of these vesicles were in positive charge range of 15 – 23 mV (Table 20). The results ranked as transfersome \approx flavosome-Q > flavosome-D. The addition of QCT did not have much impact on the zeta potential while addition of DHQ decreased the zeta potential of the vesicles. As study conducted by Katahira's group¹⁷⁶ revealed, positive liposomes demonstrated higher *in vitro* permeability than their negative counterparts. The similar findings were observed by Lin et al.¹⁷⁷. Lin reported that the cumulative amount of imperatorin permeated through the skin at 24 hours and J_{ss} from cationic-UDLs (ultra-deformable liposome) are higher than those from anionic-UDLs. Therefore, we expected that our positively charged vesicles would also have improved skin permeability.

The %EE values for MX were 69.31%, 66.37% and 62.15% for Q4, Q5 and Q6, respectively (Table 21), which displayed the same trend as observed in section 4.4.1. The %EE for MX was found to be 69.18%, 71.57% and 59.89% for D4, D5 and D6, respectively. It suggested the encapsulation efficiency for MX reached to the maximum level when DHQ concentration was 0.2% and started

decreasing with an increase in DHQ concentration. The %EE of MX in control (transfersome) was 76.52%, which is higher than the values obtained for QCT/DHQ loaded liposomes. The observed effect may be related to the fact that the flavonoids could compete with MX to reside in the vesicle bilayers. On the other hand, the diameter of the control vesicles was significantly lower which may also be an implication of this speculation.

To further determine the optimal concentration of flavonoids, the *ex vivo* skin permeation study through human cadaver skin was conducted using Franz diffusion cells. The drug permeation profiles of MX plotted as a function of time and amount of MX, QCT and QCT deposited in the epidermal and dermal layers after skin permeation study are shown in Figure 38. The values of steady state fluxes (J_{ss}), permeability coefficients (K_p) and enhancement ratio are presented in Table 22. As demonstrated in these figures, the highest amount of MX was observed in the receptor and the skin when Q5 and D5 formulations were applied, indicating that these two vesicle formulations demonstrated the highest skin permeability within their own group. Additionally, except Q4, J_{ss} , K_p and MX amount found in both dermal and epidermal layers of these two liposomal systems are higher than those of the transfersome formulation, suggesting that these systems improved MX permeability. The enhancement ratios, for these flavosomes ranged from 1.57 to 2.34, and D5 showed the highest permeation.

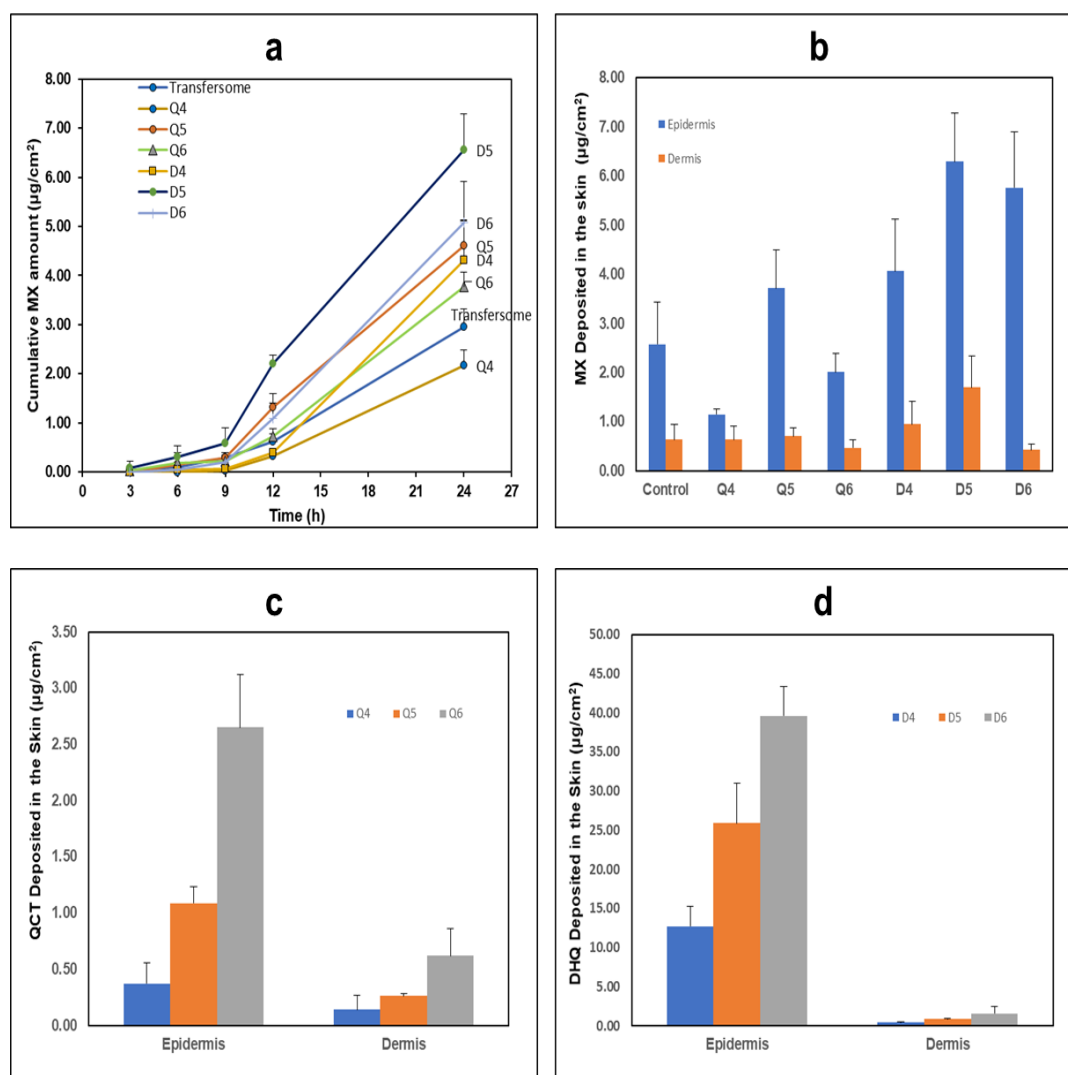


Figure 36. (a) *Ex vivo* drug permeation profiles of Meloxicam (MX) over 24 hours; (b) MX deposited in the different layers of skin after 24-hour skin permeation study, (c) Quercetin (QCT) deposited in the different layers of skin after 24-hour skin permeation study, (d) Dihydroquercetin (DHQ) deposited in the different layers of skin after 24-hour skin permeation study. Data are presented as means \pm S.D. (n=3 for each formulation).

Table 22. Steady state flux (J_{ss}) and permeation coefficients (K_p) obtained for the investigated formulations. Data are presented as means \pm S.D. (n=3 for each formulation).

Formulation	J_{ss} [$\mu\text{g cm}^{-2} \text{h}^{-1}$]	K_p [cm h^{-1}]	Enhancement Ratio
Transfersome	0.15 ± 0.02	$(23.88 \pm 3.48) \times 10^{-5}$	1
Q-4	0.11 ± 0.02	$(19.90 \pm 2.90) \times 10^{-5}$	0.83
Q-5	$0.23 \pm 0.02^*$	$(43.89 \pm 4.65) \times 10^{-5}$	1.84
Q-6	0.19 ± 0.01	$(37.46 \pm 2.21) \times 10^{-5}$	1.57

Formulation	J_{ss} [$\mu\text{g cm}^{-2} \text{h}^{-1}$]	K_p [cm h^{-1}]	Enhancement Ratio
D-4	$0.22 \pm 0.04^*$	$(39.35 \pm 7.28) \times 10^{-5}^*$	1.65
D-5	$0.32 \pm 0.03^*$	$(55.94 \pm 4.81) \times 10^{-5}^*$	2.34
D-6	$0.26 \pm 0.04^*$	$(53.84 \pm 8.52) \times 10^{-5}^*$	2.25

$*P < 0.05$ vs. transfersome

The mechanism of the observed permeation enhancement may be due to the ability of flavonoids to interact with and penetrate through the lipid bilayer of the stratum corneum of the skin. Previous studies conducted by multiple groups suggest that flavonoids may modify the lipid packing order of the cell membrane by interacting with or incorporating in the phospholipids to form flavonoid-phospholipid complexes^{178,179}. These compounds can penetrate the lipid bilayers by affecting the membrane fluidity as well as stability^{166,167}.

It was also observed that both QCT and DHQ are unstable in PBS buffer (pH 7.4), which is in agreement with the study results recorded by Buchner et al¹⁸⁰. Therefore, no QCT or DHQ was detected in the receptor medium at any time point due to the degradation of these two compounds under these conditions. The amount of both flavonoids deposited in different layers of skin was proportional to their concentration encapsulated in the liposomes. As far as skin distribution is concerned, DHQ was retained in significantly higher amounts in the epidermal layer, whereas similar amounts of QCT and DHQ were found in the dermal layer despite a higher amount of DHQ administered to the skin. These data supported the possibility of co-delivery of flavonoids and anti-inflammatory compounds in a topically applied flavosome formulation.

Based on these results, Q5 (0.06% QCT) and D5 (0.2% DHQ) were selected as the best formulations for future experiments.

4.4.3 Deformability of Flavosome

The surfactant embedded in the lipid bilayers of deformable liposomes can destabilize the bilayers and provide a flexible membrane. The flexibility enables these vesicles to penetrate through extracellular pathways among the cells within the stratum corneum, and then deform to squeeze through these passages into the deeper layers of the skin^{73,75}. Therefore, deformability is one of the important characteristics of “deformable” liposomes since this affects the ability of the vesicles to squeeze through pores smaller than the liposomal diameters. The degree of deformability of flavosomes and transfersomes were determined and are summarized in Table 23.

Table 23. Deformability index of flavosomes and transfersomes. Data are presented as means \pm S.D. (n=3 for each formulation).

Formulation	Particles Size before Extrusion (nm)	Particles Size after Extrusion (nm)	Deformability Index
Transfersome	73.9 \pm 1.9	65.5 \pm 0.8	0.886 \pm 0.011
Q5	88.5 \pm 1.0	85.6 \pm 2.7	0.967 \pm 0.031*
D5	100.2 \pm 0.6	99.5 \pm 0.7	0.993 \pm 0.007*

* $P < 0.05$ vs. transfersome

The deformability indices of Q5 and D5 were near 1 and greater than that of transfersomes, indicating that the investigated vesicles regained their

size after extrusion and were more flexible than the transfersomes. These data suggest that incorporating DHQ and QCT into the liposomes could affect the elasticity of vesicles by changing the fluidity and stability of the lipid bilayer. This observation also conformed with the permeation results discussed in section 4.4.2.

4.4.4 Skin Penetration of DiI-Labeled Liposomal Vesicles

The depth of the full thickness human cadaver skin penetration of the DiI-labeled vesicles was evaluated using fluorescence microscopy. DiI is a widely used carbocyanine membrane dye that labels cell membranes by inserting its two long (C18 carbon) hydrocarbon chains into the lipid bilayers (Lukas, Aigner et al. 1998). Therefore, it has been used as a fluorescent probe to visualize the effect of liposomal vesicles on dermal delivery of encapsulated substances into skin (Alvarez-Roman, Naik et al. 2004). According to the Confocal Laser Scanning Microscopy (CLSM) images displayed in Fig 39, transfersome, Q5 and D5 vesicles penetrated into the deeper layers of the skin up to 280, 320 and 320 μm , respectively.

The observed results indicated flavonoids containing deformable liposomes had higher skin permeability than transfersomes due to their higher deformability and their interaction with the lipid bilayer of cell membranes.

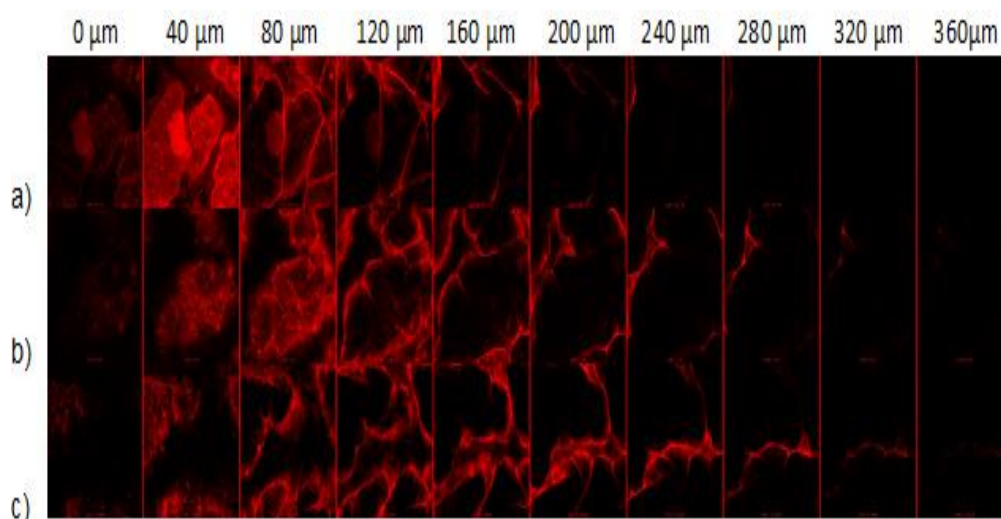


Figure 37. Confocal Laser Scanning Microscopy Images taken at different depths of the full thickness human cadaver skin after 24 hours permeation of Dil-labeled vesicles a) transfersome, b) Q5, c) D5 (magnification 10X)

4.5. Conclusions

In this study, flavosomes, novel deformable liposomes containing flavonoids, were developed and tested as a potential drug delivery carrier for topical use in skin preparations. These vesicles exhibited homogeneous particle sizes less than 150 nm with a higher degree of deformability as compared to conventional liposomes. Compared to transfersomes, the investigated formulations demonstrated improved permeability for MX, a potent NSAID, through the skin. CLSM images suggested that these deformable vesicles could deliver MX to the deeper layers of skin. Additionally, significant skin distribution of the two flavonoids, DHQ and QCT, was observed in *ex vivo* skin permeation studies. Since flavonoids are natural anti-inflammatories, flavosomes should be further explored as potential nanocarriers for co-delivery of other anti-inflammatory compounds such as meloxicam.

4.6. Publication Information

This chapter is a slightly modified version of Flavosomes, novel deformable liposomes for the co-delivery of anti-inflammatory compounds to skin published in *International Journal of Pharmaceutics* (Zhang ZJ, Michniak-Kohn B. Flavosomes, novel deformable liposomes for the co-delivery of anti-inflammatory compounds to skin. *Int J Pharm.* 2020;585:119500) and has been reproduced here.

Chapter 5. Development and Characterization of Meloxicam-loaded Deformable Liposomal Topical Gel Formulation

5.1. Introduction

Meloxicam is a Biopharmaceutical Classification System (BCS) class II non-steroidal anti-inflammatory drug (NSAID) structurally related to the enolic acid class of compounds.¹⁸¹ As a preferential cyclo-oxygenase-2 (COX-2) inhibitor, it has been used clinically to treat osteoarthritis, rheumatoid arthritis and ankylosing spondylitis by reducing pain and inflammatory symptoms.⁹¹⁻⁹³ Additionally, it has been widely explored as a potential therapeutic agent for Alzheimer's disease and various tumors, such as lung, colorectal, prostate and urinary bladder cancers.⁶⁻⁹ However, many adverse effects, especially gastro-intestinal toxicity/bleeding, have been frequently reported when it is administrated orally.^{11,94,95} Therefore, topical administration is an appealing alternative because it provides many advantages over the oral route: selective on-site local and systemic effects, avoidance of first pass effect, reduction of gastro-intestinal toxicity and improvement of patient compliance. As a zwitterionic drug, MX has a relatively high melting point (254 °C), low aqueous solubility (7.15 mg/L at 25 °C),⁹⁶ and lipophilicity (logP = 3.43) out of the ideal range of 1-3²⁰ indicating that it is not a suitable candidate for topical delivery.

In order to improve its solubility and lipophilicity, one of the available options is to encapsulate the MX in a deformable liposomal formulation that will improve the solubility and permeability through the *stratum corneum*. Transfersomes are

considered the first generation of deformable vesicles developed by Cevc and Blume⁷³ and Cevc et al.⁷⁴ They are generally prepared by addition of a surfactant (edge activator) into the conventional liposomes.⁷² Compared to conventional liposomes, the denaturant embedded in the lipid bilayers can destabilize the bilayers and provide a flexible membrane, which enables these vesicles to open extracellular pathways among the cells in the *stratum corneum*, and then deform to squeeze through these passages into the deeper layers of the skin^{54,88,89}.

Flavosomes, novel deformable liposomes containing flavonoids, specifically quercetin (QCT) and dihydroquercetin (DHQ), have been developed in the previous studies. It was demonstrated that flavonoid-loaded liposomes could be a potential drug delivery system to affect the permeability of encapsulated drugs by modulating the deformability of the liposomal vesicles and fluidity of the *stratum corneum* membrane¹⁸².

In the previous studies (Chapters 3 and 4), I have used both transfersomes¹⁸³ and flavosomes¹⁸² to encapsulate MX and observed improved solubility and skin permeability of MX into the deeper layers of human skin. However, the physiochemical stability of MX loaded liposomal suspension was an issue.

The physical stability of liposomes can be affected by a number of factors, such as¹⁸⁴: the liposome integrity, the size distribution of the lipid vesicles, unsaturation of the fatty acid groups. Some liposomes are susceptible to fusion (i.e., irreversible coalition of smaller liposomes to form larger liposomes), aggregation (i.e., reversible

conglomeration or pooling of two or more liposomes without fusion), and leakage of the contained drug substance during storage, which can be affected by the lipid components in the liposome or by the contained drug substance. Lipids with unsaturated fatty acids are subject to oxidative degradation, while both saturated and unsaturated lipids are subject to hydrolysis to form lysolipids and free fatty acids.

By optimizing the size distribution, pH and ionic strength, as well as the addition of antioxidants and chelating agents, liquid liposome formulations can be stable¹⁸⁵. Two types of chemical degradation reactions can affect the performance of phospholipid bilayers: hydrolysis of the ester bonds linking the fatty acids to the glycerol backbone and peroxidation of unsaturated acyl chains. The oxidation and hydrolysis of lipids may lead to the appearance of short-chain lipids and then soluble derivatives will form in the membrane, resulting in the decrease of the quality of liposome products. Moreover, physical processes such as aggregation/flocculation and fusion/coalescence that affect the shelf life of liposomes can result in loss of liposome associated drug and changes in size. Aggregation is the formation of larger units of liposomal material; these units are still composed of individual liposomes. In principle, this process is reversible e.g. by applying mild shears forces, by changing the temperature or by binding metal ions that initially induced aggregation. However, the presence of aggregation can accelerate the process of coalescence of liposomes, which indicates that new colloidal structures are formed. As coalescence is an irreversible process; the original liposomes cannot be retrieved.

Although suspension dosage forms are easy to apply, the suspended particles are prone to agglomerate, coalesce and separate, which can lead to nonuniform dosing and instabilities.¹⁸⁶ To overcome this, liposomal loaded gel formulation is an appealing alternative dosage form.

Hydrogels are three-dimensional networks consisting of hydrophilic polymers, which have been used for a wide range of applications because of their characteristic properties, such as biocompatibility, biodegradability and good tolerability.¹⁸⁷ Among these, poloxamer 407 (P407) based hydrogels have been widely studied because of thermoreversible gelation, solubilizing capacity, low toxicity, drug release characteristics, and compatibility with numerous biomolecules and excipients.^{188,189} The most beneficial property of topical formulations based on P407 is reverse thermal gelation of its aqueous solutions. It is the process of viscosity increase upon increasing temperature, which means that P407-based vehicles bearing liquid-like behavior at lower temperatures and become semi-solid as the temperature increases.⁸² The sol-gel transition point ($T_{\text{sol-gel}}$) strongly depends on composition of the formulation, including concentration of the polymer, active pharmaceutical ingredients and the additives. This property is considered to be particularly beneficial for skin formulations. By applying a gel with reduced viscosity, it is possible to fill the furrows and crevices in the skin, as well as skin appendages and thus obtain a larger contact surface, followed by better bioavailability.¹⁸⁹

However, the concentration of the MX in the liposomal suspensions developed was too low to make a viable gel formulation. To solve these issues, the formulation/process have been optimized to further increase the MX entrapment efficiency and the resulting optimized formulations would be incorporating in gel formulations.

In the present study, a P407 based hydrogel system has been prepared as a potential topical therapeutic vehicle to incorporate MX-loaded liposomal vesicles. A flow diagram is demonstrated in Figure 40.

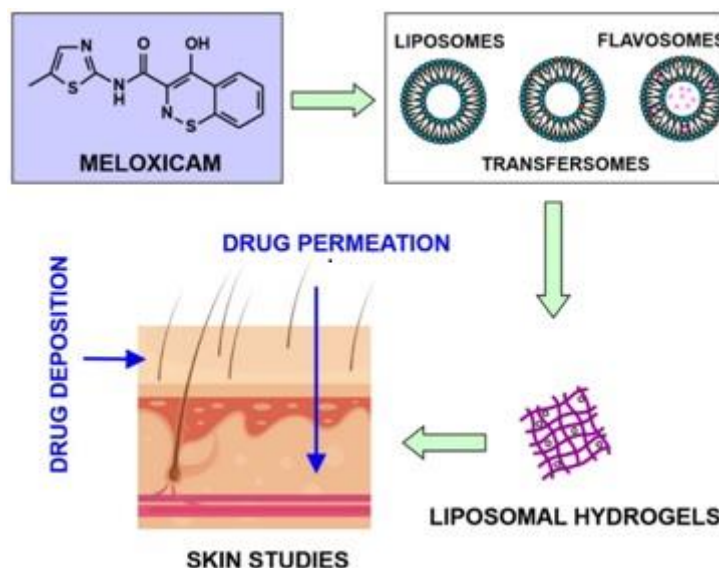


Figure 38. Flow diagram of liposomal hydrogel formulation preparation.

5.2. Materials

Phosphatidylcholine (PC) from soybean source was a gift from LIPOID LLC (Newark, NJ, USA). Kolliphor® P407 (P407) was generously donated by BASF Corporation (Tarrytown, NY, USA). Cholesterol (Chol) was purchased from Alfa Aesar (Haverhill, MA, USA). Cetylpyridinium chloride (CPC), quercetin (QCT), ethanol and isopropanol were purchased from Sigma-Aldrich (St. Louis, MO, USA).

Meloxicam (MX) was supplied from Acros Organics (Morris Plains, NJ). Dihydroquercetin (DHQ) was purchased from Cayman Chemical Company (Ann Arbor, MI, USA). High-performance liquid chromatography (HPLC) grade water and acetonitrile were purchased from Sigma-Aldrich (St. Louis, MO, USA) and Midland Scientific (Omaha, NE, USA), respectively. 1,1-Dioctadecyl-3,3,3,3-tetramethylindocarbocyanine perchlorate (Dil) was procured from AAT Bioquest (Sunnyvale, CA, USA). Dermatomed human cadaver skin was obtained from New York Firefighter Skin Bank (NY, USA). All other chemicals used were of reagent grade and purchased from VWR International (Radnor, PA, USA).

5.3. Methodology

5.3.1 Preparation of Liposomes

Meloxicam loaded liposomes were prepared by the thin film hydration method followed by sonication.^{119,183} The compositions of each formulation are listed in Table 24.

Specific amounts of PC, Chol, CPC, MX and flavonoids (QCT or DHQ) were first dissolved in chloroform. The lipid mixture was then evaporated under a nitrogen gas stream and the obtained film was placed in a vacuum desiccator overnight to remove any remaining solvent. The dried lipid film was subsequently hydrated with sodium acetate buffer solution (pH 5.5) and sonicated in a sonicator bath (Tru-sweep Crest Bath Ultrasonicator, Cortland, NY, USA) for one hour followed by 15 minutes of probe sonication (SFX Branson Ultrasonic Processor,

Emerson Industrial Automation, U.S.A.) in an ice-water bath. The liposomal suspension was then centrifuged for 30 minutes at 3,000g. The supernatant was collected in airtight containers and stored under refrigerated conditions prior to use.

Table 24. The composition and type of the vesicles investigated in the study

ID	Description	PC ^a	MX ^b	Chol ^c	CPC ^d	QCT ^e	DHQ ^f
		(3.2% w/v)	(0.32% w/v)	(0.16% w/v)	(0.96% w/v)	(0.24% w/v)	(0.8% w/v)
CLP	Conventional Liposome	✓	✓	✓			
TFS	Transfersome	✓	✓	✓	✓		
FLSQ	Flavosome Q	✓	✓	✓	✓	✓	
FLSD	Flavosome D	✓	✓	✓	✓		✓

a: Phosphatidylcholine; b: Meloxicam; c: Cholesterol; d: Cetylpyridinium chloride; e: Quercetin; f: Dihydroquercetin

5.3.2. HPLC Method of the Quantification of MX

MX was analyzed using high pressure liquid chromatography (HPLC) with UV detection. The HPLC system was an Agilent 1100 Series liquid chromatograph (Agilent Technologies, Santa Clara, CA, USA) and Agilent Chemstation software (OpenLab CDS, ChemStation Edition, Rev. C.01.10, Agilent Technologies, Santa Clara, CA, USA). A reversed-phase C18 column (Agilent Plus C18, 5 μ m, 4.6 \times 150 mm, Agilent Technologies, Santa Clara, CA, USA) was used as the stationary phase. The column temperature was maintained at 30.0 \pm 0.2°C. The mobile phase was composed of 1% phosphoric acid (A) and

acetonitrile (B) at a flow rate of 1.0 mL/min. The gradient program was: 0 minutes, 32% B; 3.7 minutes, 70% B; 6.7 minutes, 32% B. The UV detector was set at a wavelength of 360 nm for MX. The method was linear at a concentration range 0.05–50 µg/ml with R^2 of 0.9995 for meloxicam. The limit of detection (LOD) was found to be 0.01 µg/mL and the limit of quantification (LOQ) was 0.05 µg/mL. The relative standard deviation for both intra-day and inter-day precision was less than 3%.

5.3.3. Measurement of Vesicle Size, Size Distribution and Zeta Potential

Average size and size distribution (Polydispersity Index, PDI) of the liposome vesicles were measured by Dynamic Light Scattering (DLS) (Zetasizer Nano-S, Malvern Panalytical, USA) with a 632.8 nm He-Ne laser light source (4 mW). Liposomal vesicles were measured as is without any dilution. 100 mg of each gel formulation was dispersed in 1 mL of acetate buffer (pH 5.5) using a vortex mixer. Each sample was filled in a disposable polystyrene low volume cuvette (ZEN0118) without further treatment and equilibrated prior to the experiment for 180 seconds. The measurements were done at 25.0 °C using non-invasive backscatter mode (NIBS) at an angle of 173°.

Zeta potential was determined by Electrophoretic Light Scattering (ELS) (Zetasizer Nano series, Malvern Panalytical, USA). All formulation samples without further treatment were filled in disposable capillary zeta cells (DTS1070) and analyzed at 25°C.

5.3.4. Determination of MX Entrapment Efficiency and Drug Loading

The prepared liposomal vesicles were disrupted with 50% v/v ethanol in water and sonicated for 10 minutes in a sonicator bath (Tru-sweep Crest Bath Ultrasonicator, Cortland, NY). The resulting solution was then filtered with a 0.45 μm nylon syringe filter (Midland Scientific, Omaha, NE) and the concentrations of MX in the vesicle formulation were determined using HPLC analysis. The entrapment efficiency of MX loaded in the liposomes was calculated as per Equation 1,¹²⁰ whereas the drug loading (drug-to-lipid ratio) was calculated as per Equation 2.¹⁹⁰

$$\% \text{ entrapment efficiency} = (C_M/C_i) \times 100 \quad (5)$$

$$\% \text{ drug loading} = (C_M/C_L) \times 100 \quad (6)$$

where C_M is the concentration of MX loaded in the liposome, as described in the above methods, C_i is the initial concentration of MX added into the vesicle formulation and C_L is the concentration of phosphate lipid added into the vesicle formulation.

5.3.5. Degree of Deformability

The vesicles were passed through a 50 nm polycarbonate membrane (GE Healthcare, Chicago, IL, USA) fitted on an extruder (Avanti Polar Lipids, Alabaster, Alabama, USA). Vesicles before and after extrusion were analyzed for vesicle size and deformability index. Vesicle size was analyzed following the

procedure described in *Measurement of Vesicle Size* (5.3.3). The deformability index was calculated by dividing vesicle size before and after extrusion.¹⁶⁹

5.3.6. Preparation of Liposomal Gel

Liposomal gel was prepared using P407 by “cold method” as described by Dumortier et al.¹⁸⁹ Specified amounts of P407 (20% w/w) and liposomal formulations were mixed in an ice-water bath with continuous magnetic stirring, until a homogeneous dispersion was obtained. Concurrently, a specific amount of P407 (20% w/w) dispersed in MX saturated PBS (pH 7.4) was prepared as the plain (liposome-free) gel formulation. The mixture was then kept overnight at 4°C to ensure complete dissolution of P407. Subsequently, the dispersion was gently mixed at room temperature until a consistent gel formed.

5.3.7. Morphology of Liposomal Vesicles and Gel Formulations

The morphology of liposomal vesicles and gel formulations was characterized by transmission electron microscopy (TEM) (CM 12 TEM, Philips, Amsterdam, Netherlands). 100 mg of each gel formulation was dispersed in 1 mL of acetate buffer (pH 5.5) using a vortex mixer. One drop of liposomal vesicle or prepared gel formulation solution was placed onto a copper grid and the excess solution was immediately adsorbed using filter paper. The sample was then stained by adding a drop of 2% phosphotungstic acid. The excess solution was immediately removed by filter paper, and then the sample was dried at room temperature. Afterward, the grid was observed using a TEM with AMT Image

Capture Engine V602 (Advance, Microscopy Techniques Corp, Woburn, MA, USA).

5.3.8. Oscillatory Rheology Studies

The oscillatory rheological measurements were performed on Kinexus Ultra+ (Malvern Pananalytical Ltd., USA) rotational rheometer with rSpace software (ver. 1.75.2326, Malvern Pananalytical Ltd., USA). The samples were tested with the use of stainless-steel plate-plate geometry ($\Phi=20$ mm). The measuring gap was set at 1.0 mm. Prior to the experiments the samples were placed on the lower plate. After lowering down of the upper plate, the excess was removed with a spatula. Each measurement was conducted in triplicate using fresh samples and the mean values of the parameters were reported.

The measurements including oscillatory stress sweeping (SS) and temperature sweeping (TS), were performed sequentially in a single run. After being placed in the rheometer, the samples were equilibrated for 2 minutes at 32.0 ± 0.5 °C. Then the SS study was performed in the range of 1.0 - 12000.0 Pa. In the second step, the samples were cooled to 5.0 ± 0.5 °C and a TS ramp was conducted in the range of 5.0 - 30.0 °C, at constant stress of 2.0 Pa. For both SS and TS measurements, the oscillation frequency was set at 1.0 Hz.

The results for SS studies were presented as the dependence of storage (G') and loss (G'') moduli vs. oscillatory stress (τ), plotted in a logarithmic scale.

Additionally, the G' / G'' cross-over points were calculated. Temperature sweeping results were plotted as G' dependence on temperature.

5.3.9 *Ex Vivo* Skin Permeation Study

Full thickness dermatomed (approximately 500 μm) human cadaver skin from the posterior torso was obtained from the New York Firefighters Skin Bank (New York, NY, USA). On the day of study, the skin was quickly thawed in pH 7.4 PBS at room temperature for 20 minutes. An appropriate size of skin was cut using a pair of scissors and carefully mounted on the receptor chamber of a vertical Franz Diffusion Cell (FDC) (Logan Instruments, Somerset, NJ, USA) filled with a known volume of pH 7.4 PBS buffer and an orifice size of 0.64 cm^2 , the *stratum corneum* facing the donor chamber. The FDC was then placed into a dry block heater (Logan Instruments, Somerset, NJ) set at $37.0 \pm 0.5^\circ\text{C}$, and was stirred continuously with a small PTFE-coated magnetic bar at 600 rpm.

After the assembled FDC was equilibrated for at least 30 minutes, approximately 500 mg of each MX loaded liposomal gel formulations and liposome-free gel formulation was applied to the skin. At appropriate time intervals, an aliquot of the receptor medium was withdrawn, and the same volume of fresh buffer solution was replaced to the receptor chamber. The concentration of MX in the aliquot was analyzed using the HPLC method described above.

At the end of the permeation study (24 hours), the donor compartment was removed. The skin sample was washed with PBS buffer (pH 7.4) to remove the

residual formulations and carefully dried with a cotton swab. Next, the section of skin exposed to the test formulation was cut out with scissors and the dermal and epidermal layers were separated manually with tweezers. Separated layers were cut into small pieces and collected into a BeadBug prefilled tube. Then the obtained samples were homogenized with 1 mL of 50% ethanol using a BeadBug Microtube Homogenizer (Model D1030, Benchmark Scientific Inc., Sayreville, NJ, USA) for 3 cycles of 3 minutes (total 9 minutes). The resulting solutions were centrifuged at 10000 rpm for 5 minutes (Eppendorf Centrifuge 5415c, Brinkmann Instruments, Inc., Westbury, NY, USA). The supernatant was then filtered and collected into an HPLC vial using 0.45 µm syringe filters. Collected samples were analyzed using the HPLC method described above.

The cumulative amount of MX permeated per unit area was calculated according to Equation 3 ¹²²:

$$Q_n = \frac{C_n V_r + \sum_{i=0}^{n-1} C_i V_s}{A} \quad (3)$$

where Q_n is the cumulative amount of the drug permeated per unit area ($\mu\text{g}/\text{cm}^2$) at different sampling times, C_n is the drug concentration in the receiving medium at different sampling times ($\mu\text{g}/\text{mL}$), C_i is the drug concentration in the receiving medium at the i th ($n-1$) sampling time ($\mu\text{g}/\text{mL}$), V_r is the volume of the receptor solution (mL), V_s is the volume of the sample withdrawn (mL), and A is the effective permeation area of the diffusion cell (cm^2). The Q_n values were

plotted against time, and then the steady-state flux (J_{ss}) was calculated from the slope of the linear portion of the plot.

The permeability coefficient (K_p) was calculated with Equation 4¹⁷⁷:

$$K_p = \frac{J_{ss}}{C_0} \quad (4)$$

where C_0 represents the initial concentration of MX in the donor compartment.

5.3.10. Fluorescence Microscopy

The depth of the skin penetration of the liposomal gel was evaluated by fluorescence microscopy (LSM 780 Confocal Laser Scanning Microscope; Zeiss Research Microscopy Solutions, Pleasanton, USA). Dil dye was prepared and added in the lipid-drug-chloroform solution (at a 1:50 ratio, w/w) before the drying process. Dil-loaded liposomal formulations were then prepared as the procedure described in the *Preparation of Liposomes* section. Subsequently, these Dil-labeled vesicles were incorporated in 20% (w/w) P407 gel formulations prepared using the procedure described in *Preparation of Liposomal Gel*. Permeation studies of these liposomal gel formulations were then performed under the same conditions as described in the *Ex Vivo Skin Permeation Study* section. After application for 24 hours, the residual amount of the gel formulations was removed from the donor compartment. The skin exposed to the formulation was washed with deionized water and then dried with

a cotton swab. Subsequently, the skin sample was mounted on a microscope slide. The specimen was optically scanned at 10 μm increments without any additional staining or treatment through a 10 \times objective using a fluorescence microscope equipped with a filter for Dil dye. The images were then analyzed using ImageJ 1.52p software (NIH, USA).

5.3.11. Effect of Storage

The effect of storage study for liposomal suspensions and liposomal gel formulations was conducted at $5 \pm 3^\circ\text{C}$ and $25 \pm 5^\circ\text{C}$, respectively, for a period of 90 days. The content of MX contained in these vesicles and gel formulations were evaluated by HPLC method described above at an interval of 30, 60 and 90 days.

5.3.12 Statistical Analysis

The data were reported as means \pm S.D. ($n = 3$). The obtained results were analyzed with one-way analysis of variance (ANOVA) followed with post-hoc Tukey test. Statistical significance in the differences of the means was determined by Student's t-test. The statistical significance level in all tests was set at 5%. All calculations were performed with JMP[®] Pro 14.2.0 (SAS Institute Inc., Cary, NC, USA).

5.4. Results

5.4.1. Characterization of MX-loaded Liposomes

The formulations developed in the previous studies^{182,183} had low MX content, so the resulting gel formulations did not yield any meaningful permeation results. Therefore, we modified the liposomal formulations as summarized in Table 24 in the present study to increase the content of MX. As demonstrated in many published studies,¹⁷²⁻¹⁷⁴ the composition of the liposome systems determines their efficacy by affecting the size, size distribution, zeta potential, drug content, and entrapment efficiency of the vesicle formulations. For example, many studies revealed that cholesterol has a significant effect on the physicochemical properties of liposomes. However, numerous studies have reported contradictory effects of cholesterol on size, zeta potential and drug entrapment. For example, Tavano, et al¹⁷² reported the incorporation of cholesterol decreased the size of liposome. On the contrary, the study of Lopez-Pinto et al¹⁷¹ revealed the increase of liposomal size with the incorporation of cholesterol. However, as our study¹⁸³ revealed, the addition of cholesterol did not have much effect on the physiochemical properties of the investigated liposomal vesicles. As the size, vesicle surface charge and amount of encapsulated drugs of the vesicles can affect their permeability, it is important to characterize the prepared MX-loaded liposomes with respect to their particle size, polydispersity index (PDI), zeta potential and %EE (Table 25).

Table 25. Physiochemical properties of the obtained vesicles. Data are presented as means \pm S.D. (n=3)

Sample ID	Description	MX ^a			Average	PDI ^d	Zeta
		%EE ^b	%DL ^c	Content (mg/mL)	Diameter (nm)		Potential (mV)
CLP	Conventional Liposome	9.13 \pm 1.13	0.91 \pm 0.11	0.292 \pm 0.036	111.4 \pm 0.2	0.257 \pm 0.008	+2.1 \pm 0.3
TFS	Transfersome	96.04 \pm 1.98	9.61 \pm 0.20	3.075 \pm 0.063	62.3 \pm 0.3	0.287 \pm 0.013	+32.2 \pm 0.6
FLSQ	Flavosome-Q	94.39 \pm 1.57	9.44 \pm 0.16	3.022 \pm 0.050	66.0 \pm 0.6	0.281 \pm 0.002	+27.8 \pm 0.5
FLSD	Flavosome-D	92.24 \pm 0.36	9.23 \pm 0.04	2.954 \pm 0.011	97.0 \pm 1.3	0.298 \pm 0.023	+23.6 \pm 0.7

a: Meloxicam; b: % Entrapment Efficiency; c: % Drug Loading; d: Polydispersity Index

The entrapment rates of MX in the vesicles were in the range of approximately 0.3 - 3 mg/mL. The solubility of MX in acetate buffer solution (pH 5.5) was determined to be $6.82 \pm 0.30 \mu\text{g/mL}$ (n=3), indicating that liposomal formulations provided substantial enhancement of MX solubility. It was observed that %EE for MX was significantly higher in deformable liposomes compared to those in conventional liposomes. These results might be attributed to the intrinsic properties of the cationic surfactant, CPC, as a solubilizer and the interactions among the surfactants, MX and lipid bilayer. The presence of embedded edge activator (surfactant), CPC, can help solubilize MX in the liposomal lipid bilayer, which could significantly increase the %EE of the encapsulated drugs. This observation is in agreement with the data obtained by Duangjit et al.^{120,191} The authors state that cationic surfactants act as solubilizers for the drug in the liposomal bilayer. Moreover, they can affect the net positive charge of the bilayer, destabilize it and increase the elasticity of the vesicles. The similar effect

has also been observed in the case of ethosomes. As Marto et al.⁸⁸ disclosed in their study, incorporating ethanol into the liposomal formulation can solubilize the drug and create deformable lipid structures which could easily pass between skin corneocytes and subsequently enhance the skin retention and permeation.

The isoelectric point (pI) of MX was reported to be 2.6,¹²⁰ which is lower than the pH of hydration buffer (pH 5.5). Therefore, MX is presented in negatively charged form in our developed formulations. As it was mentioned above, CPC is a cationic surfactant which may contribute to the increased entrapment efficiency as a result of attractive electrostatic interactions between the negatively charged drug molecules and the surfactant.

The %EE of MX in transfersome was 96.04%, which was higher than the values obtained for QCT/DHQ loaded flavosomes (94.39% and 92.24%, respectively). The observed effect may be due to the fact that the flavonoids could compete with MX to reside in the vesicle bilayers. Furthermore, the diameter of the transfersome vesicles was significantly lower than these two flavosomes types, which may also be an indication that the effect described above does happen. Moreover, higher %EE correlated with lower vesicle diameter observed for transfersomes have also been reported by other authors.^{155,192}

The vesicle sizes of all these liposomal formulations were in the nano-size range of 60 – 110 nm with the size distribution (polydispersity index; PDI) of 0.2 - 0.3. Deformable liposomes had smaller vesicle sizes compared to

conventional liposomes, due to the incorporation of edge activator, CPC, which can achieve higher curvature, thus resulting in a decrease in vesicle size compared to conventional liposomes. The particle size in flavosomes was higher than that in transfersomes probably because more components had been encapsulated in these liposomes, which is in agreement with our prior study.¹⁸²

Zeta potential was used to quantitate the surface charge of these vesicles. The zeta potentials of these vesicles were in the positive range of 2 – 32 mV (Table 2). The results ranked in order of positive charge as transfersomes > flavosome-Q > flavosome-D >> conventional liposomes. The observed differences indicate that deformable liposomes reveal a higher tendency to resist aggregation and therefore provide better stability.

As disclosed by Cevc and Blume⁷³ and Hua⁷⁵, the embedded edge activator can destabilize the deformable liposomal lipid bilayers and enable these vesicles to penetrate through extracellular pathways among the skin cells within the stratum corneum. Then these flexible vesicles could deform to squeeze into the deeper layers of the skin. Therefore, deformability is one of the important characteristics of these flexible vesicles to measure their ability to squeeze through pores smaller than the liposomal diameters. The degree of deformability of each liposomal formulation were determined and are summarized in Table 26.

Table 26. Deformability index of liposomal vesicles. Data are presented as means \pm S.D. (n=3 for each formulation).

Formulation	Particles Size before Extrusion (nm)	Particles Size after Extrusion (nm)	Deformability Index
CLP	105.2 \pm 0.7	59.0 \pm 0.4	0.561 \pm 0.004
TFS	80.8 \pm 0.6	67.6 \pm 1.0	0.837 \pm 0.012*
FLSQ	82.4 \pm 0.7	79.8 \pm 0.7	0.969 \pm 0.008*
FLSD	96.1 \pm 1.4	95.8 \pm 0.1	0.997 \pm 0.001*

* $P < 0.05$ vs. CLP

The deformability index of conventional liposomes was found to be around 50 nm, which coincided with the size of the polycarbonate membranes (50 nm) used, indicating that the vesicles were quite rigid. However, the deformability indices of deformable liposomes, ie, transfersomes and flavosomes, were much greater than those of conventional liposomes. This suggested that the deformable vesicles regained their size after extrusion. It is noteworthy that the deformability indices of flavosomes were found to be close to 1, indicating that incorporating DHQ and QCT into the liposomes could affect the elasticity of vesicles by changing the fluidity and stability of the lipid bilayer.

To further characterize these vesicle systems, a TEM study was conducted for these developed liposomal vesicles. Figures 41 (A) to (D) present the TEM images for CLP, TFS, FLSQ and FLSD, respectively, which show spherical shapes for all these vesicle formulations.

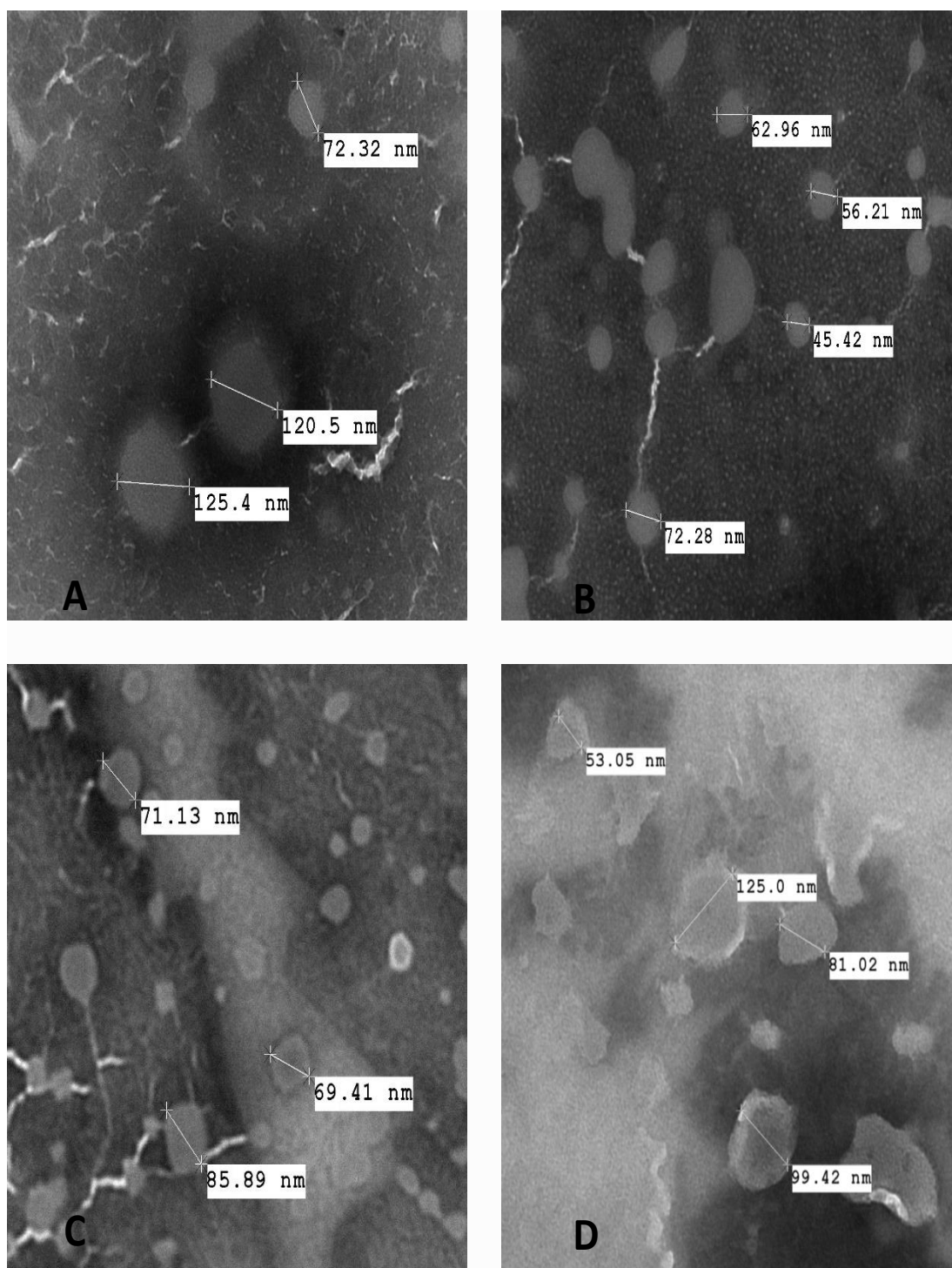


Figure 39. Transmission Electron Microscopy images of (A) conventional liposomes; (B) transfersomes; (C) flavosomes-Q; (D) flavosomes-D.

5.4.2. Characterization of MX-Loaded Hydrogels

Gels are transparent semisolid emulsions which contain a gelling agent to provide stiffness to a solution or colloidal dispersion (suspension) for external application to the skin.¹⁹³ This dosage form provides many advantages over suspensions, because it has less long-term stability issues, good adherence property to the site of application and better patient compliance. Furthermore, it can be used as a controlled release formulation.¹⁹⁴

Assessment of the mechanical properties is one of the crucial stages in the development of semi-solid formulations. For this purpose, multiple techniques are used, including tension/compression analysis, dynamic mechanical analysis (DMA) and oscillatory rheology. The latter one is a very precise tool that provides data on the viscoelastic properties. Viscoelasticity describes materials that can behave both like elastic solids and viscous fluids. Viscoelastic properties correlate with the physical appearance of semi-solid drug delivery systems, influence patient's perception but also affect the therapeutic efficiency.^{195,196}

The oscillatory stress sweeping (SS) was performed to monitor the values of storage (G') and loss moduli (G'') upon increasing oscillatory stress. The angular frequency of the oscillation was constant during the experiments ($1.0 \text{ Hz} = 6.2832 \text{ rad/s}$). To analyze the effects of drug and carriers on the polymer network stability, the measurements were conducted for all liposomal gels and compared to the properties of a blank liposomal gel (BLK-Gel) without actives (MX/QCT/DHQ)

and a gel containing the drug in a dissolved form, without liposomes (MX-Gel). The logarithmic plots presented in Figure 3a showed that all gels revealed a wide range of linear viscoelasticity, termed LVR (Linear Viscoelastic Region), where the values of storage modulus (G') remained constant and independent of the increasing stress. As observed, the values of G' in LVR were predominantly higher than those of G'' , which clearly indicates that the tested gels were more elastic than fluid-like. The LVR was also determined to depict the stability of the gels structure, since structural properties are best related to elasticity. Samples with broad LVR can be classified as well-dispersed and stable.

Also demonstrated in Figure 42a, the values of both moduli became less distinct above LVR, which can be attributed to maximum extension of the polymer chains and partial breakage of hydrogen bonds. From the SS plots, the cross-over points were determined and graphed in Figure 42b. This parameter is the value of stress at which the moduli equalize and depicts the moment of entire gel structure breakage. As revealed in Figure 42b, the BLK-Gel was the most durable, while the MX-Gel turned out to be most prone to deformation, which was depicted by lower value of cross-over point, of approximately 55%. The mechanical stability of MX-loaded liposomal gel formulations decreased about 20% in comparison to BLK-Gel. It can be stated that addition of MX decreased the gel durability, most probably by weakening the interactions between hydrophobic polypropylene oxide (PPO) chains. In the case of MX loaded liposomal gels, the

effect was less significant because of partial incorporation of the drug, however the observed effect could also be related to adherence of PPO blocks to the surface of liposomes or partial embedding into the phospholipid layer.¹⁹⁷

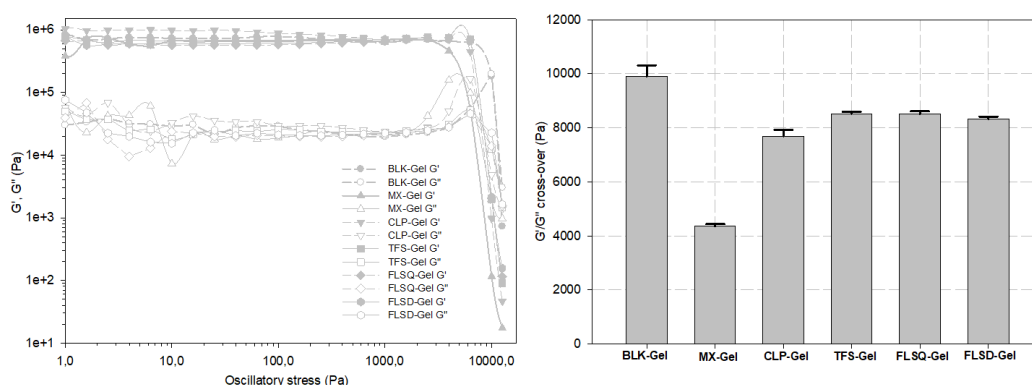


Figure 40. Amplitude sweeping plots obtained for the gels (a) and calculated cross-over values (b) ($n=3$ for each formulation, data are presented as means \pm S.D.)

Oscillatory measurements were also performed to determine the thermal transition of the gels. Samples were subjected to increasing temperature in the range of 5.0°C to 40°C and the G' value was monitored. As presented in Figure 43, none of the gels revealed a sharp transition from liquid to semi-solid form ($T_{\text{sol-gel}}$). In all cases the structure was forming in a wide temperature range. The highest $T_{\text{sol-gel}}$ was observed for MX-Gel which was correlated with the data obtained in the previous experiment. This confirmed that the weaker the structure, the higher the gelation temperature. The BLK-Gel started to thicken at the lowest temperature ($\sim 6-7^\circ\text{C}$). Similar behavior was observed for the MX-loaded deformable liposomal gels, while a conventional liposomal gel formulation recorded similar $T_{\text{sol-gel}}$ as that

of MX-Gel, indicating it was less stable than the deformable liposomal gel formulations.

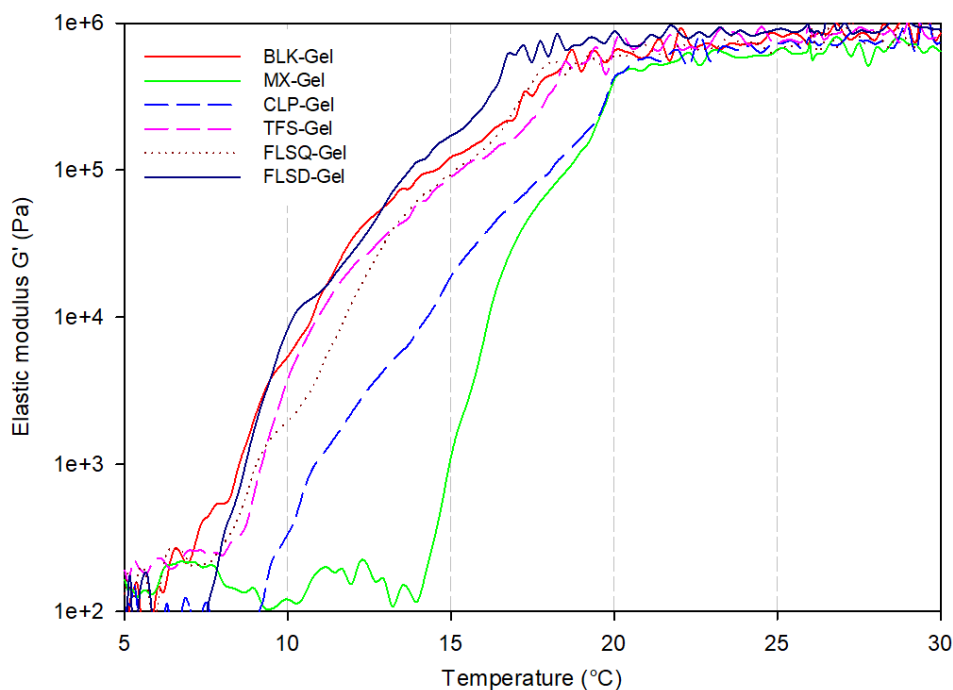


Figure 41. Temperature sweeping of the gels. (n=3 for each formulation, data are presented as means \pm S.D.).

To study the morphology of these prepared gel formulations, a TEM analysis was performed. Figures 44 (A) to (E) present the obtained TEM images for MX-Gel, CLP-Gel, TFS-gel, FLSQ-Gel and FLS-D gel, respectively. Stained spherical shape vesicles were observed in liposomal gel formulations, but it was absent in MX-loaded plain Poloxamer P407 gel, as expected.

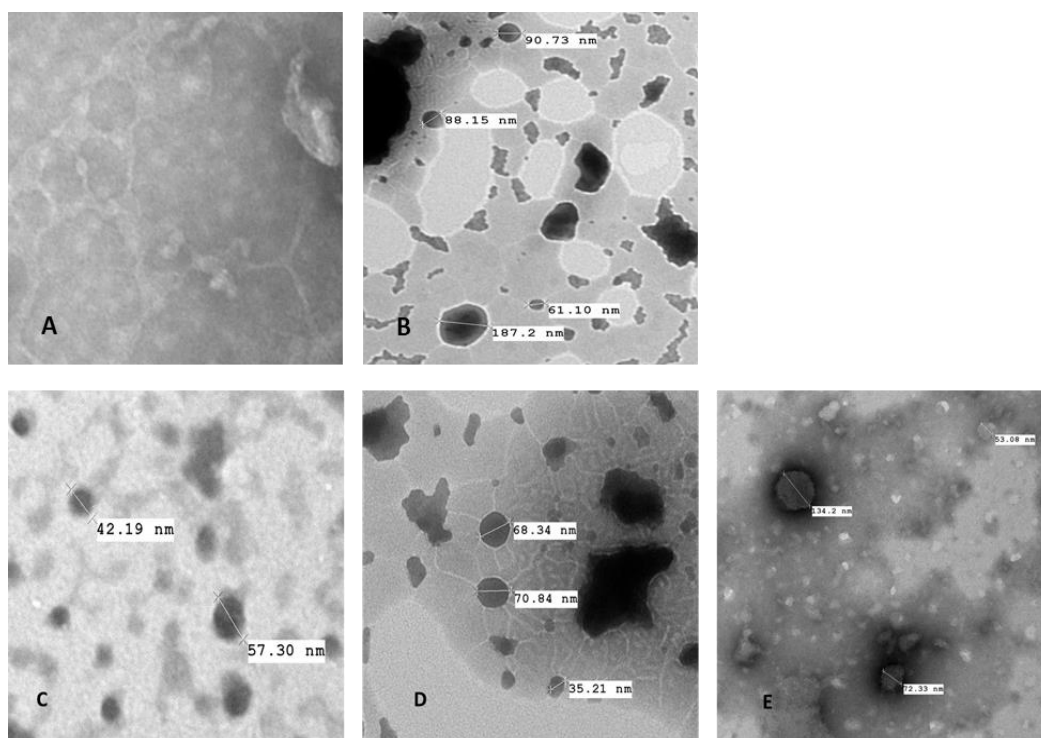


Figure 42. Transmission Electron Microscopy images of (A) MX-Gel (B) CLP-Gel (C) TFS-Gel (D) FLSQ-Gel (E) FLSD-Gel.

The apparent particle size and size distribution were also determined for these liposomal gel formulations and the data obtained was compared with those of the liposomal vesicles and summarized in Table 27. It suggested that the particle size increased with the addition of poloxamer P407. A similar observation was also disclosed in the study conducted by Pandita et al.¹⁹⁸ In the study, they suggested that the increased viscosity of the outer phase caused by the increase of poloxamer concentration might be the reason of the particle size increase. As stated in the technical note provided by Malvern Instrument,¹⁹⁹ the particle size determination using Dynamic Light Scattering technique can be affected by the ionic strength of medium, surface structure, viscosity and non-spherical particles. Therefore, the apparent particle size observed in these gel formulations might not directly

describe the particle size of the embedded vesicles. This is supported by the TEM images shown in Figure 44, in which the liposomal vesicles embedded in the hydrogel had a similar particle size with those in the suspensions.

Table 27. Physiochemical properties of the obtained vesicles. Data are presented as means \pm S.D. (n=3)

Sample ID	Description	Liposomal Vesicles		Liposomal Gel	
		Average Diameter (nm)	PDI ^a	Average Diameter (nm)	PDI ^c
CLP	Conventional Liposome	111.4 \pm 0.2	0.257 \pm 0.008	245.4 \pm 3.4	0.133 \pm 0.012
TFS	Transfersome	62.3 \pm 0.3	0.287 \pm 0.013	231.0 \pm 1.2	0.147 \pm 0.015
FLSQ	Flavosome-Q	66.0 \pm 0.6	0.281 \pm 0.002	236.2 \pm 1.8	0.187 \pm 0.015
FLSD	Flavosome-D	97.0 \pm 1.3	0.298 \pm 0.023	246.8 \pm 5.2	0.178 \pm 0.023

a: Polydispersity Index

5.4.3. Ex Vivo Skin Permeation Study

To study the potential of topical delivery of MX using these liposomal hydrogel prototypes, the *ex vivo* skin permeation study through human cadaver skin was conducted using Franz diffusion cells. The content of MX in the liposomal gel was targeted at 2 mg/g with the exception of CLP-gel due to its low entrapment efficiency. A gel formulation with MX dissolved in pH 7.4 PBS (MX-Gel) was also prepared as control. The concentration of MX in each formulation is summarized in Table 28. The drug permeation profiles of MX plotted as a function of time and amount of MX deposited in the epidermal and dermal layers after skin permeation study are shown in Figures 6a and 6b,

respectively. The values of steady state fluxes (J_{ss}), permeability coefficients (K_p), enhancement ratio, lag time and correlation coefficient (r^2) are presented in Table 28.

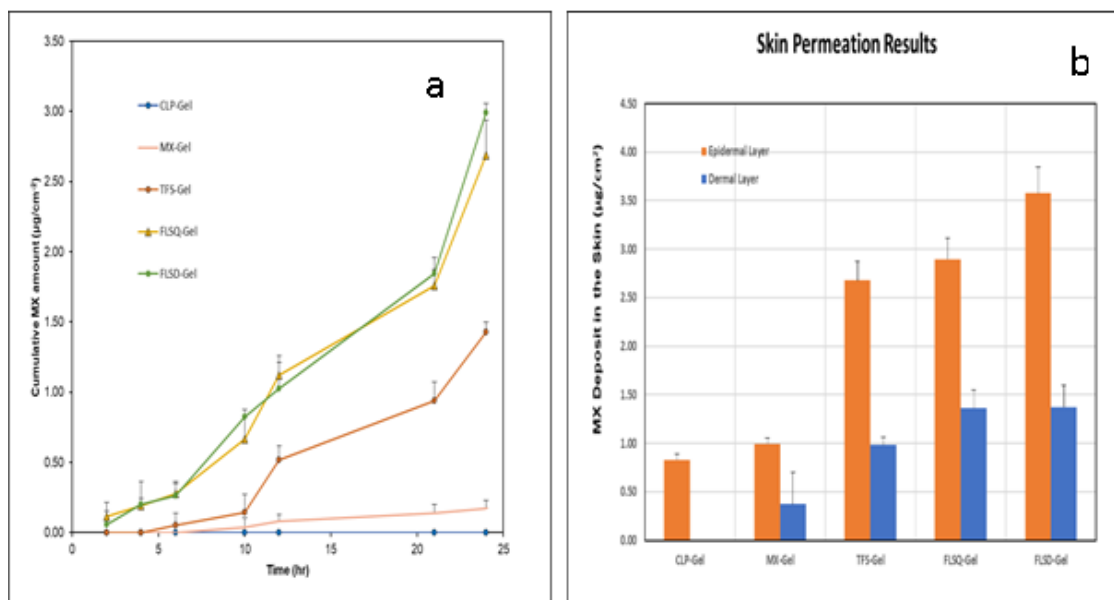


Figure 43. (a) *Ex Vivo* drug permeation profiles of Meloxicam (MX) loaded liposomal gel formulations over 24 hours; (b) MX deposited in the different layers of skin after 24-hour skin permeation study from formulations tested (n =3 for each formulation, data are presented as means \pm S.D.).

As demonstrated in Figure 45, compared to MX-gel, no MX content was observed in donor compartments and the dermis when the CLP-gel formulation was applied, despite that a similar level of MX was obtained in the epidermis. This may indicate that the rigid structure of conventional liposomes prevented their transport to the deeper layer of the skin. Therefore, it revealed that conventional liposomal gel did not produce any benefit over a simple MX gel formulation.

However, deformable liposomal gel formulations, TFS-gel, FLSQ-Gel and FLSD-gel, recorded a higher amount of MX observed in the receptor

compartments and distributed in the different layers of skin, compared to the controls, CLP-gel and MX-gel. Moreover, the highest MX content was obtained when flavosome loaded gel formulations were applied on the skin.

Table 28. Permeation parameter obtained for the investigated gel formulations. Data are presented as means \pm S.D. (n=3 for each formulation).

Formulation	J _{ss} ^a ($\mu\text{g}/\text{cm}^2/\text{h}$)	Concentration ($\mu\text{g}/\text{mg}$) ^c	K _p ^b ($\text{mg}/\text{cm}^2/\text{h}$)	Enhancement Ratio	Lag Time (h)
CLP-Gel	-	0.219 \pm 0.005	-	-	-
MX-Gel	0.017 \pm 0.006	0.428 \pm 0.057	(3.93 \pm 1.47) $\times 10^{-2}$	1	4.17 \pm 1.34
TFS-Gel	0.128 \pm 0.010*	1.906 \pm 0.014	(6.71 \pm 0.52) $\times 10^{-2}$ *	1.71	4.42 \pm 0.60
FLSQ-Gel	0.222 \pm 0.014*#	1.885 \pm 0.030	(11.78 \pm 0.76) $\times 10^{-2}$ *#	3.00	2.54 \pm 0.77#
FLSD-Gel	0.245 \pm 0.010*#	2.064 \pm 0.042	(11.89 \pm 0.50) $\times 10^{-2}$ *#	3.03	2.89 \pm 0.55#

* $P < 0.05$ vs. MX-Gel; # $P < 0.05$ vs. TFS-Gel

a: J_{ss}: steady-state flux; b: K_p: permeability coefficient;

c: Concentration is expressed as μg of meloxicam/mg of gel formulation

To discount the effect of different MX concentrations, K_p of these investigated formulations was determined and recorded in Table 28. Subsequently, the enhancement ratios were calculated by dividing K_p of each deformable liposomal gel formulation against K_p of MX-gel. The enhancement ratios of TFS-gel, FLSQ-Gel and FLSD-gel were found to be 1.71, 3.00 and 3.03, respectively, indicating flavosomal loaded gel formulations showed the highest permeation. Additionally, the lag time for flavosomal gel formulations are shorter than those found for TFS-gel and MX-gel, revealing a faster on-site release of MX by these two formulations. This indicated a potential benefit for faster pain relief and anti-inflammatory effect by utilization of the flavosomal drug delivery system.

The obtained results are in good agreement with numerous studies which confirm that classical liposomes have limited value of promoting skin delivery of various drugs due to the fact of insufficient skin penetration ability, which is the result of low deformability.²⁰⁰ As it was proven, intact liposomes are not able to penetrate into the granular layers of the epidermis.²⁰¹ The positive effect of flavonoids on skin penetration of MX can be the result of two mechanisms. First, it can be attributed to their influence on the deformability of the vesicles followed by deeper penetration into the skin. Second, by interaction with *stratum corneum*, flavonoids can increase the fluidity of lipid layers and therefore promote translocation of the drug. Numerous studies confirmed that QCT and DHQ reveal a high ability to interact with the lipid bilayers and increase the fluidity of phosphatidylcholine liposome membranes.²⁰²⁻²⁰⁴ The interaction is described as strongly concentration and pH dependent.^{166,205} The changes in physical properties of the lipid bilayers are the result of interstitial embedding into the hydrophobic domains or the polar headgroup domains. Such behavior may be related to both the lipophilic nature of QCT/DHQ and their interactions with the polar headgroups of phospholipids.

The release kinetics of these liposomal gel formulations was calculated using zero order, first order and Higuchi model, and the obtained results are summarized in Table 29. The best fit with the highest correlation coefficient (r^2) was found to be zero-order for all formulations. Therefore, J_{ss} was determined over the period of 0

to 24 hours with the correlation coefficient (r^2) for these formulations ranging from 0.94 to 0.97, displaying a zero-order release profile.

Table 29. Kinetic models for the investigated gel formulations.

Formulation	Zero order		First order		Higuchi model	
	K ^a	r ² ^b	K	r ²	K	r ²
MX-Gel	0.008	0.969	0.04	0.873	0.053	0.919
TFS-Gel	0.064	0.936	0.074	0.873	0.399	0.861
FLSQ-Gel	0.111	0.955	0.059	0.924	0.701	0.898
FLSD-Gel	0.123	0.947	0.067	0.867	0.774	0.889

a: K: slope; b: r²: correlation coefficient

Moreover, the release profiles of TFS-Gel and FLS-Gel displayed a two-phases release, as demonstrated in Figure 45a. The permeation rate accelerated after 10 hours for TFS-Gel and 6 hours for FLS-Gel, respectively. As illustrated in detail by El Maghraby et al,⁵⁴ the transdermal delivery mechanisms of liposomal systems can be categorized into: a) free drug, b) penetration enhancing, c) vesicle adsorption to and/or fusion with the SC, d) intact vesicular skin penetration and e) transappendageal penetration.

The main potential delivery routes could be b), c) and d) for these deformable liposomes under these testing conditions. However, the efficiency and the extent of each route contributing to the delivery of MX into the receptor compartment may be very different. Therefore, for phase 1, the passive diffusion of MX might be driven by one or two of these delivery mechanisms while all three of delivery routes contribute to accelerate the permeation rate in phase 2.

5.4.4. Skin Penetration of DiI-Labeled Liposomal Gel Formulations

The depth of the full thickness human cadaver skin penetration of the DiI-labeled vesicles containing gel formulations was evaluated using fluorescence microscopy. According to the Confocal Laser Scanning Microscopy (CLSM) images displayed in Figure 46, CLP-gel, TFS-gel, FLSQ-gel, and FLSD-gel penetrated into the skin up to 30, 120, 180 and 210 μm , respectively.

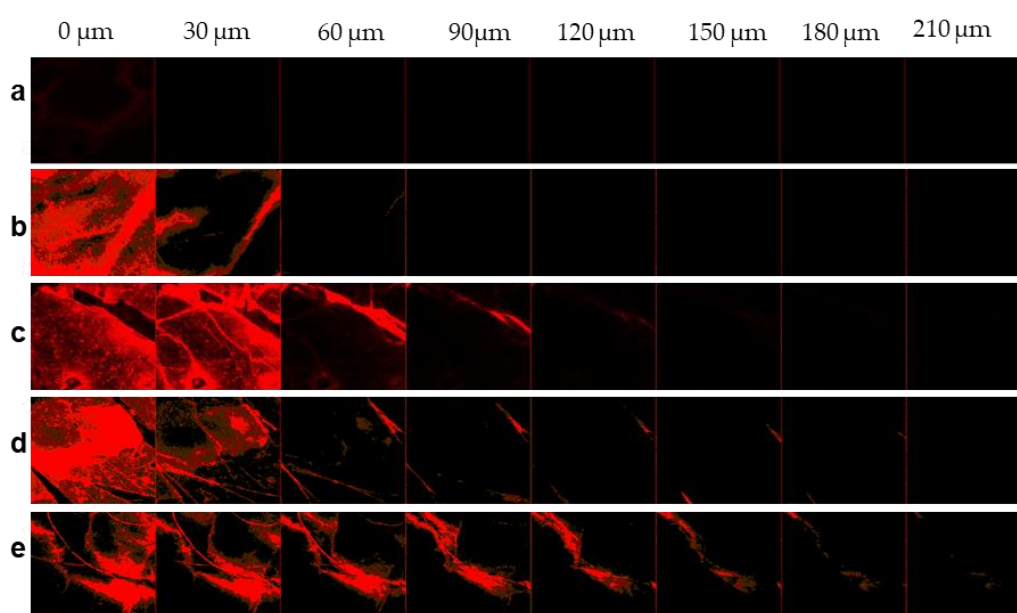


Figure 44. Confocal Laser Scanning Microscopy Images taken at different depths of the full thickness human cadaver skin after 24 hours permeation of DiI-labeled gel formulations containing a) Untreated skin, b) CLP-gel, c) TFS-gel, d) FLSQ-gel and e) FLSD-gel (magnification 10X).

The observed results indicated gel formulations containing deformable liposomes had higher skin permeability than conventional liposomes. Among the deformable liposomal formulations, flavosomal gel formulations displayed the highest permeability through the deeper layers of the skin. These findings confirmed with the observations described above.

5.4.5. Effect of Storage Study for Liposomal Formulation and Gel Formulation

The effect of storage study has been conducted on liposomal suspensions and gel formulations for 90 days. As the obtained data in Figure 8a demonstrated, deformable liposomes were stable with negligible loss of entrapped drug under refrigerated condition for 90 days; while conventional liposomes showed 60% loss of drug content after 30 days and then plateaued through 90 days. The significant drug loss observed in CLP was due to the agglomeration of the vesicles, which was affected by their surface charge.

In the present study, zeta potential has been employed to estimate the surface charge. As many studies revealed,¹⁰⁰⁻¹⁰² higher positive or negative values of zeta potential of nano vesicles indicate good physical stability due to electrostatic repulsion of individual particles. On the other hand, zeta potential value close to zero can result in particle aggregation and flocculation due to the van der Waals attractive forces.

As data summarized in Table 25 showed, zeta potential of conventional liposomes was found to be around 2 mV while those of deformable liposomes ranged from 24-32 mV. These results confirmed with those obtained in the stability data.

The % drug lost in CLP-gel was found to be 3%, 8% and 10% at 30, 60 and 90-day storage at room temperature, which is a significant improvement if compared to the stability data observed in the suspension. High viscosity of the

hydrogel medium may be considered as a factor preventing agglomeration of the dispersed vesicles which could also contribute to higher drug stability. The deformable liposomal gel formulations were all stable for 90 days at room temperature, as displayed in Figure 47.

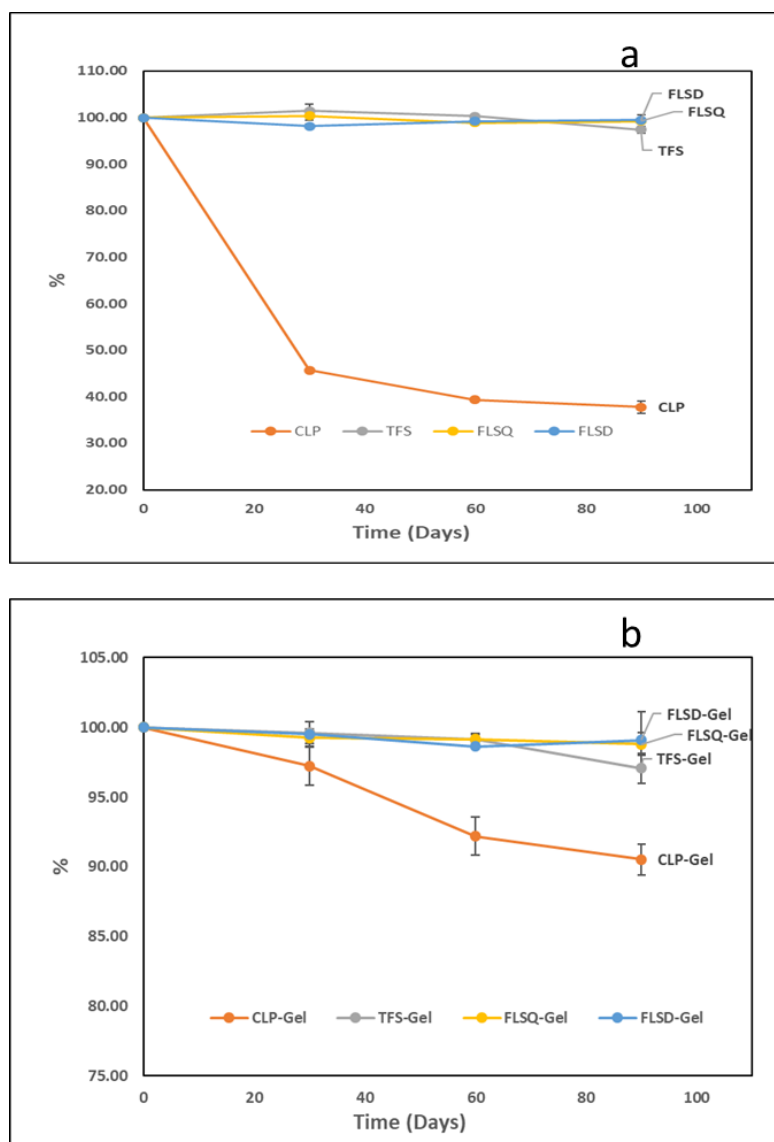


Figure 45. Stability study results of a) meloxicam loaded liposomal suspensions at 5±3 °C for 30, 60 and 90 days, b) meloxicam loaded liposomal gel formulations at 25±5 °C for 30, 60 and 90 days (n=3 for each formulation).

5.5. Conclusions

In this study, MX loaded deformable liposomal gel formulations containing transfersomes or flavosomes were prepared and tested as potential drug delivery carriers for topical use. These vesicles exhibited homogeneous particle sizes less than 120 nm with a higher entrapment rate as compared to conventional liposomes. These liposomal suspensions were then incorporated into 20% (w/w) poloxamer P407 hydrogel and characterized using rheological analysis, *ex vivo* permeation study through human cadaver skin and stability tests. It was shown that despite of thickening of the poloxamer 407 gel structure in comparison to the liposome-free gel, the deformable liposomal gel formulations promoted drug permeation across the skin to the deeper layers with high efficiency. The enhancement effect was also clearly visible by CLSM in comparison to the formulation containing conventional liposomes. Notably, the flavosomal drug delivery system produced a shorter lag time compared to the transfersomal gel formulation, indicating a potential benefit for faster pain relief and anti-inflammatory effects.

5.6. Publication Information

This chapter is a slightly modified version of Deformable liposomal hydrogel for dermal and transdermal delivery of meloxicam published in *International Journal of Nanomedicine* (Zhang ZJ, Osmałek T, Michniak-Kohn B. Deformable Liposomal Hydrogel for Dermal and Transdermal Delivery of Meloxicam. *Int J Nanomedicine*.

2020;15:9319-9335, <https://doi.org/10.2147/IJN.S274954>) and has been reproduced here.

The rheological analysis of gel formulations was performed by Dr. Tomasz Osmalek from Chair and Department of Pharmaceutical Technology, Poznań University of Medical Sciences, Poland.

Chapter 6. Thesis Study Conclusions and Future Plans

The purpose of the study is to investigate and improve dermal and transdermal delivery of the model oxica drug, meloxicam (MX), using deformable liposome delivery system. The preset goals are listed below:

Aim 1: To Develop and Validate Analytical Methodology for the Characterization of Liposomal Formulations, including both Liposomes and Liposomal Hydrogel Formulations

Aim 2: To Develop and Optimize MX Loaded Deformable Liposomal Formulations and Preparation Processes

Aim 3: To Develop and Characterize MX Loaded Deformable Liposomal Topical Gel formulations

All these specific aims have been achieved and the obtained results reported in this dissertation demonstrated that the developed deformable liposomes, transfersomes and flavosomes, can significantly enhance both dermal and transdermal delivery of MX, compared to conventional liposomes.

Initially, an HPLC method was developed and validated to show that it is specific, linear, sensitive, accurate, reproducible and stable at room temperature for the simultaneous quantitation of MX, DHQ and QCT. This method has been used for the determination of drug entrapment efficiency, drug loading and drug content in permeation study samples.

To conduct bioavailability assessment of topical formulations, I have used the dermatopharmacokinetic (DPK) approach suggested by FDA, in which the drug concentration in the skin is determined continuously or intermittently for a period of time. Human or animal skin permeation study using Franz Diffusion Cell is one of the standard in vitro tests to assess the skin kinetics of topical formulations. In our study, we have used human cadaver skin model to generate a concentration profile following topical application of liposomal suspension or hydrogel formulations by conducting skin deposition study on both epidermal and dermal layers, flux determination on permeated samples, and visualization using CLSM.

Secondly, the composition and preparation process of conventional liposomes and transfersomes were investigated. It was found that the type, grade and the content of phospholipids played a key role in the characteristics of liposomes, such as vesicle size, PDI, zeta potential, entrapment efficiency, etc. Based on the obtained data, vesicles prepared using 0.8% USPC has the highest loading of MX, particle size less than 200 nm with uniform size distribution (PDI less than 0.3). Therefore, liposomal formulations would be prepared using 0.8% USPC in the further experiments.

Then, the prepared vesicles along with two different types of microemulsions were evaluated as potential dermal delivery carriers for meloxicam. When comparing the w/o and o/w microemulsion performance with the use of an *ex vivo* model involving human cadaver skin, the highest flux and permeation values were obtained

for transfersomes, indicating these drug carriers as the most promising in terms of topical drug delivery.

Used the transfersome composition developed in aim2 as the base formulation, flavosomes, novel deformable liposomes containing flavonoids, were developed and tested as a potential drug delivery carrier for topical use in skin preparations. These vesicles exhibited homogeneous particle sizes less than 150 nm with a higher degree of deformability as compared to transfersome. Compared to transfersomes, the investigated formulations demonstrated improved permeability for MX, a potent NSAID, through the skin. CLSM images suggested that these deformable vesicles could deliver MX to the deeper layers of skin. The mechanism of the observed permeation enhancement may be due to the ability of flavonoids to interact with and penetrate through the lipid bilayer of the stratum corneum of the skin. Previous studies conducted by multiple groups suggest that flavonoids may modify the lipid packing order of the cell membrane by interacting with or incorporating in the phospholipids to form flavonoid-phospholipid complexes. These compounds can penetrate the lipid bilayers by affecting the membrane fluidity as well as stability.

Notably, significant skin distribution of the two flavonoids, DHQ and QCT, was observed in *ex vivo* skin permeation studies. Since flavonoids are natural anti-inflammatories, flavosomes might be used as potential nanocarriers for co-delivery of other anti-inflammatory compounds such as meloxicam.

Although many studies have been conducted for the development of gel formulations or liposomal formulations of MX, the researches on the liposomal hydrogel formulations for MX via topical route were scarce. In this study, MX loaded deformable liposomal gel formulations containing transfersomes or flavosomes were prepared and tested as potential drug delivery carriers for topical use.

Liposomal suspension is not a practical dosage form due to its instability at room temperature, which was observed during the aim 2 studies. In addition, the liposomal formulations developed in aim 2 had low MX content, so the resulting liposomal gel formulations did not yield any meaningful permeation results. Therefore, the liposomal formulations were modified in aim 3 to increase the content of MX by 5 folds and greatly improve the stability of the liposome suspensions.

During development, both P407-based and Carbomer-based gel formulations have been evaluated. The P407 gel formulation, was selected because it provided better homogeneity and stability due to the “cold method” preparation procedure.

It was decided to use a 20% concentration of poloxamer in order to achieve stable semi-solid consistency during application which is of high importance in the case of convenient patient use.

These optimized liposomal vesicles exhibited homogeneous particle sizes less than 120 nm with a higher entrapment rate as compared to conventional liposomes. These liposomal suspensions were then incorporated into 20% (w/w) poloxamer P407 hydrogel and characterized using rheological analysis, *ex vivo* permeation study

through human cadaver skin and stability tests. It was shown that despite of thickening of the poloxamer 407 gel structure in comparison to the liposome-free gel, the deformable liposomal gel formulations promoted drug permeation across the skin to the deeper layers with high efficiency. The enhancement effect was also clearly visible by CLSM in comparison to the formulation containing conventional liposomes. Furthermore, flavosomal drug delivery system produced a shorter lag time compared to the MX loaded plain gel and the transfersomal gel formulation, indicating a potential benefit for faster pain relief and anti-inflammatory effects.

To develop a commercially viable formulation containing flavosomes, the most promising deformable liposome drug delivery system, we could conduct the below experiments to expand the current study:

- Currently, the batch size of liposomal suspensions is limited to 40 mL and the process is time consuming due to the nitrogen drying technique used. Therefore, various scale up processes and efficient technique can be evaluated and validated to produce larger batch size of liposomal suspensions with reproducible physiochemical properties;
- In this study, a 20% poloxamer P407 hydrogel was prepared as a model gel system, which is not a commercially viable formulation due to the material and manufacturing cost and lack of safety/stability data. Therefore, in depth hydrogel formulation development using other thickening agents/polymers, antioxidant, preservatives, etc. can be investigated;

- The characterization, mechanistic analysis, pharmacokinetics and toxicological studies on the optimized flavosomal gel formulations can be conducted, including but not limited to homogeneity analysis, stability evaluation, rheological characterization, skin permeation study, fluorescent imaging, skin irritation/sensitization studies and screening of anti-inflammatory activity using animal models.

References

1. Xu S, Rouzer CA, Marnett LJ. Oxicams, a class of nonsteroidal anti-inflammatory drugs and beyond. *IUBMB Life*. 2014;66(12):803-811.
2. Lombardino JG, Wiseman EH, McLamore WM. Synthesis and antiinflammatory activity of some 3-carboxamides of 2-alkyl-4-hydroxy-2H-1,2-benzothiazine 1,1-dioxide. *J Med Chem*. 1971;14(12):1171-1175.
3. Lombardino JG, Wiseman EH. Sudoxicam and related N-heterocyclic carboxamides of 4-hydroxy-2H-1,2-benzothiazine 1,1-dioxide. Potent nonsteroidal antiinflammatory agents. *J Med Chem*. 1972;15(8):848-849.
4. Tasaki Y, Yamamoto J, Omura T, et al. Oxicam structure in non-steroidal anti-inflammatory drugs is essential to exhibit Akt-mediated neuroprotection against 1-methyl-4-phenyl pyridinium-induced cytotoxicity. *Eur J Pharmacol*. 2012;676(1-3):57-63.
5. Miceli A. Piroxicam (Feldene): Long-Lasting FANS/NSAID da spostare.
6. Goldman AP, Williams CS, Sheng H, et al. Meloxicam inhibits the growth of colorectal cancer cells. *Carcinogenesis*. 1998;19(12):2195-2199.
7. Montejo C, Barcia E, Negro S, Fernandez-Carballido A. Effective antiproliferative effect of meloxicam on prostate cancer cells: development of a new controlled release system. *Int J Pharm*. 2010;387(1-2):223-229.
8. Patel MM, Amin AF. Formulation and development of release modulated colon targeted system of meloxicam for potential application in the prophylaxis of colorectal cancer. *Drug Deliv*. 2011;18(4):281-293.
9. Arantes-Rodrigues R, Pinto-Leite R, Ferreira R, et al. Meloxicam in the treatment of in vitro and in vivo models of urinary bladder cancer. *Biomed Pharmacother*. 2013;67(4):277-284.
10. Tsubouchi Y, Mukai S, Kawahito Y, et al. Meloxicam inhibits the growth of non-small cell lung cancer. *Anticancer Res*. 2000;20(5A):2867-2872.
11. Patoia L, Santucci L, Furno P, et al. A 4-week, double-blind, parallel-group study to compare the gastrointestinal effects of meloxicam 7.5 mg, meloxicam 15 mg, piroxicam 20 mg and placebo by means of faecal blood loss, endoscopy and symptom evaluation in healthy volunteers. *Br J Rheumatol*. 1996;35 Suppl 1:61-67.
12. Altman RD, Barthel HR. Topical therapies for osteoarthritis. *Drugs*. 2011;71(10):1259-1279.
13. Chandrashekar NS, Shobha Rani RH. Physicochemical and pharmacokinetic parameters in drug selection and loading for transdermal drug delivery. *Indian J Pharm Sci*. 2008;70(1):94-96.
14. Kalia YN, Guy RH. Modeling transdermal drug release. *Adv Drug Deliv Rev*. 2001;48(2-3):159-172.

15. Moser K, Kriwet K, Naik A, Kalia YN, Guy RH. Passive skin penetration enhancement and its quantification in vitro. *Eur J Pharm Biopharm.* 2001;52(2):103-112.
16. Farahmand S, Maibach HI. Transdermal drug pharmacokinetics in man: Interindividual variability and partial prediction. *Int J Pharm.* 2009;367(1-2):1-15.
17. Williams AC, Barry BW. Penetration enhancers. *Adv Drug Deliv Rev.* 2004;56(5):603-618.
18. Ruela ALM, Perissinato AG, Lino MEdS, Mudrik PS, Pereira GR. Evaluation of skin absorption of drugs from topical and transdermal formulations %J Brazilian Journal of Pharmaceutical Sciences. 2016;52:527-544.
19. Benson HAE, Grice JE, Mohammed Y, Namjoshi S, Roberts MS. Topical and Transdermal Drug Delivery: From Simple Potions to Smart Technologies. *Curr Drug Deliv.* 2019;16(5):444-460.
20. Chen J, Gao Y. Strategies for meloxicam delivery to and across the skin: a review. *Drug Deliv.* 2016;23(8):3146-3156.
21. Organization GWH. WHO Guidelines on Hand Hygiene in Health Care: First Global Patient Safety Challenge Clean Care Is Safer Care. . 2009.
22. Organization GWH. Physiology of normal skin. *WHO Guidelines on Hand Hygiene in Health Care: First Global Patient Safety Challenge Clean Care Is Safer Care* 2009(6).
23. Bharkatiya M, Nema, RK. Skin penetration enhancement techniques. *J Young Pharmacists* 2009;1:5.
24. Benson HA. Transdermal drug delivery: penetration enhancement techniques. *Curr Drug Deliv.* 2005;2(1):23-33.
25. Din FU, Aman W, Ullah I, et al. Effective use of nanocarriers as drug delivery systems for the treatment of selected tumors. *Int J Nanomedicine.* 2017;12:7291-7309.
26. Mishra B, Patel BB, Tiwari S. Colloidal nanocarriers: a review on formulation technology, types and applications toward targeted drug delivery. *Nanomedicine.* 2010;6(1):9-24.
27. Sun T, Zhang YS, Pang B, Hyun DC, Yang M, Xia Y. Engineered nanoparticles for drug delivery in cancer therapy. *Angew Chem Int Ed Engl.* 2014;53(46):12320-12364.
28. Aljuffali IA, Hsu CY, Lin YK, Fang JY. Cutaneous delivery of natural antioxidants: the enhancement approaches. *Current pharmaceutical design.* 2015;21(20):2745-2757.
29. Mehdi R, Shaker AM. Lipid Nanoparticles and their Application in Nanomedicine. *Current Pharmaceutical Biotechnology.* 2016;17(8):662-672.
30. Müller RH, Radtke M, Wissing SA. Solid lipid nanoparticles (SLN) and nanostructured lipid carriers (NLC) in cosmetic and dermatological preparations. *Adv Drug Deliv Rev.* 2002;54 Suppl 1:S131-155.

31. Weng Y, Liu J, Jin S, Guo W, Liang X, Hu Z. Nanotechnology-based strategies for treatment of ocular disease. *Acta pharmaceutica Sinica B*. 2017;7(3):281-291.
32. Rao JP, Geckeler KE. Polymer nanoparticles: Preparation techniques and size-control parameters. *Progress in Polymer Science*. 2011;36(7):887-913.
33. Wang X, Wang Y, Chen ZG, Shin DM. Advances of cancer therapy by nanotechnology. *Cancer Res Treat*. 2009;41(1):1-11.
34. Kahraman E, Gungor S, Ozsoy Y. Potential enhancement and targeting strategies of polymeric and lipid-based nanocarriers in dermal drug delivery. *Ther Deliv*. 2017;8(11):967-985.
35. Singh N, Joshi A, Toor AP, Verma G. Chapter 27 - Drug delivery: advancements and challenges. In: Andronescu E, Grumezescu AM, eds. *Nanostructures for Drug Delivery*. Elsevier; 2017:865-886.
36. Okoro Uchechi JDNOaAAA. Nanoparticles for Dermal and Transdermal Drug Delivery. *Application of Nanotechnology in Drug Delivery*. 2014.
37. Wang Z, Itoh Y, Hosaka Y, et al. Novel transdermal drug delivery system with polyhydroxyalkanoate and starburst polyamidoamine dendrimer. *J Biosci Bioeng*. 2003;95(5):541-543.
38. Chauhan AS, Sridevi S, Chalasani KB, et al. Dendrimer-mediated transdermal delivery: enhanced bioavailability of indomethacin. *J Control Release*. 2003;90(3):335-343.
39. Cheng Y, Man N, Xu T, et al. Transdermal delivery of nonsteroidal anti-inflammatory drugs mediated by polyamidoamine (PAMAM) dendrimers. *J Pharm Sci*. 2007;96(3):595-602.
40. Venuganti VV, Perumal OP. Effect of poly(amidoamine) (PAMAM) dendrimer on skin permeation of 5-fluorouracil. *Int J Pharm*. 2008;361(1-2):230-238.
41. Niederhafner P, Sebestík J, Jezek J. Peptide dendrimers. *Journal of peptide science : an official publication of the European Peptide Society*. 2005;11(12):757-788.
42. Esfand R, Tomalia DA. Poly(amidoamine) (PAMAM) dendrimers: from biomimicry to drug delivery and biomedical applications. *Drug Discov Today*. 2001;6(8):427-436.
43. D'Emanuele A, Attwood D. Dendrimer-drug interactions. *Adv Drug Deliv Rev*. 2005;57(15):2147-2162.
44. Loong KKSaWV. Introductory Chapter: From Microemulsions to Nanoemulsions. *Nanoemulsions - Properties, Fabrications and Applications*. 2019.
45. Sonnevile-Aubrun O, Simonnet JT, L'Alloret F. Nanoemulsions: a new vehicle for skincare products. *Adv Colloid Interface Sci*. 2004;108-109:145-149.
46. Bangham AD. Model membranes. *Chem Phys Lipids*. 1972;8(4):386-392.
47. Bangham AD. Lipid bilayers and biomembranes. *Annu Rev Biochem*. 1972;41:753-776.

48. Bangham AD, Horne RW. Negative Staining of Phospholipids and Their Structural Modification by Surface-Active Agents as Observed in the Electron Microscope. *J Mol Biol.* 1964;8:660-668.
49. Bangham AD, Horne RW, Glauert AM, Dingle JT, Lucy JA. Action of saponin on biological cell membranes. *Nature.* 1962;196:952-955.
50. Deshpande PP, Biswas S, Torchilin VP. Current trends in the use of liposomes for tumor targeting. *Nanomedicine (Lond).* 2013;8(9):1509-1528.
51. Malam Y, Loizidou M, Seifalian AM. Liposomes and nanoparticles: nanosized vehicles for drug delivery in cancer. *Trends in pharmacological sciences.* 2009;30(11):592-599.
52. Beltrán-Gracia E, López-Camacho A, Higuera-Ciapara I, Velázquez-Fernández JB, Vallejo-Cardona AA. Nanomedicine review: clinical developments in liposomal applications. *Cancer Nanotechnology.* 2019;10(1):11.
53. advantage of LNP in topical (figure 5).
54. El Maghraby GM, Barry BW, Williams AC. Liposomes and skin: from drug delivery to model membranes. *Eur J Pharm Sci.* 2008;34(4-5):203-222.
55. Ganesan MG, Weiner ND, Flynn GL, Ho NFH. Influence of liposomal drug entrapment on percutaneous absorption. *International Journal of Pharmaceutics.* 1984;20(1):139-154.
56. El Maghraby GM, Williams AC, Barry BW. Skin delivery of oestradiol from deformable and traditional liposomes: mechanistic studies. *J Pharm Pharmacol.* 1999;51(10):1123-1134.
57. Kato A, Ishibashi Y, Miyake Y. Effect of egg yolk lecithin on transdermal delivery of bunazosin hydrochloride. *J Pharm Pharmacol.* 1987;39(5):399-400.
58. Zellmer S, Pfeil W, Lasch J. Interaction of phosphatidylcholine liposomes with the human stratum corneum. *Biochimica et Biophysica Acta (BBA) - Biomembranes.* 1995;1237(2):176-182.
59. Kirjavainen M, Mönkkönen J, Saukkosaari M, Valjakka-Koskela R, Kiesvaara J, Urtti A. Phospholipids affect stratum corneum lipid bilayer fluidity and drug partitioning into the bilayers. *J Control Release.* 1999;58(2):207-214.
60. Weiner N, Williams N, Birch G, Ramachandran C, Shipman C, Jr., Flynn G. Topical delivery of liposomally encapsulated interferon evaluated in a cutaneous herpes guinea pig model. *Antimicrobial agents and chemotherapy.* 1989;33(8):1217-1221.
61. Du Plessis J, Weiner, N., Muller, D.G. The influence of in vivo treatment of skin with liposomes on the topical absorption of a hydrophilic and a hydrophobic drug in vitro. *Int J Pharm* 1994;103:5.
62. Schaller M, Korting HC. Interaction of liposomes with human skin: the role of the stratum corneum. *Advanced Drug Delivery Reviews.* 1996;18(3):303-309.
63. Kirjavainen M, Urtti A, Jääskeläinen I, et al. Interaction of liposomes with human skin in vitro--the influence of lipid composition and structure. *Biochim Biophys Acta.* 1996;1304(3):179-189.

64. Keith AD, Snipes, W. Phospholipids as moisturizing agents. . *Principles of Cosmetics for the Dermatologist* 1982:10.
65. Foldvari M, Gesztes A, Mezei M. Dermal drug delivery by liposome encapsulation: clinical and electron microscopic studies. *J Microencapsul.* 1990;7(4):479-489.
66. Korting HC, Zienicke H, Schäfer-Korting M, Braun-Falco O. Liposome encapsulation improves efficacy of betamethasone dipropionate in atopic eczema but not in psoriasis vulgaris. *European journal of clinical pharmacology.* 1990;39(4):349-351.
67. Du Plessis J, Ramachandran, C., Weiner, N., Muller, D.G. The influence of particle size of liposomes on the disposition of drug into skin. . *Int J Pharm* 1994;103:6.
68. KORTING HC, STOLZ W, SCHMID MH, MAIERHOFER G. Interaction of liposomes with human epidermis reconstructed in vitro. 1995;132(4):571-579.
69. El Maghraby GM, Williams AC, Barry BW. Skin hydration and possible shunt route penetration in controlled estradiol delivery from ultradeformable and standard liposomes. *J Pharm Pharmacol.* 2001;53(10):1311-1322.
70. Han I, Kim M, Kim J. Enhanced transfollicular delivery of adriamycin with a liposome and iontophoresis. *Experimental dermatology.* 2004;13(2):86-92.
71. Dayan N, Tuitou E. Carriers for skin delivery of trihexyphenidyl HCl: ethosomes vs. liposomes. *Biomaterials.* 2000;21(18):1879-1885.
72. Dorrani M, Garbuzenko OB, Minko T, Michniak-Kohn B. Development of edge-activated liposomes for siRNA delivery to human basal epidermis for melanoma therapy. *J Control Release.* 2016;228:150-158.
73. Cevc G, Blume G. New, highly efficient formulation of diclofenac for the topical, transdermal administration in ultradeformable drug carriers, Transfersomes. *Biochim Biophys Acta.* 2001;1514(2):191-205.
74. Cevc G, Gebauer D, Stieber J, Schatzlein A, Blume G. Ultraflexible vesicles, Transfersomes, have an extremely low pore penetration resistance and transport therapeutic amounts of insulin across the intact mammalian skin. *Biochim Biophys Acta.* 1998;1368(2):201-215.
75. Hua S. Lipid-based nano-delivery systems for skin delivery of drugs and bioactives. *Front Pharmacol.* 2015;6:219.
76. Elsayed MM, Abdallah OY, Naggar VF, Khalafallah NM. Deformable liposomes and ethosomes: mechanism of enhanced skin delivery. *Int J Pharm.* 2006;322(1-2):60-66.
77. Elsayed MM, Abdallah OY, Naggar VF, Khalafallah NM. Lipid vesicles for skin delivery of drugs: reviewing three decades of research. *Int J Pharm.* 2007;332(1-2):1-16.
78. Geusens B, Strobbe T, Bracke S, et al. Lipid-mediated gene delivery to the skin. *Eur J Pharm Sci.* 2011;43(4):199-211.

79. Touitou E, Dayan N, Bergelson L, Godin B, Eliaz M. Ethosomes - novel vesicular carriers for enhanced delivery: characterization and skin penetration properties. *J Control Release*. 2000;65(3):403-418.
80. Duangjit S, Obata Y, Sano H, et al. Mentosomes, novel ultradeformable vesicles for transdermal drug delivery: optimization and characterization. *Biol Pharm Bull*. 2012;35(10):1720-1728.
81. Song YK, Kim CK. Topical delivery of low-molecular-weight heparin with surface-charged flexible liposomes. *Biomaterials*. 2006;27(2):271-280.
82. Ban E, Park M, Jeong S, et al. Poloxamer-Based Thermoreversible Gel for Topical Delivery of Emodin: Influence of P407 and P188 on Solubility of Emodin and Its Application in Cellular Activity Screening. *Molecules*. 2017;22(2).
83. Kazi KM, Mandal AS, Biswas N, et al. Niosome: A future of targeted drug delivery systems. *J Adv Pharm Technol Res*. 2010;1(4):374-380.
84. Babaie S, Bakhshayesh ARD, Ha JW, Hamishehkar H, Kim KH. Invasome: A Novel Nanocarrier for Transdermal Drug Delivery. *Nanomaterials (Basel)*. 2020;10(2).
85. Song YK, Hyun SY, Kim HT, Kim CK, Oh JM. Transdermal delivery of low molecular weight heparin loaded in flexible liposomes with bioavailability enhancement: comparison with ethosomes. *J Microencapsul*. 2011;28(3):151-158.
86. Al-Mahallawi AM, Abdelbary AA, Aburahma MH. Investigating the potential of employing bilosomes as a novel vesicular carrier for transdermal delivery of tenoxicam. *Int J Pharm*. 2015;485(1-2):329-340.
87. Hu C, Rhodes DG. Proniosomes: a novel drug carrier preparation. *Int J Pharm*. 1999;185(1):23-35.
88. Marto J, Vitor C, Guerreiro A, et al. Ethosomes for enhanced skin delivery of griseofulvin. *Colloids Surf B Biointerfaces*. 2016;146:616-623.
89. Roberts MS, Mohammed Y, Pastore MN, et al. Topical and cutaneous delivery using nanosystems. *J Control Release*. 2017;247:86-105.
90. Oluwatosin A, Ogunsola ea. Structural analysis of “flexible” liposome formulations: new insights into the skin-penetrating ability of soft nanostructures. *Soft Matter*. 2012;8:6.
91. Pairet M, van Ryn J, Schierok H, Mauz A, Trummlitz G, Engelhardt G. Differential inhibition of cyclooxygenases-1 and -2 by meloxicam and its 4'-isomer. *Inflamm Res*. 1998;47(6):270-276.
92. Degner F, Sigmund R, Zeidler H. Efficacy and tolerability of meloxicam in an observational, controlled cohort study in patients with rheumatic disease. *Clin Ther*. 2000;22(4):400-410.
93. Deeks JJ, Smith LA, Bradley MD. Efficacy, tolerability, and upper gastrointestinal safety of celecoxib for treatment of osteoarthritis and

- rheumatoid arthritis: systematic review of randomised controlled trials. *BMJ*. 2002;325(7365):619.
94. Distel M, Mueller C, Bluhmki E, Fries J. Safety of meloxicam: a global analysis of clinical trials. *Br J Rheumatol*. 1996;35 Suppl 1:68-77.
 95. Lanes SF, Rodriguez LA, Hwang E. Baseline risk of gastrointestinal disorders among new users of meloxicam, ibuprofen, diclofenac, naproxen and indomethacin. *Pharmacoepidemiol Drug Saf*. 2000;9(2):113-117.
 96. Wishart DS KC, Guo AC, Shrivastava S, Hassanali M, Stothard P, Chang Z, Woolsey J. . Drugbank: a comprehensive resource for in silico drug discovery and exploration. *Nucleic Acids Res*. 2006;1(34 (Database issue)):D668-672.
 97. Verma DD, Verma S, Blume G, Fahr A. Particle size of liposomes influences dermal delivery of substances into skin. *Int J Pharm*. 2003;258(1-2):141-151.
 98. Chen M, Liu X, Fahr A. Skin penetration and deposition of carboxyfluorescein and temoporfin from different lipid vesicular systems: In vitro study with finite and infinite dosage application. *Int J Pharm*. 2011;408(1-2):223-234.
 99. Dragicevic-Curic N, Scheglmann D, Albrecht V, Fahr A. Temoporfin-loaded invasomes: development, characterization and in vitro skin penetration studies. *J Control Release*. 2008;127(1):59-69.
 100. Agarwal S, Murthy RSR, Harikumar SL, Garg R. Quality by Design Approach for Development and Characterisation of Solid Lipid Nanoparticles of Quetiapine Fumarate. *Curr Comput Aided Drug Des*. 2020;16(1):73-91.
 101. Kedar U, Phutane P, Shidhaye S, Kadam V. Advances in polymeric micelles for drug delivery and tumor targeting. *Nanomedicine*. 2010;6(6):714-729.
 102. Beck-Broichsitter M, Ruppert C, Schmehl T, et al. Biophysical investigation of pulmonary surfactant surface properties upon contact with polymeric nanoparticles in vitro. *Nanomedicine*. 2011;7(3):341-350.
 103. Robson AL, Dastoor PC, Flynn J, et al. Advantages and Limitations of Current Imaging Techniques for Characterizing Liposome Morphology. *Front Pharmacol*. 2018;9:80.
 104. Herkenne C, Alberti I, Naik A, et al. In vivo methods for the assessment of topical drug bioavailability. *Pharm Res*. 2008;25(1):87-103.
 105. Nair A, Jacob S, Al-Dhubiab B, Attimarad M, Harsha S. Basic considerations in the dermatokinetics of topical formulations %J Brazilian Journal of Pharmaceutical Sciences. 2013;49:423-434.
 106. FDA. Draft Guidance on Acyclovir. 2016.
 107. Abd E, Yousef SA, Pastore MN, et al. Skin models for the testing of transdermal drugs. *Clin Pharmacol*. 2016;8:163-176.
 108. PermeGear. <http://www.permegear.com/franz.htm>.
<http://www.permegear.com/franzhtm>.
 109. Tsubouchi H, Ogawa H. Exo1 roles for repair of DNA double-strand breaks and meiotic crossing over in *Saccharomyces cerevisiae*. *Mol Biol Cell*. 2000;11(7):2221-2233.

110. Lawrence MJ, Rees GD. Microemulsion-based media as novel drug delivery systems. *Adv Drug Deliv Rev.* 2000;45(1):89-121.
111. Gannu R, Palem CR, Yamsani VV, Yamsani SK, Yamsani MR. Enhanced bioavailability of lacidipine via microemulsion based transdermal gels: formulation optimization, ex vivo and in vivo characterization. *Int J Pharm.* 2010;388(1-2):231-241.
112. Heuschkel S, Goebel A, Neubert RH. Microemulsions--modern colloidal carrier for dermal and transdermal drug delivery. *J Pharm Sci.* 2008;97(2):603-631.
113. El Maghraby GM. Transdermal delivery of hydrocortisone from eucalyptus oil microemulsion: effects of cosurfactants. *Int J Pharm.* 2008;355(1-2):285-292.
114. Lopes LB. Overcoming the cutaneous barrier with microemulsions. *Pharmaceutics.* 2014;6(1):52-77.
115. Shukla T, Upmanyu N, Agrawal M, Saraf S, Saraf S, Alexander A. Biomedical applications of microemulsion through dermal and transdermal route. *Biomed Pharmacother.* 2018;108:1477-1494.
116. Ita K. Progress in the use of microemulsions for transdermal and dermal drug delivery. *Pharm Dev Technol.* 2017;22(4):467-475.
117. Hoar TP, Schulman JH. Transparent Water-in-Oil Dispersions: the Oleopathic Hydro-Micelle. *Nature.* 1943;152(3487):2.
118. Kreilgaard M. Influence of microemulsions on cutaneous drug delivery. *Adv Drug Deliv Rev.* 2002;54 Suppl 1:S77-98.
119. Akbarzadeh A, Rezaei-Sadabady R, Davaran S, et al. Liposome: classification, preparation, and applications. *Nanoscale Res Lett.* 2013;8(1):102.
120. Duangjit S, Obata Y, Sano H, et al. Comparative study of novel ultradeformable liposomes: mentosomes, transfersomes and liposomes for enhancing skin permeation of meloxicam. *Biol Pharm Bull.* 2014;37(2):239-247.
121. Shah B, Khunt D, Misra M, Padh H. Formulation and In-vivo Pharmacokinetic Consideration of Intranasal Microemulsion and Mucoadhesive Microemulsion of Rivastigmine for Brain Targeting. *Pharm Res.* 2018;35(1):8.
122. Zeb A, Qureshi OS, Kim HS, Cha JH, Kim HS, Kim JK. Improved skin permeation of methotrexate via nanosized ultradeformable liposomes. *Int J Nanomedicine.* 2016;11:3813-3824.
123. Gabizon A, Goren D, Cohen R, Barenholz Y. Development of liposomal anthracyclines: from basics to clinical applications. *J Control Release.* 1998;53(1-3):275-279.
124. Sahoo SK, Labhasetwar V. Nanotech approaches to drug delivery and imaging. *Drug Discov Today.* 2003;8(24):1112-1120.
125. Allen TM. Liposomes. Opportunities in drug delivery. *Drugs.* 1997;54 Suppl 4:8-14.
126. Yongju He LL, Shuquan Liang, Mengqiu Long & Hui Xu. Influence of probe-sonication process on drug entrapment efficiency of liposomes loaded

- with a hydrophobic drug. *International Journal of Polymeric Materials and Polymeric Biomaterials*. 2019;68(4):5.
127. Silva R, Ferreira H, Little C, Cavaco-Paulo A. Effect of ultrasound parameters for unilamellar liposome preparation. *Ultrason Sonochem*. 2010;17(3):628-632.
 128. Nam JH, Kim SY, Seong H. Investigation on Physicochemical Characteristics of a Nanoliposome-Based System for Dual Drug Delivery. *Nanoscale Res Lett*. 2018;13(1):101.
 129. Yuan Y, Li SM, Mo FK, Zhong DF. Investigation of microemulsion system for transdermal delivery of meloxicam. *Int J Pharm*. 2006;321(1-2):117-123.
 130. Panapisal V, Charoensri S, Tantituvanont A. Formulation of microemulsion systems for dermal delivery of silymarin. *AAPS PharmSciTech*. 2012;13(2):389-399.
 131. Yanng B, Kuo, S., Hariyadi, P., Parkin, K. . Solvent suitability for lipase-mediated acyl-transfer and esterification reactions in microaqueous milieu is related to substrate and product polarities. . *Enzyme Microb Technol* 1994;16:7.
 132. Soo ELS, A.B.; Basri, M.; Rahman, R.N.Z.A.; Kamaruddin, K. . Response surface methodological study on lipase-catalyzed synthesis of amino acid surfactants. *Process Biochem* 2004;39:8.
 133. Yang JH, Kim YI, Kim KM. Preparation and evaluation of aceclofenac microemulsion for transdermal delivery system. *Arch Pharm Res*. 2002;25(4):534-540.
 134. Warisnoicharoen W, Lansley AB, Lawrence MJ. Nonionic oil-in-water microemulsions: the effect of oil type on phase behaviour. *Int J Pharm*. 2000;198(1):7-27.
 135. Mehta SK, Kaur G, Bhasin KK. Incorporation of antitubercular drug isoniazid in pharmaceutically accepted microemulsion: effect on microstructure and physical parameters. *Pharm Res*. 2008;25(1):227-236.
 136. Mehta SK, Kaur G, Bhasin KK. Analysis of Tween based microemulsion in the presence of TB drug rifampicin. *Colloids Surf B Biointerfaces*. 2007;60(1):95-104.
 137. Kumar R, Sinha VR. Preparation and optimization of voriconazole microemulsion for ocular delivery. *Colloids Surf B Biointerfaces*. 2014;117:82-88.
 138. Podlogar F, Bester Rogac M, Gasperlin M. The effect of internal structure of selected water-Tween 40-Imwitor 308-IPM microemulsions on ketoprofen release. *Int J Pharm*. 2005;302(1-2):68-77.
 139. Fanun M. Conductivity, viscosity, NMR and diclofenac solubilization capacity studies of mixed nonionic surfactants microemulsions. *J Mol Liq* 2007;135:9.
 140. Fanun M. MICROEMULSIONS : Properties and Applications, 1st ed. *CRC Press: Boca Raton, FL, USA*. 2008.

141. Fanun M. Properties of microemulsions with sugar surfactants and peppermint oil. . *Colloid Polym Sci* 2009;287:2.
142. Jeirani ZMJ, B.; Si Ali, B.; Mohd Noor, I.; Chun Hwa, S.; Saphanuchart, W. . Prediction of Water Percolation Threshold of a Microemulsion Using Electrical Conductivity Measurements and Design of Experiments. . *Ind Eng Chem Res* 2012;51:9.
143. Mitra RK, Paul BK. Physicochemical investigations of microemulsification of eucalyptus oil and water using mixed surfactants (AOT+Brij-35) and butanol. *J Colloid Interface Sci.* 2005;283(2):565-577.
144. Fisher S, Wachtel EJ, Aserin A, Garti N. Solubilization of simvastatin and phytosterols in a dilutable microemulsion system. *Colloids Surf B Biointerfaces.* 2013;107:35-42.
145. Tabor RF, Zaveer MI, Dagastine RR, Grillo I, Garvey CJ. Phase behavior, small-angle neutron scattering and rheology of ternary nonionic surfactant-oil-water systems: a comparison of oils. *Langmuir.* 2013;29(11):3575-3582.
146. Benson HA. Transfersomes for transdermal drug delivery. *Expert Opin Drug Deliv.* 2006;3(6):727-737.
147. Cevc G, Blume G. Lipid vesicles penetrate into intact skin owing to the transdermal osmotic gradients and hydration force. *Biochim Biophys Acta.* 1992;1104(1):226-232.
148. Pena-Rodriguez E, Moreno MC, Blanco-Fernandez B, Gonzalez J, Fernandez-Campos F. Epidermal Delivery of Retinyl Palmitate Loaded Transfersomes: Penetration and Biodistribution Studies. *Pharmaceutics.* 2020;12(2).
149. Honeywell-Nguyen PL, Wouter Groenink HW, de Graaff AM, Bouwstra JA. The in vivo transport of elastic vesicles into human skin: effects of occlusion, volume and duration of application. *J Control Release.* 2003;90(2):243-255.
150. Zhang J, Michniak-Kohn B. Investigation of microemulsion microstructures and their relationship to transdermal permeation of model drugs: ketoprofen, lidocaine, and caffeine. *Int J Pharm.* 2011;421(1):34-44.
151. Naoui W, Bolzinger MA, Fenet B, et al. Microemulsion microstructure influences the skin delivery of an hydrophilic drug. *Pharm Res.* 2011;28(7):1683-1695.
152. El-Badry M, Fetih G, Shakeel F. Comparative topical delivery of antifungal drug croconazole using liposome and micro-emulsion-based gel formulations. *Drug Deliv.* 2014;21(1):34-43.
153. Duangjit S, Opanasopit P, Rojanarata T, Ngawhirunpat T. Evaluation of meloxicam-loaded cationic transfersomes as transdermal drug delivery carriers. *AAPS PharmSciTech.* 2013;14(1):133-140.
154. Alvi IA, Madan J, Kaushik D, Sardana S, Pandey RS, Ali A. Comparative study of transfersomes, liposomes, and niosomes for topical delivery of 5-fluorouracil

- to skin cancer cells: preparation, characterization, in-vitro release, and cytotoxicity analysis. *Anticancer Drugs*. 2011;22(8):774-782.
155. Gupta PN, Mishra V, Rawat A, et al. Non-invasive vaccine delivery in transfersomes, niosomes and liposomes: a comparative study. *Int J Pharm*. 2005;293(1-2):73-82.
 156. Mahrhauser D, Nagelreiter C, Baierl A, Skipiol J, Valenta C. Influence of a multiple emulsion, liposomes and a microemulsion gel on sebum, skin hydration and TEWL. *Int J Cosmet Sci*. 2015;37(2):181-186.
 157. Niu XQ, Zhang DP, Bian Q, et al. Mechanism investigation of ethosomes transdermal permeation. *Int J Pharm X*. 2019;1:100027.
 158. Kopustinskiene DM, Jakstas V, Savickas A, Bernatoniene J. Flavonoids as Anticancer Agents. *Nutrients*. 2020;12(2).
 159. Yahfoufi N, Alsadi N, Jambi M, Matar C. The Immunomodulatory and Anti-Inflammatory Role of Polyphenols. *Nutrients*. 2018;10(11).
 160. Abotaleb M, Samuel SM, Varghese E, et al. Flavonoids in Cancer and Apoptosis. *Cancers (Basel)*. 2018;11(1).
 161. Hussain T, Tan B, Murtaza G, et al. Flavonoids and type 2 diabetes: Evidence of efficacy in clinical and animal studies and delivery strategies to enhance their therapeutic efficacy. *Pharmacol Res*. 2020;152:104629.
 162. O'Fallon KS, Kaushik D, Michniak-Kohn B, Dunne CP, Zambraski EJ, Clarkson PM. Effects of quercetin supplementation on markers of muscle damage and inflammation after eccentric exercise. *Int J Sport Nutr Exerc Metab*. 2012;22(6):430-437.
 163. Sharp MA, Hendrickson NR, Staab JS, McClung HL, Nindl BC, Michniak-Kohn BB. Effects of short-term quercetin supplementation on soldier performance. *J Strength Cond Res*. 2012;26 Suppl 2:S53-60.
 164. Chen Y, Deuster P. Comparison of quercetin and dihydroquercetin: antioxidant-independent actions on erythrocyte and platelet membrane. *Chem Biol Interact*. 2009;182(1):7-12.
 165. Nataša Poklar Ulrih AO, Marjeta Šentjurc, Sandra Kure, Veronika Abram. Flavonoids and cell membrane fluidity. *Food Chemistry*. 2010;121(1):7.
 166. Saija A, Scalese M, Lanza M, Marzullo D, Bonina F, Castelli F. Flavonoids as antioxidant agents: importance of their interaction with biomembranes. *Free Radic Biol Med*. 1995;19(4):481-486.
 167. Arora A, Byrem TM, Nair MG, Strasburg GM. Modulation of liposomal membrane fluidity by flavonoids and isoflavonoids. *Arch Biochem Biophys*. 2000;373(1):102-109.
 168. Huang M, Su E, Zheng F, Tan C. Encapsulation of flavonoids in liposomal delivery systems: the case of quercetin, kaempferol and luteolin. *Food Funct*. 2017;8(9):3198-3208.

169. Garg V, Singh H, Bhatia A, et al. Systematic Development of Transethosomal Gel System of Piroxicam: Formulation Optimization, In Vitro Evaluation, and Ex Vivo Assessment. *AAPS PharmSciTech*. 2017;18(1):58-71.
170. Alvarez-Roman R, Naik A, Kalia YN, Fessi H, Guy RH. Visualization of skin penetration using confocal laser scanning microscopy. *Eur J Pharm Biopharm*. 2004;58(2):301-316.
171. Lopez-Pinto JM, Gonzalez-Rodriguez ML, Rabasco AM. Effect of cholesterol and ethanol on dermal delivery from DPPC liposomes. *Int J Pharm*. 2005;298(1):1-12.
172. Tavano L, Muzzalupo R, Cassano R, Trombino S, Ferrarelli T, Picci N. New sucrose cocoate based vesicles: Preparation, characterization and skin permeation studies. *Colloids Surf B Biointerfaces*. 2010;75(1):319-322.
173. Taladrid D, Marin D, Aleman A, Alvarez-Acero I, Montero P, Gomez-Guillen MC. Effect of chemical composition and sonication procedure on properties of food-grade soy lecithin liposomes with added glycerol. *Food Res Int*. 2017;100(Pt 1):541-550.
174. Bozzuto G, Molinari A. Liposomes as nanomedical devices. *Int J Nanomedicine*. 2015;10:975-999.
175. Luger P, Danec, K., Engel, W., Trummlitz, G., and Wagner, K. . Structure and physicochemical properties of meloxicam, a new NSAID. *European Journal of Pharmaceutical Sciences* 1996;4(3):13.
176. Katahira N, Murakami T, Kugai S, Yata N, Takano M. Enhancement of topical delivery of a lipophilic drug from charged multilamellar liposomes. *J Drug Target*. 1999;6(6):405-414.
177. Lin H, Xie Q, Huang X, et al. Increased skin permeation efficiency of imperatorin via charged ultradeformable lipid vesicles for transdermal delivery. *Int J Nanomedicine*. 2018;13:831-842.
178. Pawlikowska-Pawlega B, Gruszecki WI, Misiak LE, Gawron A. The study of the quercetin action on human erythrocyte membranes. *Biochem Pharmacol*. 2003;66(4):605-612.
179. Sanver D, Murray BS, Sadeghpour A, Rappolt M, Nelson AL. Experimental Modeling of Flavonoid-Biomembrane Interactions. *Langmuir*. 2016;32(49):13234-13243.
180. Buchner N, Krumbein A, Rohn S, Kroh LW. Effect of thermal processing on the flavonols rutin and quercetin. *Rapid Commun Mass Spectrom*. 2006;20(21):3229-3235.
181. Davies NM, Skjodt NM. Clinical pharmacokinetics of meloxicam. A cyclo-oxygenase-2 preferential nonsteroidal anti-inflammatory drug. *Clin Pharmacokinet*. 1999;36(2):115-126.
182. Zhang ZJ, Michniak-Kohn B. Flavosomes, novel deformable liposomes for the co-delivery of anti-inflammatory compounds to skin. *Int J Pharm*. 2020;585:119500.

183. Zhang J, Froelich A, Michniak-Kohn B. Topical Delivery of Meloxicam using Liposome and Microemulsion Formulation Approaches. *Pharmaceutics*. 2020;12(3).
184. FDA. Liposome Drug Products Chemistry, Manufacturing, and Controls; Human Pharmacokinetics and Bioavailability; and Labeling Documentation Guidance for Industry. April, 2018.
185. Yadav A.V MMS, Shete A. S and Sfurti Sakhare. Stability Aspects of Liposomes. *Ind J Pharm Edu Res*. 2011;45(4):12.
186. Mayba JN, Gooderham MJ. A Guide to Topical Vehicle Formulations. *J Cutan Med Surg*. 2018;22(2):207-212.
187. Buwalda SJ, Boere KW, Dijkstra PJ, Feijen J, Vermonden T, Hennink WE. Hydrogels in a historical perspective: from simple networks to smart materials. *J Control Release*. 2014;190:254-273.
188. Jung YS, Park W, Park H, Lee DK, Na K. Thermo-sensitive injectable hydrogel based on the physical mixing of hyaluronic acid and Pluronic F-127 for sustained NSAID delivery. *Carbohydr Polym*. 2017;156:403-408.
189. Dumortier G, Grossiord JL, Agnely F, Chaumeil JC. A review of poloxamer 407 pharmaceutical and pharmacological characteristics. *Pharm Res*. 2006;23(12):2709-2728.
190. Xu X, Khan MA, Burgess DJ. A quality by design (QbD) case study on liposomes containing hydrophilic API: II. Screening of critical variables, and establishment of design space at laboratory scale. *Int J Pharm*. 2012;423(2):543-553.
191. Duangjit S, Opanasopit P, Rojanarata T, Ngawhirunpat T. Characterization and In Vitro Skin Permeation of Meloxicam-Loaded Liposomes versus Transfersomes. *J Drug Deliv*. 2011;2011:418316.
192. Bragagni M, Mennini N, Maestrelli F, Cirri M, Mura P. Comparative study of liposomes, transfersomes and ethosomes as carriers for improving topical delivery of celecoxib. *Drug Deliv*. 2012;19(7):354-361.
193. Buhse L, Kolinski R, Westenberger B, et al. Topical drug classification. *Int J Pharm*. 2005;295(1-2):101-112.
194. Li J, Mooney DJ. Designing hydrogels for controlled drug delivery. *Nat Rev Mater*. 2016;1(12).
195. Yu T, Malcolm K, Woolfson D, Jones DS, Andrews GP. Vaginal gel drug delivery systems: understanding rheological characteristics and performance. *Expert Opin Drug Deliv*. 2011;8(10):1309-1322.
196. R As, Sirivat A, Vayumhasuwan P. Viscoelastic properties of Carbopol 940 gels and their relationships to piroxicam diffusion coefficients in gel bases. *Pharm Res*. 2005;22(12):2134-2140.
197. Fakhari A, Corcoran M, Schwarz A. Thermogelling properties of purified poloxamer 407. *Heliyon*. 2017;3(8):e00390.

198. Pandita D, Ahuja A, Lather V, et al. Development of lipid-based nanoparticles for enhancing the oral bioavailability of paclitaxel. *AAPS PharmSciTech*. 2011;12(2):712-722.
199. Instruments M. DLS Technical Note, MRK656-01.
200. Liu D, Hu H, Lin Z, et al. Quercetin deformable liposome: preparation and efficacy against ultraviolet B induced skin damages in vitro and in vivo. *J Photochem Photobiol B*. 2013;127:8-17.
201. Kirjavainen M, Urtti A, Valjakka-Koskela R, Kiesvaara J, Monkkonen J. Liposome-skin interactions and their effects on the skin permeation of drugs. *Eur J Pharm Sci*. 1999;7(4):279-286.
202. Pawlikowska-Pawlega B, Gruszecki WI, Misiak L, et al. Modification of membranes by quercetin, a naturally occurring flavonoid, via its incorporation in the polar head group. *Biochim Biophys Acta*. 2007;1768(9):2195-2204.
203. Hendrich AB, Malon R, Pola A, Shirataki Y, Motohashi N, Michalak K. Differential interaction of Sophora isoflavonoids with lipid bilayers. *Eur J Pharm Sci*. 2002;16(3):201-208.
204. Kim YA, Tarahovsky YS, Yagolnik EA, Kuznetsova SM, Muzafarov EN. Lipophilicity of flavonoid complexes with iron(II) and their interaction with liposomes. *Biochem Biophys Res Commun*. 2013;431(4):680-685.
205. Movileanu L, Neagoe I, Flonta ML. Interaction of the antioxidant flavonoid quercetin with planar lipid bilayers. *Int J Pharm*. 2000;205(1-2):135-146.